NATIONAL TECHNICAL UNIVERSITY OF ATHENS

School of Mechanical Engineering

Interdepartmental Program of Postgraduate Studies

Automation Systems

Postgraduate Thesis

by

Loucas Poufos

Dipl. Mechanical Engineer NTUA

Optimization of tank vehicle suspension characteristics

Advisor: Dr.- Ing. Dimitrios Koulocheris

Athens 2010

ΕΘΝΙΚΟ ΜΕΤΣΟΒΙΟ ΠΟΛΥΤΕΧΝΕΙΟ

Σχολή Μηχανολόγων Μηχανικών

Διατμηματικό Πρόγραμμα Μεταπτυχιακών Σπουδών

Συστήματα Αυτοματισμού

Μεταπτυχιακή εργασία

Πούφου Λουκά

Διπλωματούχου Μηχανολόγου Μηχανικού Ε.Μ.Π.

Βελτιστοποίηση χαρακτηριστικών ανάρτησης βυτιοφόρου οχήματος

Επιβλέπων: Δρ.-Μηχ. Δ. Κουλοχέρης

Αθήνα 2010

Abstract

In the design of a vehicle, the engineer today more than ever has to perform a balancing act of sorts, in an attempt to satisfy the requirements of safety and practicality but also minimize the constructional and operational costs. Efficiency goes hand in hand with optimization and the empirical rules of designing have now been augmented by automated optimization procedures.

The complexity of vehicle dynamics problems increases the need for deeper comprehension of the complex theory involved in the movement of a vehicle and the interaction with the environment it moves in. A solid knowledge of vehicle dynamics as well as vibration analysis is required. Moreover, the theoretical approach to the solution of such problems can be enhanced greatly by creating appropriate models which represent the vehicle and its behavior in simulated conditions. The engineer, with the correct implementation and use of such a model is able to predict the behavior of a vehicle, given the applicable conditions, and also optimize certain vehicle parameters in order to achieve a desired goal.

The objective of this study is to examine certain aspects of a tri-axle tank-truck's dynamic behavior under different loading conditions and modify this behavior in a desirable way by optimizing a number of vehicle parameter values. The loading cases examined represent typical conditions for such a vehicle in real-life practice.

In particular, it is attempted to determine an optimum set of values from within an allowable range for the vehicle's suspension characteristics in order to minimize the tank's roll angle time-response. Different patterns of filling the tank will be examined and the movement of the vehicle will be simulated for different types of roads. The optimization of the vehicle parameters will be take place using both a deterministic quasi-Newton line search method (BFGS) and a stochastic genetic algorithm. The two methods will be compared to each other with regards to global search capabilities and overall convergence characteristics. In the process useful conclusions will be drawn regarding both the nature of the problem as well as the nature of the algorithms.

Περίληψη

Κατά τον σχεδιασμό ενός οχήματος, ο μηχανικός σήμερα πρέπει να επιτελέσει το δύσκολο έργο της εύρεσης μίας ισορροπίας μεταξύ των απαιτήσεων ασφάλειας και πρακτικότητας με την ελαχιστοποίηση του κατασκευαστικού και λειτουργικού κόστους. Η αποδοτικότητα είναι συνυφασμένη με την βελτιστοποίηση και οι εμπειρικοί κανόνες σχεδίασης έχουν πλέον επαυξηθεί με αυτοματοποιημένες διαδικασίες βελτιστοποίησης.

Η πολυπλοκότητα των προβλημάτων της δυναμικής οχημάτων αυξάνει την ανάγκη για βαθύτερη κατανόηση της σύνθετης θεωρίας που αναλύει την κίνηση ενός οχήματος και την αλληλεπίδρασή του με το περιβάλλον στο οποίο κινείται. Η στιβαρή γνώση δυναμικής οχημάτων και ανάλυσης κραδασμών είναι απαραίτητη. Επιπλέον, η θεωρητική προσέγγιση για την λύση τέτοιων προβλημάτων μπορεί να ενισχυθεί σημαντικά με την δημιουργία κατάλληλων μοντέλων που αντιπροσωπεύουν το όχημα και την συμπεριφορά του σε συνθήκες προσομοίωσης . Ο μηχανικός, με την σωστή εφαρμογή και χρήση ενός τέτοιου μοντέλου, είναι σε θέση να προβλέπει την συμπεριφορά του οχήματος για δεδομένες συνθήκες, και να βελτιστοποιεί παραμέτρους του οχήματος ώστε να επιτυγχάνεται ένας επιθυμητός στόχος.

Ο σκοπός της παρούσας εργασίας είναι να εξετάσει συγκεκριμένα χαρακτηριστικά της δυναμικής συμπεριφοράς ενός τριαξονικού βυτιοφόρου οχήματος υπό διαφορετικές συνθήκες φόρτωσης και να τροποποιήσει την δεδομένη συμπεριφορά βελτιστοποιώντας τις τιμές κάποιων από τις παραμέτρους του οχήματος. Οι περιπτώσεις φόρτωσης που εξετάζονται αντιπροσωπεύουν τυπικές συνθήκες ρεαλιστικής πρακτικής για ένα τέτοιο όχημα.

Συγκεκριμένα, επιχειρείται να προσδιοριστεί ένα βέλτιστο σύνολο τιμών, εντός επιτρεπτών ορίων, για τα χαρακτηριστικά των αναρτήσεων του οχήματος έτσι ώστε να ελαχιστοποιείται η απόκριση της γωνίας στρέψης του βυτίου. Εξετάζονται διαφορετικές περιπτώσεις πλήρωσης του βυτίου ενώ η κίνηση του οχήματος προσομοιώνεται σε διάφορα είδη οδοστρώματος. Η βελτιστοποίηση των εν λόγω παραμέτρων του οχήματος πραγματοποιείται με την χρήση ντετερμινιστικού quasi-Newton αλγορίθμου αναζήτησης γραμμής (BFGS) και με την χρήση στοχαστικού γενετικού αλγορίθμου. Μεταξύ των δύο μεθόδων πραγματοποιείται σύγκριση όσον αφορά της ικανότητες αναζήτησης του ολικού ελαχίστου της κάθε μίας αλλά και των γενικότερων χαρακτηριστικών της σύγκλισης. Από αυτήν την διαδικασία εξάγονται χρήσιμα συμπεράσματα για την φύση του προβλήματος και την φύση των αλγορίθμων.

Acknowledgements

I would very much like to thank Dr.- Ing. Dimitrios Koulocheris of the School of Mechanical Engineering, National Technical University of Athens (NTUA) for entrusting me with the current assignment but also for his support and assistance throughout the preparation and fruition of this study.

Athens, October 2010

Loucas Poufos

Table of Contents

Abstract ..... **i**

Περίληψη ..... **iii**

Acknowledgements ..... **v**

Table of Contents ..... **vii**

List of Figures ..... **ix**

List of Tables ..... **xi**

1 Optimization **1**

1.1 The general concept of optimization in engineering 1
1.2 Mathematical formulation of a single-objective optimization problem 2
1.2.1 Mathematical definitions 3
1.3 Optimization algorithms 6
1.3.1 Line search methods 7
1.3.2 Evolutionary Algorithms (EAs) 11
1.3.3 Genetic Algorithm (GA) 13
1.3.4 Evolution Strategies (ES) 22
1.4 Constraint Handling Techniques 24

2 Vehicle Dynamics **29**

2.1 Introduction to vehicle dynamics 29
2.2 Coordinate systems and movement 30
2.3 Road Loads 32
2.4 Excitations 34
2.5 Suspensions 37
2.6 General concept of modeling 38

3 Applications **41**

3.1 Model of the vehicle 41

3.2 Optimization with the Genetic Algorithm 47
3.2.1 Load Case 1: All compartments filled at 100% 47
3.2.2 Load Case 2: All compartments filled at 80% 53
3.2.3 Load Case 3: All compartments filled at 50% 56
3.2.4 Load Case 4: All compartments filled at 20% 59
3.3 Optimization with the BFGS method 62
3.3.1 Load Case 1: All compartments filled at 100% 62
3.3.2 Load Case 2: All compartments filled at 80% 65
3.3.3 Load Case 3: All compartments filled at 50% 68
3.3.4 Load Case 4: All compartments filled at 20% 71

4 Conclusions 75

4.1 Optimization algorithms 75
4.2 Excitation input 77
4.3 Load cases 78
4.4 Topology of the solution space 82
4.5 Optimum solution 86
4.6 Future Work 91

Bibliography 93

List of Figures

Figure 1.1 (a) convex and (b) non-convex (i.e. concave) set..... 3
Figure 1.2 Convex function and its epigraph. 4
Figure 1.3: Algorithmic steps of a basic steepest descend method. 9
Figure 1.4 Algorithmic steps of a basic BFGS method..... 11
Figure 1.5 Algorithmic steps of a basic GA..... 18
Figure 1.6 Algorithmic steps of a basic ES. 23
Figure 2.1 ISO and SAE Vehicle-fixed (S) and Earth-fixed (N) axis coordinate systems. 31
Figure 2.2 Vehicle in an Earth-fixed coordinate system 32
Figure 3.1 Vehicle layout and dimensions..... 42
Figure 3.2 Tank's compartment numbering 42
Figure 3.3 Model of the vehicle along the ABCD section of Figure 3.1..... 45
Figure 3.4 Obstacle profile (a) left track, (b) right track 46
Figure 3.5 Road profile (a) left track, (b) right track..... 46
Figure 3.6 GA Case 1: Roll angle (a) obstacle excitation, (b) road excitation 49
Figure 3.7 GA Case 1: Front suspension stiffness (a) obstacle excitation, (b) road excitation..... 50
Figure 3.8 GA Case 1: Supports' damping (a) obstacle excitation, (b) road excitation.... 51
Figure 3.9 GA Case 1: Supports' damping sum (a) obstacle excitation, (b) road excitation..... 51
Figure 3.10 GA Case 1: Optimized responses (a) obstacle excitation, (b) road excitation 52
Figure 3.11 GA Case 2: Roll angle (a) obstacle excitation, (b) road excitation 54
Figure 3.12 GA Case 2: Supports' damping sum (a) obstacle excitation, (b) road excitation..... 54
Figure 3.13 Relation between roll angle and front suspension damping..... 55
Figure 3.14 GA Case 2: Optimized responses (a) obstacle excitation, (b) road excitation 56
Figure 3.15 GA Case 3: Roll angle (a) obstacle excitation, (b) road excitation..... 57
Figure 3.16 GA Case 3: Supports' damping sum (a) obstacle excitation, (b) road excitation..... 58

Figure 3.17 GA Case 3: Optimized responses (a) obstacle excitation, (b) road excitation 59

Figure 3.18 GA Case 4: Roll angle (a) obstacle excitation, (b) road excitation 60

Figure 3.19 GA Case 4: Optimized responses (a) obstacle excitation, (b) road excitation 61

Figure 3.20 LS Case 1: Roll angle (a) obstacle excitation, (b) road excitation 63

Figure 3.21 LS Case 1: Support stiffness parameters (a) obstacle excitation, (b) road excitation 64

Figure 3.22 LS Case 1: Optimized responses (a) obstacle excitation, (b) road excitation 65

Figure 3.23 LS Case 2: Roll angle (a) obstacle excitation, (b) road excitation 67

Figure 3.24 LS Case 2: Optimized responses (a) obstacle excitation, (b) road excitation 68

Figure 3.25 LS Case 3: Roll angle (a) obstacle excitation, (b) road excitation 69

Figure 3.26 LS Case 3: Optimized responses (a) obstacle excitation, (b) road excitation 71

Figure 3.27 LS Case 4: Roll angle (a) obstacle excitation, (b) road excitation 72

Figure 3.28 LS Case 4: Optimized responses (a) obstacle excitation, (b) road excitation 74

Figure 4.1 Roll angles per load case (a) obstacle excitation, (b) road excitation 76

Figure 4.2: Optimized responses for the obstacle excitation 79

Figure 4.3: Optimized responses for the road excitation 79

Figure 4.4 Supports' damping sum vs tank fill percent (a) obstacle excitation, (b) road excitation 81

Figure 4.5 Roll angle vs tank fill percent for the road excitation 82

Figure 4.6 Roll angle response vs supports' damping 85

Figure 4.7 Roll angle response vs support damping (a) obstacle excitation, (b) road excitation 87

Figure 4.8 Roll angle response vs support damping (a) obstacle excitation, (b) road excitation 89

List of Tables

Table 2.1 Aerodynamic force analysis 33
Table 3.1 Vehicle Parameters 43
Table 3.2 Geometric and structural constraints 43
Table 3.3 Linear translational elements in mechanical systems 44
Table 3.4 GA Case 1: Obstacle excitation 48
Table 3.5 GA Case 1: Road excitation 48
Table 3.6 GA Case 1: Optimum design vectors 52
Table 3.7 GA Case 2: Obstacle excitation 53
Table 3.8 GA Case 2: Road excitation 53
Table 3.9 GA Case 3: Optimum design vectors 56
Table 3.10 GA Case 3: Obstacle excitation 57
Table 3.11 GA Case 3: Road excitation 57
Table 3.12 GA Case 3: Optimum design vectors 58
Table 3.13 GA Case 4: Obstacle excitation 59
Table 3.14 GA Case 4: Road excitation 60
Table 3.15 GA Case 4: Optimum design vectors 61
Table 3.16 LS Case 1: Obstacle excitation 62
Table 3.17 LS Case 1: Road excitation 62
Table 3.18 LS Case 1: Optimum design vectors 65
Table 3.19 LS Case 2: Obstacle excitation 66
Table 3.20 LS Case 2: Road excitation 66
Table 3.21 LS Case 2: Optimum design vectors 68
Table 3.22 LS Case 3: Obstacle excitation 69
Table 3.23 LS Case 3: Road excitation 69
Table 3.24 LS Case 3: Optimum design vectors 70
Table 3.25 LS Case 4: Obstacle excitation 72
Table 3.26 LS Case 4: Road excitation 72
Table 3.27 LS Case 4: Optimum design vectors 74

Table 4.1 Optimum design vectors for the obstacle excitation 80
Table 4.2 Optimum design vectors for the road excitation.....80

Chapter 1

1 Optimization

1.1 The general concept of optimization in engineering

Optimization is the process of finding the best solution from a set of feasible solutions to a given problem. The concept of optimization is closely connected with engineering since there is always the demand of designing and creating something new, such as a structure or a machine, which besides serving the initial purpose for which it was created, is even more functional, safer and more economical than the previous one.

Since the beginning of engineering history, optimization has been a very important priority. Though, for lack of optimization algorithms or computer methods available, optimization was mostly done empirically. It was not until a few decades ago, that a breakthrough in modeling and analysis by numerical methods took place which in combination with the rapid development of computer technology made optimization a vital part of today's modern designing. The engineer is now able to use more advanced algorithms and techniques to solve even more complicated problems which in turn helps design better products.

In order to obtain a usable solution to an optimization problem two steps are required. The first step is the mathematical formulation of the optimization problem with the definition of the design variables, the objective function and the corresponding constraint functions. The second step is the selection and computer implementation of an optimization algorithm appropriate for the specific type of problem which will allow the evaluation of the available solutions and search for better ones.

An engineer uses their experience to formulate the problem, striking a balance between accuracy and solvability, but also to choose and implement the right optimization algorithm for the specific type of problem. Only then is the solution fast but also reliable.

1.2 Mathematical formulation of a single-objective optimization problem

The generic Single-objective Optimization Problem (SOP) of any type can be formulated in the same sense as any mathematical optimization. Essentially, this means minimizing or maximizing a real-value multivariable function by systematically choosing the values of its variables from within a set of allowed values.

Let X be the design space and $\vec{x} = [x_1, ..., x_n]^T$, $\vec{x} \in X$ be a vector of the design variables. The design space X can be continuous or discrete. Let $f(\vec{x}) : X \subseteq \mathbb{R}^n \to \mathbb{R}$ be the objective function, which we are trying to maximize or minimize.
Since

$$\arg\max_{\vec{x} \in X} f(\vec{x}) = \arg\min_{\vec{x} \in X} (-f(\vec{x})) \tag{1.1}$$

all optimization problems can be considered to be equivalent to minimization problems and then it is safe to say that the generic mathematical formulation is as follows:

$$\min_{\vec{x} \in X} f(\vec{x}), \ \vec{x} = [x_1, ..., x_n]^T \in X, \ f : X \subseteq \mathbb{R}^n \to \mathbb{R} \tag{1.2}$$

subject to:

$$g(\vec{x}) \leq 0, \ g \in \mathbb{R}^p \tag{1.3}$$

$$h(\vec{x}) = 0, \ h \in \mathbb{R}^q \tag{1.4}$$

where:

- $g(\vec{x}) = [g_1(\vec{x}), ..., g_p(\vec{x})]^T$ are the p inequality constraints
- $h(\vec{x}) = [h_1(\vec{x}), ..., h_q(\vec{x})]^T$ are the q equality constraints
- the condition that $\vec{x} \in X$, imposes limitations on the range of values that each design variable can take of the form : $x_j^L < x_j < x_j^U$, $j = 1, ..., n$ where x_j^L, x_j^U the lower and

upper limit respectively of the design variable x_j. These inequality constraints are in addition to those imposed by Eq.(1.3) but can be treated in the same way.

Every equality constraint reduces the number of design variables (dimensionality of the problem) by one and every inequality constraint reduces the size of the available search space but without altering its dimensionality.

1.2.1 Mathematical definitions

Convex Set: A set C in a real or complex vector space is said to be convex if, for all x and y in C and all t in the interval [0, 1], the point

$$\left(1 - t\right) x + t\, y \tag{1.5}$$

is in C. In other words, every point on the line segment connecting x and y is in C (see Eq.(1.5)).

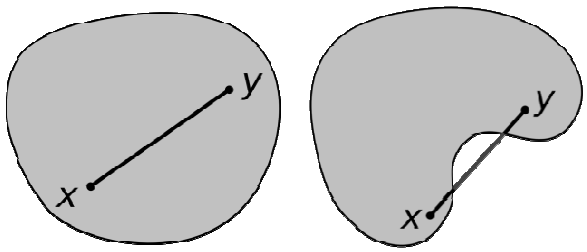

Figure 1.1 (a) convex and (b) non-convex (i.e. concave) set.

Convex Function: A real-valued function f defined on an interval (or on any convex subset of some vector space) is called convex, concave upwards, concave up or convex cup, if for any two points x and y in its domain C and any t in [0, 1],

$$f(t \cdot x + (1-t) \cdot y) \leq t \cdot f(x) + (1-t) \cdot f(y) \tag{1.6}$$

In other words, a function is convex if and only if its epigraph (the set of points lying on or above the graph) is a convex set (Figure 1.2).

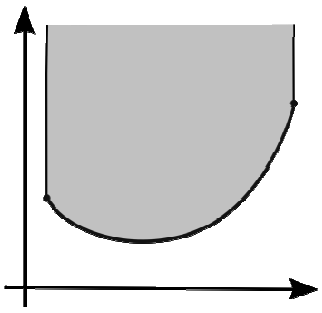

Figure 1.2 Convex function and its epigraph.

A function f is said to be ***concave*** if $-f$ is convex.

Feasible set or Feasible region: Feasible is the set F of design vectors x which satisfy the constraints of the optimization problem of Eq.(1.2). F is a subset of X

$$F = \{x \in X \mid g(x) \le 0 \mid h(x) = 0\} \tag{1.7}$$

$$F \subseteq X \tag{1.8}$$

If all constraints are convex functions and the objective is also a convex function (in minimization) or concave (in maximization) then the feasible region is also convex.

Global extrema: A real function has a global (or absolute) *maximum* point at x^* if

$$f(x^*) \ge f(x) \ \forall x \in X . \tag{1.9}$$

Similarly, a real function has a global (or absolute) *minimum* point at x^* if

$$f(x^*) \le f(x) \ \forall x \in X . \tag{1.10}$$

Local extrema: A real function has a local *maximum* point at x^* if there exists some $\varepsilon > 0$ such that

$$f(x^*) \ge f(x), \ |x - x^*| < \varepsilon, \ x \in X . \tag{1.11}$$

In other words, in a neighborhood of x^*, the size of which is determined by the value of ε, x^* acts like a global maximum.

Similarly, a real function has a local *minimum* point at x^* if there exists some $\varepsilon > 0$ such that

$$f(x^*) \le f(x), \ |x - x^*| < \varepsilon, \ x \in X . \tag{1.12}$$

Critical points (Fermat's theorem)

Let $f(\vec{x}) : A \subseteq \mathbb{R}^n \to \mathbb{R}$ be a function and suppose that $x_0 \in A$ is a local extremum of f. If f is differentiable at x_0 then $\nabla f(x_0) = 0$

The contrapositive of this statement is:

If f is differentiable at $x_0 \in A$ and $\nabla f(x_0) \neq 0$ then x_0 is not an extremum of f.

In essence this means that a local optimum can only be found where $\nabla f(x_0) = 0$.

The points $x_0 \in A$ for which $\nabla f(x_0) = 0$ holds, are called critical points.

Positive definite matrix

An $n \times n$ real symmetric matrix *M* is *positive definite* if $\vec{z}^T M \vec{z} > 0$ for all non-zero vectors z with real entries, where z^T denotes the transpose of z

Positive semi-definite matrix

An $n \times n$ real symmetric matrix *M* is *positive semi-definite* if $\vec{z}^T M \vec{z} \geq 0$ for all non-zero vectors z with real entries.

Negative definite matrix

An $n \times n$ real symmetric matrix *M* is negative *definite* if $\vec{z}^T M \vec{z} < 0$ for all non-zero vectors z with real entries.

Negative semi-definite matrix

An $n \times n$ real symmetric matrix *M* is *negative semi-definite* if $\vec{z}^T M \vec{z} \leq 0$ for all non-zero vectors z with real entries.

Second (partial) derivative test

Let $f(\vec{x}) : A \subseteq \mathbb{R}^n \to \mathbb{R}$ be a twice differentiable function and suppose that $x_0 \in A$ is a critical point of f (for critical points $\nabla f(x_0) = 0$ must hold)

If H is the Hessian matrix (square matrix of second-order partial derivatives) of f then:

- If H is positive definite at x_0 then $f(x_0)$ is a local minimum
- If H is negative definite at x_0 then $f(x_0)$ is a local maximum
- If H has both positive and negative eigenvalues then x_0 is a saddle point for f (this is true even if x is degenerate).
- Otherwise the test is inconclusive.

Quadratic Form

A quadratic form is any function $f(\vec{x}):\mathbb{R}^n \to \mathbb{R}$ of the form:

$$f(\vec{x}) = \frac{1}{2}\vec{x}^T A\vec{x} - b\vec{x} + c \tag{1.13}$$

where A is an $n \times n$ matrix, $\vec{x}$ and $\vec{b}$ are vectors of length n and c is a scalar value.

Any quadratic form with a symmetric and positive definite A will have a global minimum, and no local minima. The gradient and Hessian of the quadratic form f of Eq.(1.13) will be

$$\nabla f(\vec{x}) = A\vec{x} - \vec{b} \tag{1.14}$$

$$\nabla^2 f(\vec{x}) = A \tag{1.15}$$

The use of the present form in optimization is that finding the minimum (or maximum) any quadratic function can be equivalent to solving the system $\nabla f(\vec{x}) = A\vec{x} - \vec{b} = 0$ using any available numerical method.

1.3 Optimization algorithms

In an optimization problem, the types of mathematical relationships among the objective function, the constraints and the design variables, determine the solvability of the problem, the type of optimization algorithm that can or should be used and the confidence that the optimum solution obtained is in fact the global optimum. The linearity or not of the problem, its dimensionality, the convexity or concavity of the solution space and the continuity or not of the design space, all demand different approaches and characteristics from a method in order to locate the global optimum. The use of the right algorithm is vital in obtaining a fast and usable solution to any optimization problem.

One very basic categorization among the optimization methods is between:

- deterministic (or mathematical) methods and
- probabilistic (or stochastic) methods.

A deterministic algorithm is an algorithm whose each state is *solely* determined by the previous one and nothing else. Given a particular input, it will always produce the same output and the intermediate sequence of states will always be the same. This family of algorithms is

used in optimization for every scientific field such as mathematics, economics, logistics, etc. The search is based on the use of derivatives of the objective function or approximations thereof and basic infinitesimal calculus to locate local extrema in the objective function.

Their main advantage is that convergence is rather quick compared to the other types of methods. However, the results are not satisfactory when it comes to non-convex functions that have more than one local extrema. The final result is determined by the initial point of the optimization process and since the search is based on theorems of differentiable real functions which have local validity, these algorithms are unable to qualitatively distinguish local from global extrema and are therefore easily "trapped" in local extrema. Consequently, these algorithms perform very well for finding the global extremum in convex problems or finding fast the nearest local optimum.

On the other hand, stochastic methods insert probabilistic elements, either in the problem data (the objective function, the constraints, etc.), in the algorithm itself (random parameter values, random choices, search directions, etc.), or in both. This makes the final result independent from the initial point or points of the optimization and therefore the algorithm is less likely to be trapped in local optima. They are easier to program as they require less or no mathematical background knowledge compared to deterministic methods and can be more easily modified to be used for different problems or kinds of problems. However they lack in speed compared to deterministic algorithms.

1.3.1 Line search methods

The basic principle of an iterative line search method is in every iteration to improve the current position in the multi-dimensional solution space by taking a step of a certain length and toward a certain direction. The general formulation of every line search method can be described as follows:

$$\vec{x}^{n+1} = \vec{x}^{n} + a^{n} \cdot \vec{p}^{n} \tag{1.16}$$

where:

n is the number of the iteration (not an exponent)

$\vec{x}$ is the position in the solution space

a is the step size and

p is the search direction

There are many different methods in the line search family. Their basic difference lies primarily in the way that the search direction is estimated in every iteration and secondarily in the estimation of the step length. Some methods maintain a constant step size throughout all the iterations and others estimate a different one after the search direction has been selected.

The selection of a constant value for the step size may obviously the simplest but not the optimum. A small constant value for a will increase the possibility that the algorithm will eventually converge but the process will be slow, whereas with a large step size the process moves faster but convergence may not be achieved. In any case, once the search direction has been selected, there is one value for the step size which minimizes what is now a one-parameter optimization problem within the current iteration. By estimating this new step size in every iteration one can achieve the maximum gain, however this increases the computational cost since the minimization problem $\min_a f(x^n + a^n \cdot p^n)$ must be solved for a^n every time, at least to some extent. Especially in non-linear problems this can be rather time consuming while depending on the method and the way that the search direction is estimated, this process might even be unnecessary or harmful to convergence.

The most commonly used methods of this family are the steepest descent method, the Newton method, many of the latter's variations (quasi-Newton) such as the BFGS, the method of conjugate gradients, etc.

Steepest descent method

In the steepest descent method, the search direction of Eq.(1.16) is selected to be that of the most rapid decrease of the objective function. This can be easily proved to be the negative gradient of the objective function in the current position, i.e.

$$\vec{p}^n = -\nabla f(\vec{x}^n) = -\left(\frac{\partial f}{\partial x_1}, \frac{\partial f}{\partial x_2}, ..., \frac{\partial f}{\partial x_n} \right) \tag{1.17}$$

This means that in each iteration it is necessary to calculate the first derivative of the objective function and that the search direction of every iteration is orthogonal to the contour lines of the minimization function.

This method can be used for spaces of any number of dimensions, even in infinite-dimensional ones. In the latter case the search space is typically a function space, and one calculates the Gâteaux derivative of the functional to be minimized to determine the descent direction.

The weaknesses of the algorithm include that every search direction is orthogonal to the previous one which does not inhibit the algorithm from searching the same directions more than once. Therefore, it can take a lot of iterations to converge towards a local minimum if the curvature of the function in different directions is very different and in that case the method appears to be moving in "zigzag". Moreover, finding the optimal step size can be time-consuming, especially for non-linear problems, whereas using a fixed step size can yield poor results.

1. *Initialization*: Initialize $\vec{x}^0$, a^0, $n=0$
2. *Find search direction*: Calculate $\vec{p}^n = \frac{-\nabla f(\vec{x}^n)}{\left\|\nabla f(\vec{x}^n)\right\|}$. If $\left\|\nabla f(\vec{x}^n)\right\| \le \varepsilon$, stop
3. *New solution:* $\vec{x}^{n+1} = \vec{x}^n + a^n \cdot \vec{p}^n$
4. *Check new Solution:* - *If* $f(\vec{x}^{n+1}) = f_{n+1} \ge f_n$, reduce a^n and Go to step 3

   - *If* $f(\vec{x}^{n+1}) = f_{n+1} < f_n$, $n = n+1$ and Go to step 2

Figure 1.3: Algorithmic steps of a basic steepest descend method.

Alternatively, the step size a^n can be explicitly calculated in every iteration instead of manually selected and modified. The minimization problem $\min_a f(x^n + a^n \cdot p^n)$ must be solved for a^n (step 2b) and is then inserted in the formula of step 3 of Figure 1.3. This produces a greater need for calculations within each iteration but a smaller number of iterations is needed. In that case the 4th step of the algorithm is redundant.

Newton method

Newton's method assumes that the minimization function can be locally approximated as a quadratic Taylor expansion in the region around the optimum, and uses the first and second derivatives to find the critical point. For $a=1$ the approximation can be written:

$$f(\vec{x}^n + \vec{p}^n) \approx f(\vec{x}^n) + \vec{p}^{n^T} \cdot \nabla f(\vec{x}^n) + \frac{1}{2} \cdot \vec{p}^{n^T} \cdot \nabla^2 f(\vec{x}^n) \cdot \vec{p}^n \qquad (1.18)$$

In order to find a local optimum the first derivative of $f(\vec{x}^n + \vec{p}^n)$ must be equal to zero and therefore:

$$\frac{\partial f(\vec{x}^n + \vec{p}^n)}{\partial \vec{p}^n} = \nabla f(\vec{x}^n) + \nabla^2 f(\vec{x}^n) \cdot \vec{p}^n = 0 \tag{1.19}$$

This means that as long as $\nabla^2 F(\vec{x}^n)$ (*Hessian matrix*) is positive definite it can be inversed and the search direction can be calculated as follows:

$$\vec{p}^n = -\left(\nabla^2 f(\vec{x}^n)\right)^{-1} \nabla f(\vec{x}^n) = -\left(B^n\right)^{-1} \nabla f(\vec{x}^n) \tag{1.20}$$

The fact that the Hessian matrix, which contains second derivatives of the objective function, is needed increases the computational cost of this method. The step size is of secondary importance in this method and should be selected to be $a = 1$ unless the reduction in the objective function value is not large enough, in which case it should be properly adjusted to a smaller value.

Quasi-Newton methods

In quasi-Newton methods the Hessian matrix of second derivatives of the function to be minimized (matrix B^n in Eq. (1.20)) does not need to be computed at any stage. The Hessian is updated by analyzing successive gradient vectors instead. Quasi-Newton methods are a generalization of the secant method to find the root of the first derivative for multidimensional problems. In multi-dimensions the secant equation is under-determined, and quasi-Newton methods differ in how they constrain the solution.

The BFGS method is one of the most popular members of this class and it was named by the initials of the researchers who first proposed it (Broyden, Fletcher, Goldfarb, Shanno). The new approximated Hessian to be used in Eq.(1.20) in order to find the new search direction for this method has to be symmetric and positive definite and is proposed to be:

$$B^{n+1} = B^n + \frac{B^n \vec{s}^n \vec{s}^{n^T} B^n}{\vec{s}^{n^T} B^n \vec{s}^n} + \frac{\vec{y}^n \vec{y}^{n^T}}{\vec{y}^{n^T} \vec{s}^n} \tag{1.21}$$

As long as B^0 is symmetric, so are all the produced matrices. For the creation of B^n two methods are generally effective. Either the actual Hessian matrix can be used or an identity matrix multiplied by a scalar factor. If Eq.(1.21) is used to produce the matrix B^{n+1}, that matrix must then be inversed to be applied in the form of Eq. (1.20). Instead, another calculation can be used in order to produce the inverse matrix in one step.:

$$H^{n+1} = \left(I - \vec{r}^{\,n}\vec{s}^{\,n}\vec{y}^{\,n^T}\right) H^n \left(I - \vec{r}^{\,n}\vec{y}^{\,n}\vec{s}^{\,n^T}\right) + \vec{r}^{\,n}\vec{s}^{\,n}\vec{s}^{\,n^T} \tag{1.22}$$

where:

$$\vec{s}^{\,n} = \vec{x}^{\,n+1} - \vec{x}^{\,n} \tag{1.23}$$

$$\vec{y}^{\,n} = \nabla f(\vec{x}^{\,n+1}) - \nabla f(\vec{x}^{\,n}) \tag{1.24}$$

$$\vec{r}^{\,n} = \frac{1}{\vec{y}^{\,n^T}\vec{s}^{\,n}} \tag{1.25}$$

The basic algorithmic steps of the BFGS method are summarized in Figure 1.4

1. *Initialization*: Initialize $\vec{x}^{\,0}$, H^0, $n=0$, $\varepsilon > 0$
2. *Find search direction*: Calculate $\vec{p}^{\,n} = -H^n \cdot \nabla f(\vec{x}^{\,n})$. If $\left\|\nabla f(\vec{x}^{\,n})\right\| \le \varepsilon$, stop
3. *Find step size: Calculate* a^n *(according to Wolfe conditions)*
4. *New solution:* $\vec{x}^{\,n+1} = \vec{x}^{\,n} + a^n \cdot \vec{p}^{\,n}$, $n = n+1$
5. Intermediate calculations: $\vec{s}^{\,n} = \vec{x}^{\,n+1} - \vec{x}^{\,n}$, $\vec{y}^{\,n} = \nabla f(\vec{x}^{\,n+1}) - \nabla f(\vec{x}^{\,n})$, $\vec{r}^{\,n} = \frac{1}{\vec{y}^{\,n^T}\vec{s}^{\,n}}$
6. Hessian matrix: $H^{n+1} = \left(I - \vec{r}^{\,n}\vec{s}^{\,n}\vec{y}^{\,n^T}\right) H^n \left(I - \vec{r}^{\,n}\vec{y}^{\,n}\vec{s}^{\,n^T}\right) + \vec{r}^{\,n}\vec{s}^{\,n}\vec{s}^{\,n^T}$
7. Update and loop: $n = n+1$. Go to step 2

Figure 1.4 Algorithmic steps of a basic BFGS method.

1.3.2 Evolutionary Algorithms (EAs)

Evolutionary Algorithms are probably the most important member of stochastic methods. They have been used with great success in a wide area of scientific fields such as engineering, biology, economics, operations research, etc. EAs are based on the model of natural evolution as proposed by Charles Darwin. They are categorized as *heuristic* algorithms, from the Greek work "ευρίσκω" which means "find", in the sense no mathematical proof can be provided that such a process provides better solutions, although better solutions are indeed produced. The theory and its implementation include imitations of biological processes such as natural selection, adaptation and survival of the fittest. An initial population of individuals, each one

representing a candidate solution, undergoes a series of evaluations and recombinations, gradually evolving to an optimum (see also section 1.3.3).

The main features of EAs involve the lack of need for derivatives and the random selection of the design variables vector. Most mathematical methods conduct their search by calculating the gradient of the objective function and moving towards the direction of decreasing values. In EAs each member of the population which is a candidate solution for the optimization problem, is directly tested on the fitness function. In the case of large-scale and highly non-linear problems such as those encountered in structural optimization or many other areas, the calculation of the gradient is a rather time consuming process. EAs, by circumventing this need, are able to significantly expedite each iteration. The progress of the algorithm comes through genetic operations on the population rather than mathematical ones. Therefore the search occurs in many directions at the same time. Moreover, as the initial population is also random in addition to scattered, almost the entire design space is explored and the process is much less likely to be trapped in a local extremum compared to deterministic methods. Thus, even though a larger amount of iterations is needed, since the population is scattered all across the design space and the search is performed in random directions, the optimization is often faster. However, there is no certainty that the solution obtained is in fact the global optimum. The rate of convergence is very high during the initial iterations and becomes very low when close to the optimum.

The above attributes make the EAs more suitable for non-convex problems or highly nonlinear ones. The two most popular and widely used Evolutionary Algorithms are the Genetic Algorithm (GA) and Evolution Strategies (ES). Both GAs and ES imitate biological evolution in nature and have some common characteristics that make them differ from other conventional optimization algorithms. Instead of a single design point, they work simultaneously with a population of design points in the space of design variables. This characteristic allows for a natural implementation on parallel computing environments which can significantly reduce the computational cost of the methodology. Moreover, in place of the usual deterministic operators, they use randomized operators such as mutation, selection and recombination, while they can also handle with minor modifications, continuous, discrete or mixed optimization problems.

1.3.3 Genetic Algorithm (GA)

Genetic algorithms are based on Darwin's theory of adaptation to the environment and natural selection through the survival of the fittest. According to this theory, in the course of evolution, species slowly adapt to their surroundings. Traits that can be beneficial to an organism and can provide a genetic advantage in their struggle for survival are becoming more predominant in a population while on the other hand, traits that do not provide an advantage are slowly becoming extinct.

In natural biological environments, the individuals in a population are always competing against each other for food and other resources. The fittest individuals are the most successful and are primarily selected for reproduction, which usually includes mixing genetic material in order to produce an offspring who shares common characteristics with both parents. Apart from those hereditary characteristics in an offspring, from time to time, there exists a small probability that a completely new characteristic will appear in place of an old one in a random process of mutation. The combination of genetic characteristics of the parents along with the small probability of mutation due to outside random factors, ensure the creation of a new generation with better or worse characteristics which will once become parents of their own. This continuing process leads to improved individuals within the population or in this case of a computer implemented genetic algorithm, better solutions to an optimization problem.

The creation of a computer implemented GA started in the early 60's by a group of biologists (Barricelli 1962; Fraser 1962; Martin and Cockerham 1960) but their current form is attributed to John Holland along with his colleagues and students in Michigan University in the mid 70's (Holland 1975). In the last few years, these types of algorithms have been improved and have proven to be rather reliable and successful in a wide range of science fields (Groves et al. 1990; Michalewicz et al 1991; Smith 1980; Carrol 1996) including computational mechanics (Galante 1996; Nagendra et al. 1996; Ohsaki 1995; Adeli and Kumar 1995; Ghasemi and Hinton 1996; Shyue-Jian Wu and Chow 1995), and in many different types of optimization problems, single or multi-objective. If fact they have proven themselves to be better than gradient based methods or other stochastic methods in locating the global optimum (Grefenstette 1990; Chen and Chen 1997; Lagaros et al. 1998).

The terminology used in GAs is borrowed from biology. Each candidate solution to an optimization problem is called an *individual*, *creature* or *phenotype* and their abstract representations are called *chromosomes* or the *genotype* of the *genome*. The chromosome is

consisted of *genes*, which represent the design variables and are located in specific positions within the chromosome called *loci*. The specific condition or value of each *gene* is called an *allele*.

The GAs operate on a population of candidate solutions which evolve toward an optimum solution. First, the initial population is generated (usually randomly) and then every member of the initial population is encoded in a binary string (chromosome). The size of the randomly selected initial population depends on the nature of the problem and its formulation, namely the number of design variables and the range of the values they can take, translated in the average bit length of the genes. The members are evaluated and ranked amongst them by the objective function, based on their fitness. The fittest individuals have increased probabilities of being selected to become the parents for the next generation. After the selection, the genetic operators of crossover and mutation are applied and the new generation is created. The same procedure is repeated for the next population until an optimum solution is obtained.

Encoding

The *chromosomes* carry the encoded information using fixed-length binary character strings, much like actual chromosomes carry encoded genetic information. Each string is divided into *n* (number of design variables of the problem) segments, the *genes*. Each gene is the binary counterpart of the real value variable in an individual. It is common practice to use Grey encoding instead of the standard binary encoding. The reason is that with Grey encoding, the neighboring real values represented, differ by only one bit and therefore slight changes in the binary string represent slight changes of the real value variable.

The bit length of all the genes in a chromosome is not necessarily the same and is selected in accordance with the range of each variable so that all possible variable values can be represented. The number of values or states represented by a gene with *m*-number of binary bits is 2^m. When choosing the value for *m* (only natural numbers), it is obvious that the step sizes between 2^m and 2^{m+1} can be rather large for high values of *m*. In the event that the possible binary values are more than the actual values that need to be encoded, the extra binary values can be handled in a number of ways (Lin and Hajela 1992). These extra binary values could represent real values outside the allowable range of the variables. In such case, when the fitness of an individual that contains such a value is calculated, some kind of penalty is imposed and that individual is ranked poorly in order to be disqualified in the selection stage.

Other techniques dictate that some real values are represented by more than one binary value or that the real values are increased in number so as to be equal to the binary ones.

Fitness Evaluation

The objective function of the problem is also called the fitness function. In structural optimization problems the fitness function is usually the weight of the structure. Each member of the population is evaluated and awarded a fitness value. Along with the fitness evaluation, the constraints and the feasibility of the solution must also be checked. This requires a complete structural analysis of the problem under the selected design variables, followed by the examination of constraint violations. In case of infeasible designs and constraint violations, the fitness value of the corresponding candidate solution must somehow receive a penalty in order to reflect the violation (see also section **1.4**). The fact that each member is evaluated independently allows for parallel implementation of the algorithm, dividing the computational cost and speeding up the optimization process.

The penalized fitness of each individual is normalized by the sum of penalized fitness values of the whole population and can provide a measure of the quality of each candidate solution compared to the rest of the population. Better solutions within the same population have a higher probability of becoming parents for the next generation.

Selection

The selection of members that will become parents and will breed the next generation can occur through a number of different proposed schemes. Most commonly used are the *Tournament* selection, *Ranking* selection and *Proportionate* selection. According to the *Tournament* selection scheme, the population is randomly divided into a number of subgroups and the best candidate from within each subgroup, based on its fitness, is selected to become a parent. According to the *Ranking* selection scheme, the solutions are ranked in an ascending order based on their fitness (best being last in the list). The probability of a solution to be picked is proportionate to its position on the list (lower in the list higher probability). The most common *Proportionate* selection scheme is the *Roulette Wheel*. Each solution is assigned a probability equal to its normalized fitness value on a pie chart or roulette wheel. A random number generator “spins the wheel” and a member is selected to become a parent.

It is possible for the best members of the population to be exempt from the selection and reproduction process and pass to the next generation unchanged. This technique is called

elitism and often increases the performance of the algorithm by ensuring that the best members and their best qualities are not lost or altered in the random processes of selection and reproduction.

After the selection, the chromosomes have to be combined in order to produce the next generation of candidate solutions. This is achieved through the genetic operators of *crossover* (or recombination) and *mutation*.

Crossover

The crossover operator acts with a set probability p_c on the selected parent chromosomes and combines parts of them to produce a new chromosome. This combination can occur in a number of different patterns.

In *one-point* crossover, a crossover point is randomly selected within a chromosome and the remaining binary string is interchanged between the two parent chromosomes producing two new offspring. Consider the following 2 parents which have been selected for crossover. The "|" symbol indicates the randomly chosen crossover point.

Parent 1: 11001|010

Parent 2: 00100|111

After interchanging the parent chromosomes at the crossover point, the following offspring are produced:

Offspring1: 11001|111

Offspring2: 00100|010

- In *two-point* crossover, two crossover points are selected instead of one and the middle part of the string is interchanged between the two parents. For example if the parents are the same as before

  Parent 1: 11|001|010

  Parent 2: 00|100|111

  After the application of the two-point crossover operator the following offspring are produced:

  Offspring1: 11|100|010

  Offspring2: 2: 00|001|111

- In *uniform* crossover, the bit strings of the parents' chromosomes are compared on a bit-by-bit level. The individual bits which are common for the same loci on both parents are passed on directly to the offspring. For the bits that differ between the two parents, there is a probability *p* (called mixing ratio), for each bit, that it comes from one parent and *(1-p)* that it comes from the other. Usually *p*=0.5 and consequently, half the genes come from each parent.

- *Arithmetic* crossover produces offspring that are linear combinations of their parents' vectors.

$$Offspring1 = a * Parent1 + (1- a) * Parent2$$

$$Offspring2 = (1 - a) * Parent1 + a * Parent2$$

  where a is a random weighting factor (chosen before each crossover operation).
  For example if we consider the following 2 parents which have been selected for crossover:

$$Parent\ 1: (0.2)(2.1)(0.5)(7.6)$$

$$Parent\ 2: (0.1)(3.7)(1.0)(3.3)$$

  If a = 0.7, the following two offspring would be produced:

$$Offspring1: (0.17)(2.58)(0.65)(6.31)$$

$$Offspring2: (0.13)(3.22)(085)(4.59)$$

  The offspring produced this way is always feasible in convex problems as it lies on the line segment between the two parents.

- The *heuristic* crossover operator uses the fitness values of the two parent chromosomes to determine the direction of the search and moves outside the range of the two, in the direction that the fitness is improved. The offspring are created according to the following equations:

$$Offspring1 = BestParent + R * (BestParent - WorstParent)$$

$$Offspring2 = BestParent$$

  where *R* is a random number between 0 and 1.

  With this operator, it is possible that *Offspring1* will not be feasible. This can happen if *R* is chosen such that one or more of its genes fall outside of the allowable upper or lower variable bounds.

Mutation

Mutation inserts a small probability p_m (usually less than 1% or 1/pop_size for large populations (Goldberg 1989)) that a single binary bit in a given chromosome will be changed from its initial value. The result will be the creation of a different chromosome that may or may not (jump mutation) be similar to any other chromosome of the population. This process maintains a genetic diversity from one generation to the next and enables the algorithm to avoid local extrema in case the chromosomes of the population evolve to become too similar to one another.

Termination

The termination of the algorithm can occur for a number of user defined reasons such as a minimum criterion (value) reached by the solution obtained, a fixed number of generations exceeded, a fixed number of objective function evaluations executed, improvement of the best solution by less than a given threshold value for a number of generations, improvement of the mean fitness value of the population by less than a given threshold value for a number of generations, etc

In conclusion the basic GA can be summarized in individual steps as follows in Figure 1.5:

1. *Initialization*: Random generation of an initial population of candidate solutions and encoding in chromosomes.
2. *Analysis and Evaluation*: The candidate solutions are evaluated by the fitness function.
3. *Selection*: Members of the population are selected to be the parents for the next generation.
4. *Genetic Operators:* Crossover and Mutation operators are applied to create the next generation.
5. *Analysis and Evaluation:* The new generation is evaluated by the fitness function.
6. *Termination Criteria:* If any one of the termination criteria is reached stop, else go back to step 3.

Figure 1.5 Algorithmic steps of a basic GA.

Holland's schema theorem

No strict mathematical proof can be provided that the methodology of the genetic algorithms will work and that the initial population will eventually locate the optimum solution. In fact, this is the reason why the whole class of population-based algorithms is called *heuristic*. However, John Holland, who first proposed the GA as an optimization technique (Holland 1975), provides an explanation why this method can indeed be used in order to drive the process towards better solutions through the *schemata theorem*

As it was described previously, every chromosome is encoded in a fixed-length binary string of, say, *m*-number of bits. Consider that each individual binary bit can also receive in addition to the fixed values of 1 or 0 the value of *. This value represents a wild card of sorts and can be interpreted as either one of the other two fixed binary values of 1 or 0. Therefore the binary string or *schema* of S =*100*1 can represent the strings of 010001, 010011, 110001 and 110011. In general, it is obvious that a schema with *r*-number *of* non-fixed or wild card bits represents 2^r strings and a string with *k*-number of bits can belong to 2^k different schemata.

The *defining length, d(*S*)* of the schema is defined as the distance between the first and last fixed-value bits of the string. For the previously mentioned schema S, the defining length is *d(*S*)*=6-2=4 (counting the positions of the bits from left to right) or alternatively *d(*S*)* = 5-1=4 (counting from right to left). Starting to count the positions in the string from either end does not change the result. If S' = **0*1* then *d(*S'*)* = 5-3 (left to right) = 4-2 (right to left)=2.

The *order, o(*S*)* of a schema is defined as the number bits in the schema that have a fixed value of 1 or 0. For the previous examples it is *o(*S*)=4 and o(*S'*)*=2.

The concept behind the definition of these quantities and the whole theory of schemata is to attempt to predict the representation of each of the competing schemata within a population in the following generations after the application of the genetic operators of selection, crossover and mutation. In order for the optimization to be driving forward, schemata of better fitness should be increasing their representation as the generations proceed and schemata of poor fitness should be slowly fading out.

a) Assume that, in the phase of selecting the parents, a schema S is represented in the population of generation g by $M(S,g)$ members which have an average fitness value of

$F(S,g)$. If the average fitness of the whole population in the same generation is $F(g)$ then in the next generation $g+1$ the representation of schema S should be:

$$M(S,g+1) = M(S,g) \cdot \frac{F(S,g)}{F(g)} \tag{1.26}$$

This is a linear approximation and the Eq.(1.26) is called *reproductive schema growth equation*. It is obvious that schemata for which $F(S,g) > F(g)$ are better than the average of the population and will increase their representation in the following generation while for schemata for which $F(S,g) < F(g)$ their representation will decrease.

If schema S produces members who are better than average then there exists a positive ε so that:

$$F(S,g) = F(g) + \varepsilon \cdot F(g) \tag{1.27}$$

and Eq.(1.26) can be rewritten as:

$$M(S,g+1) = M(S,g) \cdot (1+\varepsilon) \tag{1.28}$$

If this margin ε is considered to remain steady throughout the course of g generations then

$$M(S,g) = M(S,0) \cdot (1+\varepsilon)^g \tag{1.29}$$

which predicts that the representation of a schema S in the initial population due to the selection operator will increase exponentially in the course of the future generations.

b) The defining length of a schema is related with its preservation in a population after the crossover operator. As it was described previously, a number of crossover operators are available. Due to its simplicity, the one-point crossover operator will be described but the same general idea can be applied to the rest as well.

In a chromosome of *m*-number of bits, there are *(m-1)*-positions on which the one-point operator can act and cut the chromosome in two. Out of the *m-1* positions, only the *d(S)* of them can actually destroy the schema. So for a chromosome on which the one-point crossover operator is applied, the probability that the schema survives is:

$$p_{surv}(S) = 1 - \frac{d(S)}{m-1} \tag{1.30}$$

Considering that crossover is applied on a chromosome under the probability p_c the probability that a schema survives the operation is increased to:

$$p_{surv}(S) = 1 - p_c \cdot \frac{d(S)}{m-1} \tag{1.31}$$

There is also a small probability that even if the position where the one-point crossover operator is applied is such that the schema is affected, the parts of the chromosomes that are joined can still maintain the schema alive. For example, if the schema is S =*100*10* and exists in parent 1:

parent 1: 0100|1100

parent 2: 1001|0101

After the crossover, the schema though initially affected is still maintained alive in offspring 1

offspring 1: 0100|0101

offspring 2: 1001|1100

Therefore Eq.(1.31) is modified:

$$p_{surv}(S) \geq 1 - p_c \cdot \frac{d(S)}{m-1} \tag{1.32}$$

If Eq.(1.26) and (1.31) are combined, the reproduction of a schema after the selection and crossover operators becomes:

$$M(S, g+1) \geq M(S, g) \cdot \frac{F(S, g)}{F(g)} \cdot \left(1 - p_c \cdot \frac{d(S)}{m-1}\right) \tag{1.33}$$

c) The survival of a schema after the operator of mutation is in correlation with the order of the schema. It is obvious that only if the mutation happens in a non-fixed bit of the schema, can it still remain intact for the next generation. If the probability of mutation is p_m then the probability of survival is:

$$p_{surv}(S) = \left(1 - p_m\right)^{o(S)} \approx 1 - o(S) \cdot p_m \tag{1.34}$$

Combining the above probability for mutation with Eq.(1.33), the reproduction of a schema after the selection, crossover and mutation operators becomes:

$$M(S, g+1) \geq M(S, g) \cdot \frac{F(S, g)}{F(g)} \cdot \left(1 - p_c \cdot \frac{d(S)}{m-1} - o(S) \cdot p_m\right) \tag{1.35}$$

In interpretation of Eq.(1.35), it can be concluded that schemata with a small defining length and low order with above average fitness receive an exponential increase of representation in a population through the next generations. In other words, the final solution is comprised of fundamental blocks of small size and low order (building blocks hypothesis).

1.3.4 Evolution Strategies (ES)

Sharing a number of similarities with the Genetic Algorithm, Evolution Strategy is also a direct search optimization method in the class of Evolutionary Algorithms. ES use mutation, recombination and selection applied to a population of individuals containing candidate solutions in order to evolve iteratively better and better solutions. Evolution Strategies can be applied for single or multi-objective targets in all fields of optimization including continuous, discrete, combinatorial search spaces, with and without constraints as well as mixed search spaces. The objective function, also called *goal* function can be presented in mathematical form, via simulations, or even in terms of measurements obtained from real objects.

The basic concept of ES begins with the creation of an initial population of feasible candidates. The feasibility is ensured by evaluating the initial population and modifying the infeasible designs until they become feasible. Then the application of a mutation operator is performed on that population. Usually, in real-value search spaces, mutation is achieved by adding a normally distributed random value to each vector component. This value can be common for all components or can be calculated individually for each one. The step size or *mutation strength* (i.e. the standard deviation of the normal distribution) has to be small in general, and is governed by self-adaptation or by covariance matrix adaptation (CMA-ES).

The canonical versions of the ES are denoted by:

$$(\mu/\rho\,,\lambda)\text{-}ES \quad \text{and} \quad (\mu/\rho\,+\lambda)\text{-}ES,$$

where μ denotes the number of parents, $\rho \leq \mu$ the mixing number (i.e. the number of parents involved in the procreation of an offspring), and λ the number of offspring.

The parents are *deterministically* selected from the set of either only the λ offspring, referred to as *comma-selection* ($\mu < \lambda$ must still hold), or the set of parents and offspring ($\mu+\lambda$), referred to as *plus-selection*. Selection of the next μ parents is based on the fitness rankings within the current population and not the actual fitness values. It is obvious that in the comma-type selection, the existence of each individual is limited to one generation. This allows the ($\mu/\rho\,,\lambda$)-

ES selection to perform better on problems with an optimum moving over time, or on problems where the objective function is noisy.

For continuous optimization problems, the procedure can terminate when one of the following termination criteria is satisfied:

i. The absolute or relative difference between the best and the worst objective function values is less than a given threshold value

ii. The mean value of the objective values from all parent vectors in the last 2n generations has not improved by less than a given threshold value.

To summarize, the basic ES algorithmic steps can be written as follows in Figure 1.6:

1. *Initialization:* Selection of μ parent vectors of the design variables.
2. *Analysis and Evaluation:* Evaluation of the parents by the fitness function.
3. *Feasibility Check:* If not all parents are feasible, modification of infeasible parents and go back to step 2.
4. *Genetic Operators:* Mutation of all members and crossover every ρ parents to produce λ offspring.
5. *Analysis and Evaluation:* Evaluation of the offspring by the fitness function.
6. *Feasibility Check:* If not all offspring are feasible, discard infeasible offspring and go back to step 4.
7. *Parents Selection:* Selection of the next generation parents according to $(\mu/\rho+\lambda)$ or $(\mu/\rho, \lambda)$ selection schemes
8. *Termination Criteria:* If any one of the termination criteria is reached stop, else go back to step 4.

Figure 1.6 Algorithmic steps of a basic ES.

From what has been described in the previous sections, some differences between GAs and ES can be observed. The numerical representation of the design variables of the problem differs in these two algorithms. The basic GA operates on fixed-sized binary strings representing the real values of the design variables whereas ES work directly on real-valued vectors. Another difference can be found in the use of the genetic operators. Although, both GA and ES use the mutation and recombination (crossover) operators, the role of these genetic operators in each method is different. In GAs mutation is a secondary procedure to crossover. It affects a small number of alleles in the whole population and only serves to slightly diversify the genetic pool

in order to avoid entrapment in local extrema. Crossover is mainly responsible for finding the optimum solution by combining parts of the members of the population, in a way that could be likened to building the solution from individual independent blocks. In ES, on the other hand, mutation is more radical. It affects all the design variables at once and is the primary force that drives the optimization forward and separates one generation from the next. Crossover then takes on and multiplies the number of mutated candidate solutions. Furthermore, in ES the selection process for members that pass to the next generation is deterministic and only the fittest of each population carry on to the next. In GAs every member of the population has a probability to pass to the next generation and this probability increases according to its fitness. The selection process conducted among the candidates is probabilistic.

1.4 Constraint Handling Techniques

The generic single-objective optimization problem as it was presented previously in section 1.2 is subject to a number of equality and/or inequality constraints. These constraints impose limitations to the values that the design variables can take and limit the available search space in which the optimum solution can be searched and found. In general, different optimization methods handle constraints in different ways. Gradient-based optimization methods cannot handle directly inequality constraints while on the other hand, methods such as the GA need the allowable interval of each design variable in order to initialize the population of candidate solutions.

Constraint handling techniques are available which formulate the constraints of the problem in a way that they are incorporated in the objective function (e.g Lagrange Multipliers, Kuhn-Tucker conditions, Augmented Lagrange Multipliers, etc). The new equivalent unconstrained problem can be solved instead by methods which can handle unconstrained problems.

In the present work the penalty method will be used for handling the constraints of the problem. Any optimization method which can be used for unconstrained optimization problems can also work with the penalty method, as the constrained optimization problem is replaced by a series of unconstrained problems whose solutions ideally converge to the solution of the original constrained problem. The unconstrained problems are formed by adding a term to the objective function that consists of a penalty parameter and a measure of violation of the constraints.

Three degrees of penalty functions exist: barrier methods in which no infeasible solution is considered, partial penalty functions in which a penalty is applied near the feasibility boundary, and global penalty functions which are applied throughout the infeasible region (Schwefel 1995).

In general, a penalty function approach is as follows: Given an optimization problem,

$$\min f(x) \tag{P}$$

subject to

$$x \in A$$
$$x \in B$$

where:

x is the vector of design variables, constraints A are relatively easy to satisfy and constraints B . are relatively difficult to satisfy, the optimization problem can be reformulated as follows:

$$\min \left[f(x) + p(d(x,B)) \right] \tag{R}$$

subject to

$$x \in A$$

where $d(x,B)$ is a metric function describing the distance of the solution vector from the region B , and $p(\cdot)$ is a monotonically non-decreasing penalty function such that $p(0) = 0$. If the exterior penalty function, $p(\cdot)$, grows quickly enough outside of B , the optimal solution of (P) will also be optimal for (R). Furthermore, any optimal solution of (R) will provide an upper bound on the optimum for (P), and this bound will in general be tighter than the one obtained by simply optimizing $f(x)$ over A. In practice, the constraints $x \in B$ are expressed in the forms of Eq.(1.3) and (1.4).

Different possible distance metrics, $d(\cdot)$, include a count of the number of violated constraints, the Euclidean distance between x and B as suggested by Richardson et al. (1989), a linear sum of the individual constraint violations or a sum of the individual constraint violations raised to an exponent, k .

It can be difficult to find a penalty function which is an effective and efficient surrogate for the missing constraints. The effort required to tune the penalty function to a given problem

instance or repeatedly calculate it during search may negate any gains in eventual solution quality. As noted by Siedlecki and Sklansky (1989), much of the difficulty arises because the optimal solution will frequently lie on the boundary of the feasible region and thus many of the solutions similar to the optimum will be infeasible. Therefore, restricting the search to only feasible solutions or imposing very severe penalties makes it difficult to find the schemata that will drive the population toward the optimum as shown in the research of (Smith and Tate 1993, Anderson and Ferris 1994, Coit et al. 1995, Michalewicz 1995). Conversely, if the penalty is not severe enough, then too large a region is searched and much of the search time will be used to explore regions far from the feasible region.

Static penalty functions

A simple method for penalizing infeasible solutions is to apply a constant penalty to those solutions which violate feasibility in any way. The penalized objective function would then be the unpenalized objective function plus a penalty (for a minimization problem). A variation on this simple penalty function is to add a metric based on number of constraints violated, where there are multiple constraints. The penalty function for a problem with m constraints would then be as below (for a minimization problem):

$$f_p(x) = f(x) + \sum_i c_i \delta_i \tag{1.36}$$

where

$\delta_i = 1$, if constraint i is violated

$\delta_i = 0$, if constraint i is satisfied

$f_p(x)$ is the penalized objective function,

$f(x)$ is the unpenalized objective function,

c_i is a constant imposed for violation of constraint i and

i is the number of $p+q$ constraints of Eq.(1.3) and (1.4).

This penalty function is based only on the number of constraints violated, and is generally inferior to an approach based on some distance metric from the feasible region (Goldberg 1989, Richardson et al. 1989).

A more sophisticated and more effective penalty includes a distance metric for each constraint, and adds a penalty which becomes more severe with distance from feasibility. Distance metrics can be continuous (Juliff 1993) or discrete (Patton et al. 1995), and could be linear or non-linear (Le Riche et al. 1995).

Dynamic penalty functions

The primary deficiency with static penalty functions is the inability of the user to determine criteria for the c_i coefficients. Moreover, the exploration of the infeasible region may prove to be beneficial at times, yet the final solution must be feasible. Many of these difficulties can be alleviated if a dynamic aspect which (generally) increases the severity of the penalty for a given distance as the search progresses is incorporated, as a variation of distance based penalty function. This scheme has the property of allowing highly infeasible solutions early in the search, while by gradually increasing the penalty imposed, the final solution is coerced to eventually move into the feasible region. A general form of a distance based penalty method incorporating a dynamic aspect based on the length of search t, is as follows for a minimization problem:

$$f_p(x,t) = f(x) + \sum_i s_i(t) d_i^k \tag{1.37}$$

where $s_i(t)$ is a monotonically non-decreasing in value with t. Metrics for t include number of generations or the number of solutions searched. If $s_i(t)$ is too lenient, the resulting final solution may be infeasible and if $s_i(t)$ is too severe, the search may converge to non-optimal feasible solutions. Therefore, these penalty functions typically require problem specific tuning to perform well. Joines and Houck (1994) propose that,

$$s_i(t) = (c_i t)^a \tag{1.38}$$

where a is a constant equal to 1 or 2.

Adaptive Penalty Functions

While incorporating distance together with the length of the search into the penalty function has been generally effective, these penalties ignore any other aspects of the search. In this respect, they are not adaptive to the ongoing success (or lack thereof) of the search and cannot guide the search to particularly attractive regions or away from unattractive regions based on what has already been observed. A few authors have proposed making use of such search

specific information. Siedlecki and Sklansky (1989) discuss the possibility of self-adapting penalty functions, but their method is restricted to binary-string encodings with a single constraint, and involves considerable computational overhead.

Bean and Hadj-Alouane (1992) and Hadj-Alouane and Bean (1992) propose penalty functions which are revised based on the feasibility or infeasibility of the best penalized solution during recent generations. Smith and Tate (1993) and Tate and Smith (1995) used both search length and constraint severity feedback in their penalty function which was enhanced by the work of Coit et al. (1995). This penalty function involves the estimation of a near-feasible threshold (NFT) for each constraint. Conceptually, the NFT is the threshold distance from the feasible region at which the user would consider the search as "getting warm." The penalty function encourages the evolutionary algorithm to explore within the feasible region and the NFT-neighborhood of the feasible region, and discourage search beyond that threshold.

Chapter 2

2 Vehicle Dynamics

2.1 Introduction to vehicle dynamics

A vehicle is most often a man-made device that is designed or used to transport people or cargo. Vehicles come in many different forms and types and can be categorized according to a number of factors some of which are the terrain they move upon (land, air, water, snow, etc), their power source (fuels, such as petroleum or diesel, nuclear power, wind, waves, batteries, electrical power, solar energy, gravity, human or animal power, etc), the means they use to permit or ease movement (wheels, hulls, wings, rotors, jets or cushions of air, etc) and many others.

In the field of physics, *dynamics* is the branch which studies of the causes of motion and changes in motion. Combined with *kinematics,* which describes the motion of objects without consideration of the causes leading to it, they compose the branch of *classical mechanics*. Generally speaking, dynamics is the study of how physical systems might develop or alter over time and what their relationship with the causes of those changes is. The foundation of modern day dynamics is Newtonian mechanics and the basic elements used in the analysis are the generalized forces (including torques) acting on the bodies, the elemental properties of the bodies, particularly mass and moment of inertia, and the motion of the examined bodies measured by differences in their position, velocity or acceleration.

So, the subject of "vehicle dynamics" is concerned with the movements of vehicles and parts thereof and the forces responsible for them. Said movements include the acceleration and braking, ride, and turning of the vehicle among others. Vehicle dynamics in the broadest sense encompasses all the forms of vehicles - ships, airplanes, railroad trains, rubber-tired vehicles,

hovercrafts and so many others. Obviously the principles involved in the dynamics of these many types of vehicles are very diverse and extensive. Since the performance and movement of a vehicle is a response to the forces imposed on it, the study of vehicle dynamics must involve the study of how and why the forces are produced. Depending on the particular vehicle, the forces acting on it may be developed by fluid movement - water or air, by metal tires against rails or rubber tires against the road. In the following sections it will be attempted to present the most important types of forces acting on a motor vehicle and their origins.

2.2 Coordinate systems and movement

Two types of coordinate systems are used to describe the full range of motion of a vehicle and its components. The first one is fixed on the vehicle and the other is fixed on the earth.

By the *Vehicle Fixed Coordinate System (body frame - S)*, the vehicle's motions are defined with reference to a right-hand orthogonal coordinate system which originates at the vehicle's center of gravity (CG) and travels along with the vehicle. By SAE and ISO convention the axes of reference for the movement are (see Figure 2.1):

x - Forward and on the longitudinal plane of symmetry

y - Lateral out the left side of the vehicle

z - Upward with respect to the vehicle

p - Roll velocity about the x axis

q - Pitch velocity about the y axis

r - Yaw velocity about the z axis

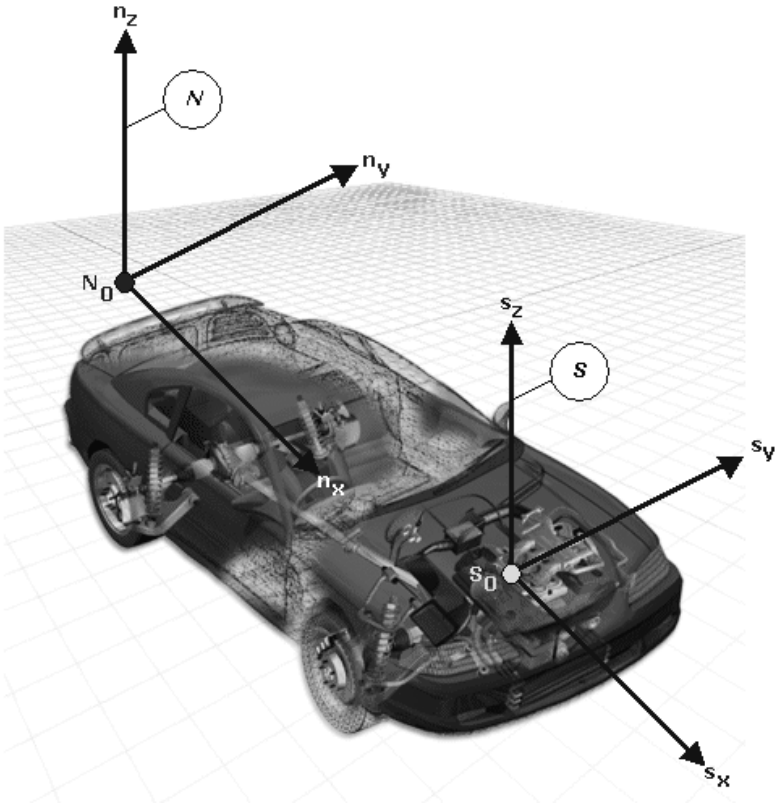

Figure 2.1 ISO and SAE Vehicle-fixed (S) and Earth-fixed (N) axis coordinate systems.

Vehicle motion is usually described by the velocities (forward, lateral, vertical, roll, pitch and yaw) with respect to the vehicle fixed coordinate system, where the velocities are referenced to the earth fixed coordinate system.

Vehicle attitude and trajectory through the course of a maneuver are defined with respect to a right-hand orthogonal axis system fixed on the earth. It is normally selected to coincide with the vehicle fixed coordinate system at the point where the maneuver is started. By the *Earth Fixed Coordinate System (world frame - N) t*he coordinates (see Figure 2.2) are:

X - Forward travel

Y - Travel to the right

Z - Vertical travel (positive downward)

ψ - Heading angle (angle between x and X in the ground plane)

v - Course angle (angle between the vehicle's velocity vector and X axis)

β - Sideslip angle (angle between x axis and the vehicle velocity vector)

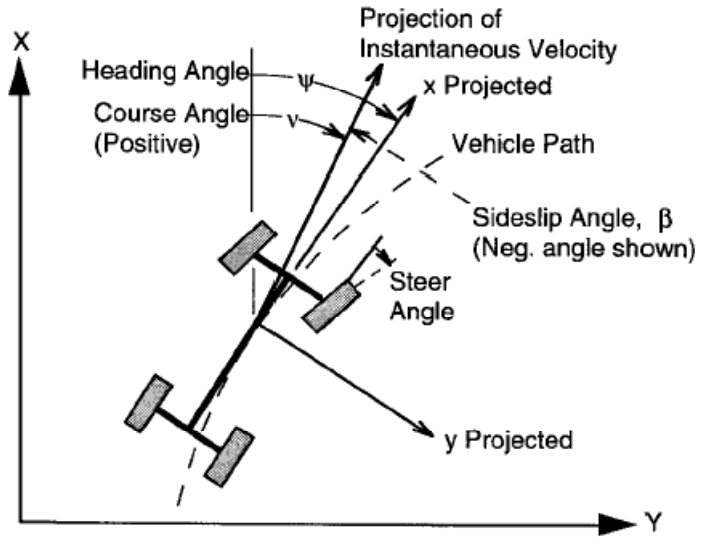

Figure 2.2 Vehicle in an Earth-fixed coordinate system

2.3 Road Loads

When a vehicle is moving and because of this movement it is susceptible to a number of loading conditions which inhibit the movement and need to be overborne in order for it to still be able to move forward and even accelerate. For a motor vehicle, as the one discussed about in the current work, the two main categories of road loads are the aerodynamic resistance and the rolling resistance.

The aerodynamic forces acting on a vehicle arise from two sources, namely the form drag and viscous friction. When a vehicle is moving through the open air, Bernoulli's principle connects velocity and pressure of the air flow around the moving vehicle. The irregularities of the shape of the vehicle alter the normal laminar flow of air, causing the air to bend around its shape and move at different velocities on different parts of the surface area of the vehicle. This generates an uneven pressure distribution on the surface of the vehicle, which in turn translates into the creation of an aerodynamic force and moment acting on the vehicle. Moreover, the friction between the air molecules and the surface of the vehicle generates a second component in the aerodynamic force affecting the vehicle. The vector sum of these forces and moments can be analyzed into components acting about the principal axes of the vehicle as shown in Table 2.1. Drag is the largest and most important aerodynamic force as it acts directly against the movement of the vehicle. Factors that influence the aerodynamic efficiency of a vehicle are the vehicle speed, the wind speed and direction, air density, the vehicle's frontal area and for the moments the wheelbase as well.

The other major vehicle resistance force is the rolling resistance of the tires. In fact, at low speeds, the rolling resistance is the primary and only significant motion resistance force. The difference from other resistances is that they act only under certain conditions of motion, while rolling resistance is present from the instant the wheels begin to turn. In addition, a large part of the power expended in a rolling wheel is converted into heat within the tire. The consequent temperature rise reduces both the abrasion resistance and the flexure fatigue strength of the tire material, and may become the limiting factor in tire performance.

There are at least seven mechanisms responsible for rolling resistance:

- Energy loss due to deflection of the tire sidewall near the contact area
- Energy loss due to deflection of the tread elements
- Scrubbing in the contact patch
- Tire slip in the longitudinal and lateral directions
- Deflection of the road surface
- Air drag on the inside and outside of the tire
- Energy loss on bumps

The most important factors affecting the tire's rolling resistance are:

- Tire Temperature
- Tire Inflation Pressure
- Velocity
- Tire Material and Design
- Tire Slip

Table 2.1 Aerodynamic force analysis

Direction	Force	Moment
Longitudinal (x-axis, positive rearward)	Drag	Roll
Lateral (y-axis positive to the right)	Side force	Pitch
Vertical (z-axis positive upward)	Lift	Yaw

2.4 Excitations

The movement of a vehicle, especially at high speeds, is responsible for causing a broad spectrum of vibrations which are transmitted through the vehicle components to the passengers onboard the vehicle. The tactile and visual vibrations are commonly referred to as “ride”, while aural vibrations are referred to as “noise”. According to their frequencies, vibrations are classified as ride when they are in the range of 0-25 Hz and as noise in the range of 25-20,000 Hz, since 25 Hz is approximately the lower frequency threshold of hearing. However, in practice, these different types of vibrations are usually so interrelated that it may be difficult to consider them separately. Vibrations in motor vehicle may be excited by multiple sources but in general two main classes of excitations are considered, road roughness and on-board sources. The on-board excitations originate from moving (rotating) components of the vehicle and in general include the tire/wheel assemblies, the driveline and the engine.

Road roughness

Road roughness includes all those major and minor abnormalities of the road surface which make the road deviate from its perfect state or absolute flatness. Road roughness is described by the elevation profile along the wheel tracks of the vehicle. Road elevation profiles can be measured either by performing close interval rod and level surveys or by high-speed profilometers. Road profiles can be considered "broad-band random signals" and therefore they can be described either by the profile itself or its statistical properties. One of the most useful representations is the Power Spectral Density (PSD) function, which is a plot of the amplitudes of the sine waves obtained after performing a Fourier transformation on the profile versus spatial frequency. Spatial frequency is expressed as the "wavenumber" with units of cycles/meter and is the inverse of the wavelength of the sine wave on which it is based.

The deviations in elevation seen by a vehicle as it moves along the road translate into a vertical displacement input to the wheels which excites the vibrations. Since vibrations are measured and perceived mainly as accelerations, the roughness of the road could also be viewed as an acceleration input at the wheels in order to have a better correlation between the two. In order to transform the displacement input into accelerations, a traveling velocity is assumed and the displacements of elevation are expressed as a function of time. By differentiating this signal once, the velocity of the input at the wheels is obtained, and by doing so once more the acceleration.

As described so far, the road roughness is a vertical input able to excite only a bounce motion on a single wheel. The longitudinal distance between the front and back wheel of a vehicle causes the same point of the road profile to reach the back wheel with a certain time delay compared to the front one. This difference in elevation can produce a pitching motion of the vehicle. Similarly, because of the lateral distance between the left and right wheeltrack, a slightly different road profile is encountered by each side. This difference in elevation between the left and right road profile points creates a roll excitation input to the vehicle. Roll excitations are, in general, more noticeable by the passengers of a vehicle when it is moving at lower speeds.

Tire/wheel assembly

The tire/wheel assembly includes rotating and stationary parts such as tires, wheels, hubs, brakes, etc and is partly responsible for absorbing road roughness excitations and isolating the vehicle from the road. Ideally, it does so without contributing any excitations of its own to the vehicle. In reality, however, numerous slight imperfections in the manufacture of the rotating parts of the assembly, when combined, can cause variations in the forces and moments the assembly experiences. These in turn are transmitted to the axle of the vehicle and act as excitation sources for ride vibrations. The imperfections can result in non-uniformities of three major types - mass imbalance, dimensional variations and stiffness variations.

Imbalance is caused by a non-uniform distribution of mass in the individual components of the assembly along or about the axis of rotation. Asymmetry about the axis of rotation causes static imbalance. The resultant effect is a force rotating in the wheel plane with a magnitude proportional to the imbalance mass, the radius from the center of rotation, and the square of the rotational speed. The excitations produced by this phenomenon are in the radial and longitudinal direction. On the other hand, asymmetric mass distribution along the axis of rotation causes dynamic imbalance. The resultant effect is a rotating torque on the wheel, affecting the overturning moment and aligning torque at the wheel rotational frequency. The two forms of imbalance are independent from one another and they do not have to be simultaneously present. The tires, wheels, hubs and brake drums may all contribute to the above imbalance effects.

A tire is a rotating elastic body loaded in the radial direction, resembling an array of radial springs which are periodically compressed as the wheel rotates. The free length of the springs, establishes the dimensional non-uniformities (free radial runout), whereas slight variations in

the radial stiffness of the tire can cause variations in the compression length of the springs at a nominal load producing rolling non-uniformities (loaded radial runout).

The non-uniformities of a tire/wheel assembly generate radial, lateral and tractive excitation forces and displacements at the axle of the vehicle as the wheel rotates causing ride and noise vibrations. In practice, the different types of non-uniformities of the tire/wheel assembly tend to be highly correlated and the resulting conditions cannot easily be separated and corrected independently.

Driveline

The driveline is considered to be everything between the transmission and the wheels, generally consisting of the driveshaft, gear reduction and differential in the drive axle, and axle shafts connecting to the wheels.

The driveshaft is the main source of ride excitations. They arise directly from two sources, namely i) a mass imbalance of the driveshaft hardware, and ii) secondary couples or moments imposed on the driveshaft due to angulation of the cross-type universal joints.

Mass imbalance of the driveshaft may result from the combination of any of the five following factors: i) asymmetry of the rotating parts, ii) off-center position of the shaft on its supporting flange and end yoke, iii) deviation from straightness of the shaft, iv) off-center position of the shaft due to running clearances, and v) deflection of the shaft due to elasticity. An initial imbalance exists as a result of the asymmetry, runouts and looseness in the structure. As the shaft rotates, a rotating force is created which imposes forces on the support means in the vertical and lateral directions. The magnitude of the excitation force is equivalent to the product of this static imbalance and the square of the rotating speed. When this force is applied on the elastic shaft it can cause it to bend thus causing additional asymmetry and increasing the dynamic imbalance of the shaft. In that sense, the apparent magnitude of the imbalance can change with speed.

Every universal joint that operates at an angle creates a secondary couple load that traverses down the centerline of the drive shaft. The magnitude and direction of this secondary couple load is proportional to the magnitude of the torque transferred through the joint and the angle of the shafts. In the same sense, in a cross-type universal joint, speed variations result in variations of torque on the driveline which result in variations of the secondary couple. Thus, the forces which are produced and transferred to the support points of the driveline on the

transmission, to the crossmembers supporting the driveline intermediate bearings and at the rear axle, vary depending on the torque applied to the driveline. Consequently, these forces can excite ride vibrations on the vehicle and torsional vibrations in the driveline. The torque variations may also act directly at the transmission and the rear axle varying the drive forces at the ground and thus generating directly longitudinal vibrations in the vehicle.

Engine

The engine is the primary power source on a motor vehicle. In piston engines the torque delivered is not constant in magnitude, rather it consists pulses corresponding to the power strokes of each cylinder, while the flywheel acts as an inertial damper between the pulses. In effect, the torque output to the driveshaft consists of a steady-state component plus superimposed torque variations. These torque variations may result in excitation forces on the vehicle similar to those produced by the secondary couple. The engine roll direction is the most important for excitation of vibrations.

2.5 Suspensions

The suspension of a vehicle is basically a system of springs, shock absorbers and linkages connecting the tire/wheel assembly (see also section 2.4) to the chassis. In that sense, the tire/wheel assembly on the lower end of the suspension is considered an *unsprung mass,* since it encounters the excitation from the road directly, and the chassis with the rest of the vehicle on the higher end of the suspension a *sprung mass*, because the excitation is filtered through the suspension.

The primary purpose of the suspension system on a vehicle is dual. For one it contributes to the good handling of the vehicle by ensuring constant contact between the wheels and the road surface during movement on a rough road, or by resisting to rolling or pitching movements during turning, accelerating or braking. At the same time it absorbs road anomalies and insulates the vehicle from road noise and vibrations, providing comfort to the passengers and protection to the vehicle's components from excessive wear. These two goals are contradicting and the appropriate selection of the setting is made according to the use of the vehicle. In general, softer springs improve the comfort of the passengers and stiffer springs provide better handling on the road.

Passive suspensions, which are most commonly used for conventional vehicles, consist of a traditional spring (leaf spring, torsion beam, coil spring, rubber bushing, air spring, etc) and a damper or shock absorber. The spring absorbs impacts by storing the potential energy in its extension or contraction and the damper is responsible for the dissipation of this energy so that the system does not resonate.

The spring rate (or suspension rate or simply stiffness) is a ratio used to measure a spring's resistance to being compressed or expanded during its deflection. The magnitude of the spring force increases as deflection increases according to Hooke's Law. It can be expressed as: $F_k = -kx$ where F is the force the spring exerts, k is the spring rate of the spring and x is the displacement from equilibrium length.

Damping is any effect that tends to reduce the amplitude of oscillations in an oscillatory system. Mathematically, damping can be modeled as a force synchronous with the velocity of the object but opposite in direction to it. Practically, with the use of hydraulic gates and valves in a vehicles shock absorber, it is attempted to dissipate the stored dynamic energy in the suspension's spring and convert it to heat, so that the oscillations of the system can be reduced and the vehicle can settle back to a normal state in a minimal amount of time. Damping also controls the travel speed and resistance of the vehicle's suspension. Most damping in modern vehicles can be controlled by increasing or decreasing the resistance to fluid flow in the shock absorber.

2.6 General concept of modeling

Besides an empirical approach to vehicle dynamics which is governed by intuition and trial and error in determining which factors influence the vehicle performance, in which way, and under what conditions, the analytical approach is mainly used by engineers in order to obtain more accurate and more reliable results. This approach attempts to describe the mechanics of the vehicle, based on the known laws of physics so that an analytical model of the phenomenon can be established. The mathematical description of a physical phenomenon dealing with dynamics is achieved by formulating a number of algebraic or differential equations which correlate forces or motions to control inputs and vehicle properties. The system of these mathematical equations, when solved, can describe the phenomenon and the state of the system at any time. The objective is to be able to evaluate the role and the importance of each vehicle property in the phenomenon of interest, predict the manner in which the system will

respond to various hypothetical inputs as well as how that response changes with different system parameter values. This way one can estimate the necessary modifications to be made to the system in order to achieve a certain goal.

A system model can always only approximate real events as best as possible, or better yet, as best as needed and not actually reproduce them. System models should generally be as simple as possible. That way they are easier and faster to solve. However they should be accurate enough so that the correct result is reached, and in this case accuracy can lead to complexity. During the analysis and creation of a model, it is often necessary that a number of assumptions are made and a number of factors ignored in order to reduce the complexity of the model and improve manageability and solvability of the system. The number and nature of these assumptions determine the credibility of the analysis and the quality of the approximation. The engineer creating the model should have an understanding of the nature of the problem as well as the nature of the factors determining the outcome in order to be able to make educated decisions about what factors are important and avoid errors which can prove fatal to the analysis.

In the past, the mathematical and computational limitations of obtaining a solution to complex systems inhibited the functionality of an analysis on complex models and confined the engineer. Every problem had to be mathematically expressed in closed forms in order to be solvable. Thus the existence of large numbers of components, systems, subsystems, and nonlinearities which are presented in vehicles made comprehensive modeling virtually impossible, limiting the scope to only simplistic models of certain mechanical systems.

Nowadays, the increase of computer power and solidity of computational methods have allowed for a much more comprehensive approach to vehicle dynamics. Much more complex models for the behavior of separate components of a vehicle can be solved and on a second level they can be integrated into larger models of the overall vehicle, allowing simulation and evaluation of its total behavior. In cases where the engineer is uncertain of the importance of specific factors, those factors can be included in the model and their importance can be later on assessed by evaluating their influence on simulated behavior. This fortifies the analysis by widening the search field in the pursuit for performance improvement and by reduces uncertainty in our knowledge and understanding of important aspects in complex systems and phenomena.

Chapter 3

3 Applications

In the current chapter, it is attempted to implement part of the aforementioned theoretical knowledge in a practical, real-life engineering problem of constrained optimization in vehicles' dynamics. The concept is the optimization of specific aspects of a vehicle's dynamic behavior by modifying certain vehicle parameter properties. In particular, an attempt is made to determine appropriate values from within a predefined range for the stiffness and damping constants of a tri-axle tank-truck's (see section 3.1) suspension system and tank support system, in order to minimize the tank's maximum occurring roll angle during movement.

3.1 Model of the vehicle

A tri-axle tank truck as the one shown in Figure 3.1 is studied. The tank is comprised of 6 separate compartments and is mounted on the vehicle chassis frame (Π) through a sub-frame (Y) in an effort to minimize the torsion transferred from the tank's movement to the chassis frame. The tank's compartment numbering is shown in Figure 3.2

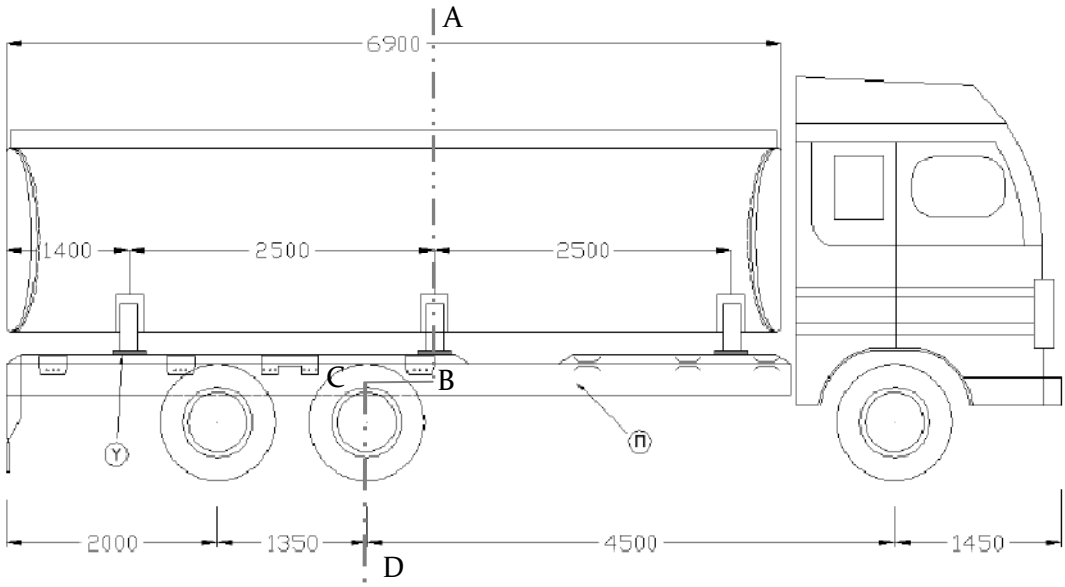

Figure 3.1 Vehicle layout and dimensions

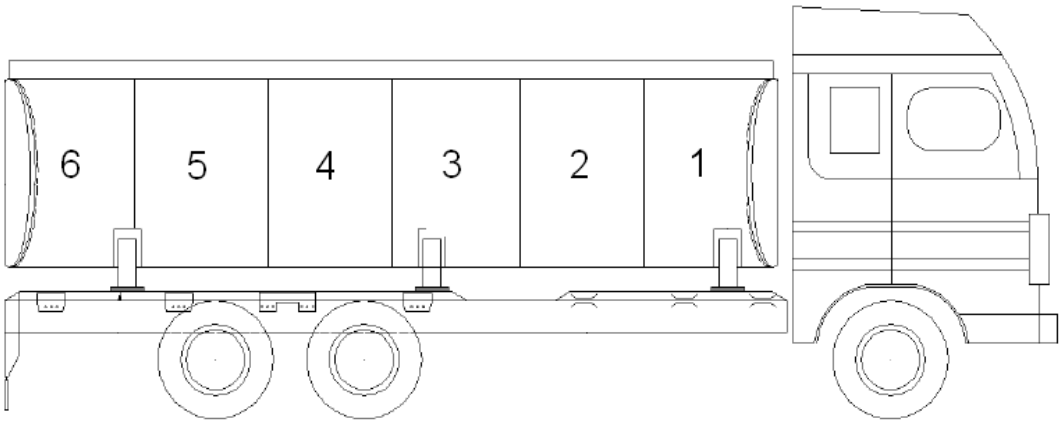

Figure 3.2 Tank's compartment numbering

The principal dimensions of the vehicle are shown in Figure 3.1 and other useful characteristics are shown in Table 3.1. The constraints imposed by structural or geometric limitations are shown in Table 3.2.

Table 3.1 Vehicle Parameters

MODEL PARAMETERS	SYMBOL	VALUE	UNITS
Front Axle mass	M_{FA}	600	kg
Middle Axle mass	M_{MA}	1300	kg
Rear Axle mass	M_{RA}	600	kg
Chassis mass	M	6500	kg
Chassis mass distribution: Front Axle / Rear Axles	-	5500/3500	kg
Tank mass (when filled)	M_T	17000	kg
Tank mass (empty)	M_E	2500	kg
Width of the chassis frame	B	0.860	m
Front/ Middle/ Rear Tires' stiffness	F_{RVi}	800/1600/1600	kN/m
Front/ Middle/ Rear wheel space	T_{Ni}	2.100/1.900/1.900	m

Table 3.2 Geometric and structural constraints

MODEL PARAMETERS	VALUE	UNITS
Suspension Stiffness	10000-500000	N/m
Suspension Damping	1000-50000	N.s/m
Supports stiffness	1000-50000	N/m
Supports damping	100-5000	N.s/m
Suspension Max. Displacement	±0.2	m
Front Axle/ Rear Axles load capacity	7000/20000	kg

The technique used for modeling the current vehicle is based on the notion of integrating numerous basic ideal system elements to form the full model of the vehicle. In particular, a lumped model was used for the individual elements of the system. The individual algebraic and differential elemental equations are derived from these elements and are then combined to form the mathematical description of the whole system. Such a model simplifies the description of physical systems, under certain assumptions (see below), by treating an

element's certain distributed property as a concentrated one acting or applied on a certain point of the element. This way the dependent variables of the element equation become disengaged from the spatial coordinate while mathematically speaking, the state space of the system is reduced to a finite number and also the partial differential equations (PDEs) of the continuous (infinite-dimensional) time and space model of the physical distributed system are transformed into ordinary differential equations (ODEs) with a finite number of parameters.

For mechanical systems the simplifying assumptions that have to be made in order for the lumped model to work, are that (a) all objects are rigid bodies and (b) all interactions between rigid bodies take place via kinematic pairs (joints), springs and dampers.

The model assumes linear full-car suspension. The description of typical linear elements and their equations in mechanical systems are the following (Table 3.3):

Table 3.3 Linear translational elements in mechanical systems

Element	Equation	Energy
Mass – m kinetic energy storage	$F_m = m\ddot{x}$	$E = \frac{1}{2} m\dot{x}^2$
Spring – k dynamic energy storage	$F_k = kx$	$U = \frac{1}{2} kx^2$
Damper – c energy dissipation	$F_c = c\dot{x}$	$V = \frac{1}{2} c\dot{x}^2$

It is also assumed that the tank has been mounted on the chassis frame using three supports (sub-frame Y), modeled as mass-less elements with equivalent stiffness and damping, which act on the left and the right side of the frame (Figure 3.3). The travelling velocity is set at 11.11 m/s.

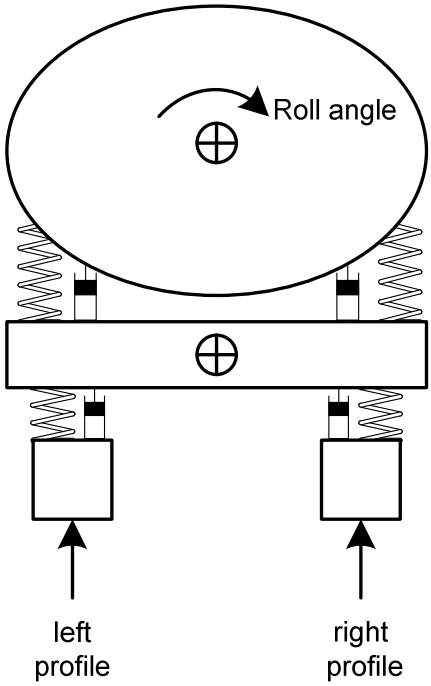

Figure 3.3 Model of the vehicle along the ABCD section of Figure 3.1

When the equations from all the elements of the system are combined, an equation of the following form is produced for the whole system:

$$[M]\cdot\ddot{x}(t)+[C]\cdot\dot{x}(t)+[K]\cdot x(t)=[P]\cdot f(t) \qquad (1.39)$$

where,

$[M]$ is the mass matrix,

$[C]$ is the damping matrix,

$[K]$ is the stiffness matrix,

$x(t)$ is the displacements vector for all the DoF's

$[P]$ is the coordinates matrix and

$f(t)$ is the excitations vector

The roll angle of the tank is acquired by conducting dynamic analyses of the model of the system (solving Eq. 3.1 for $x(t)$) and studying the respective component in the cases of different road profile excitations as inputs and different loading cases of the tank, corresponding to various realistic hypothetical scenarios.

This study examines 4 different basic loading scenarios. Each one represents a different filling pattern of the vehicle's tank (Figure 3.2). The four loading cases examined are:

- Case 1: All 6 compartments of the tank are filled at 100% of their maximum capacity.
- Case 2: All 6 compartments of the tank are filled at 80% of their maximum capacity.
- Case 3: All 6 compartments of the tank are filled at 50% of their maximum capacity.
- Case 4: All 6 compartments of the tank are filled at 20% of their maximum capacity.

The excitations of the system represent overcoming an obstacle on the road, particularly a pothole (Figure 3.4) and a typical country road based on ISO/TC 108/WGp draft No.3e, 1972 (Figure 3.5).

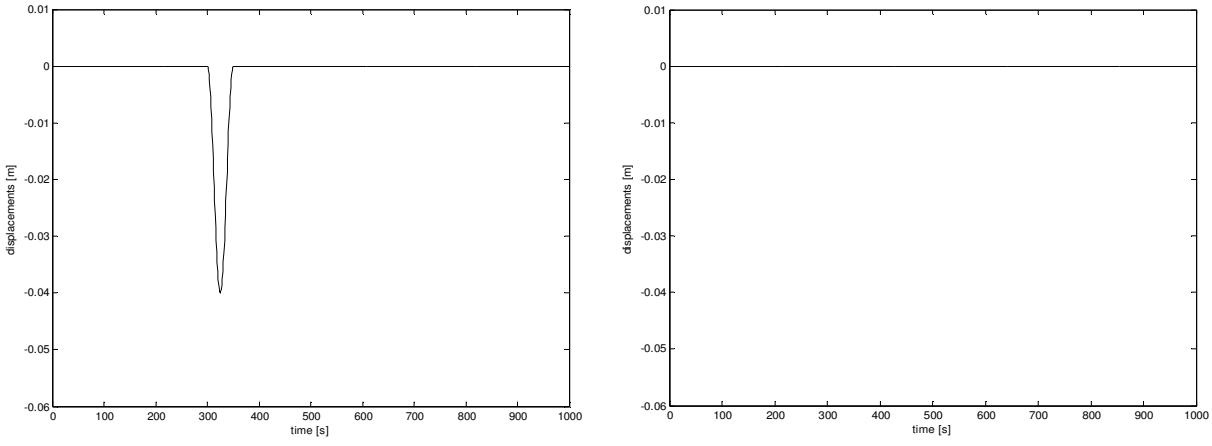

(a) (b)

Figure 3.4 Obstacle profile (a) left track, (b) right track

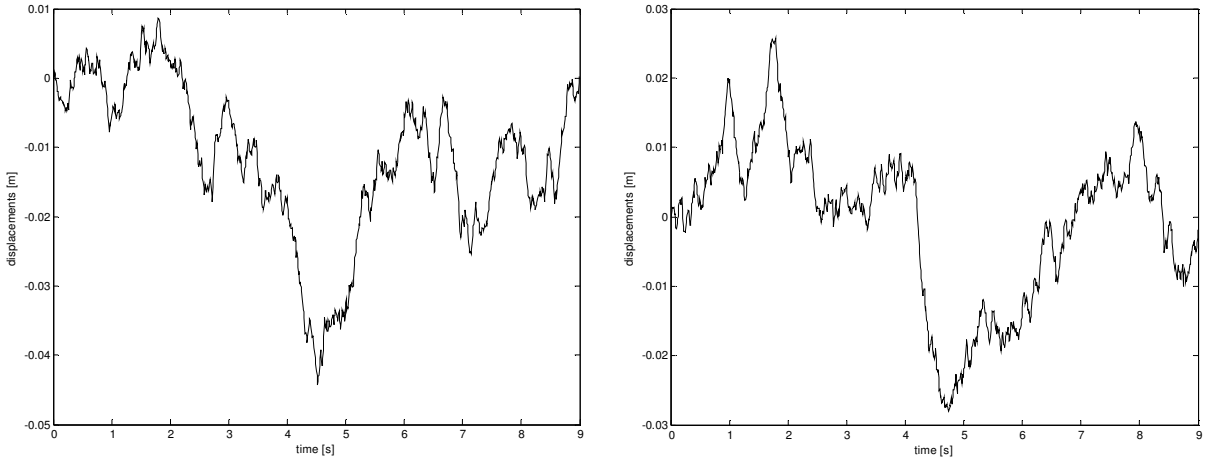

(a) (b)

Figure 3.5 Road profile (a) left track, (b) right track

Two optimization algorithms are selected for the optimization process. A stochastic genetic algorithm and a deterministic line search method are going to be compared with regards to global search capabilities and overall convergence. In the process useful conclusions will be drawn regarding both the nature of the problem and the nature of the algorithms. Since the

left and right side of the vehicle are considered to have symmetrical properties, there are a total of 12 design variables in the optimization process. Namely those variables are the front, middle and rear suspension stiffness (3) and damping (3) and the front, middle and rear tank's supports' stiffness (3) and damping (3), for a total of 12 variables.

3.2 Optimization with the Genetic Algorithm

The GA optimizer was implemented using the Genetic Algorithm and Direct Search Toolbox™ of MATLAB® R2008a. The solver of the optimization process included the modeling of the vehicle according to the Vehicles Laboratory™ Toolbox Software Version 1.5.1 (MATLAB® R2008a) in conjunction with a dynamic penalty function for violations in constraints as they are described in Table 3.2.

In order to overcome the stochastic nature of the algorithm and also to better apprehend the general behavior of the system and topology of the solution space, a number of 20 runs per load case per excitation input are executed. For every load case examined, the ten best runs of the particular excitation inputs are isolated, studied and compared in order to determine the behavior of the algorithm as well as the nature of the problem.

3.2.1 Load Case 1: All compartments filled at 100%

For this particular load case the tank of the truck is filled to the maximum possible degree. All 6 compartments of the tank of the vehicle are fully filled, therefore the weight of the liquid inside the tank is 14500 kg and the tank's center of gravity is in the middle of the tank.

A number of 20 runs for every excitation input were executed and the 10 best optimized design vectors for each are presented as follows in Table 3.4 for the obstacle excitation and Table 3.5 for the road excitation input.

Table 3.4 GA Case 1: Obstacle excitation

GA	1	2	3	4	5	6	7	8	9	10
F K susp	10001	10000	10000	10000	10000	10000	10000	350873	311152	485034
M K susp	10000	10000	10000	10000	10001	10000	10000	10000	10000	10000
R K susp	10000	10000	10000	10000	10000	10000	10000	10000	10000	10000
F c susp	49742	49382	49610	49033	45927	46875	43331	46999	40141	45260
M c susp	1003	1000	1000	1000	1000	1000	1001	1000	1001	12208
R c susp	1002	1000	1000	1000	1000	1000	1001	1001	1001	1000
F K supp	1000	1000	1000	1000	1000	1000	1000	1000	1000	1002
M K supp	1000	1000	1000	1000	1000	1000	1000	1000	1000	1000
R K supp	1001	1000	1000	1000	1000	1000	1000	1000	1000	1000
F c supp	991	4020	100	4596	4287	100	2288	2142	102	100
M c supp	1854	1917	4549	102	101	4557	3436	100	2340	4981
R c supp	3484	100	1863	827	1524	613	101	3524	2833	100
roll	0.1429	0.1430	0.1430	0.1433	0.1437	0.1440	0.1443	0.1446	0.1448	0.1451

Table 3.5 GA Case 1: Road excitation

GA	1	2	3	4	5	6	7	8	9	10
F K susp	21493	354880	292998	450897	290157	434007	10001	265421	458763	376072
M K susp	10000	10000	19330	10000	10000	10000	10001	10000	56819	10001
R K susp	10000	10001	10000	10000	10000	10000	10001	10001	10001	10001
F c susp	39024	47359	47674	49114	36592	44741	31828	30936	43326	39892
M c susp	1193	1001	1000	11975	1001	1001	1000	1001	1000	1000
R c susp	1000	1000	1810	1000	1001	1001	1000	1000	10296	1000
F K supp	1000	1000	1001	1000	1000	1000	1000	1000	1000	1001
M K supp	1000	1000	1000	1000	1000	1000	1001	1000	1000	1001
R K supp	1000	1000	1000	1000	1000	1000	1000	1000	1000	1001
F c supp	3976	2411	4031	3002	3365	4604	4899	1801	4981	4805
M c supp	4850	4853	3660	4633	4432	3319	4399	4921	3926	4413
R c supp	4012	4559	4017	4154	3689	4064	4281	4558	3155	2722
roll	0.4498	0.4507	0.4514	0.4516	0.4516	0.4516	0.4516	0.4521	0.4522	0.4524

Figure 3.6 shows the graph for the maximum roll angles as they are shown in the previous tables. It is presented here as a visual aid for ranking the quality of each solution compared to the rest in its case. For the first input, all the above solutions are located within 2% of the optimum found value and for the second within 0.5%.

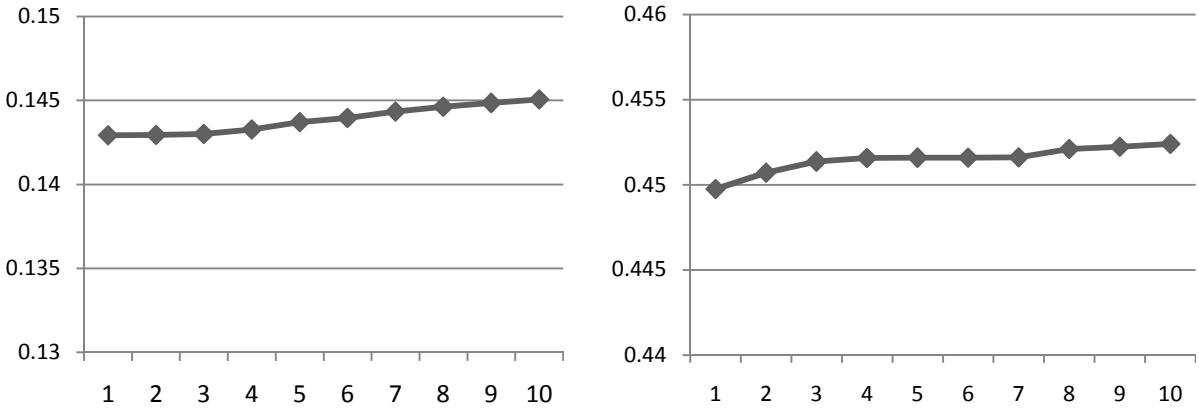

(a) (b)

Figure 3.6 GA Case 1: Roll angle (a) obstacle excitation, (b) road excitation

Table 3.4 shows a very clear general picture about where the globally optimum solution for this case is. For the first 9 parameters, the first 4 vectors are almost identical. The first 7 vectors are identical in 8 parameters and extremely close for the ninth.

Not the exact same general picture comes out from Table 3.5. The basic differences involve the front suspension stiffness and damping. There appear to be two or more potential optimal ranges for the suspension stiffness, clear sign that the algorithm was trapped in completely different local optima. See for example design vectors 1, 2 and 4. For the first, the stiffness is very low, as the one found in the previous case. For the others it ranges from medial to very high within the allowable range. In order to assess the resulting difference between these instances, the roll angle time-response is plotted in Figure 3.7, as it is determined by changes on the stiffness of the front suspension. The second vector of Table 3.5 is used as a template and the difference in the respective responses by changing the front suspension stiffness from high (50) to medial (25) to low (1) are plotted for both excitation inputs.

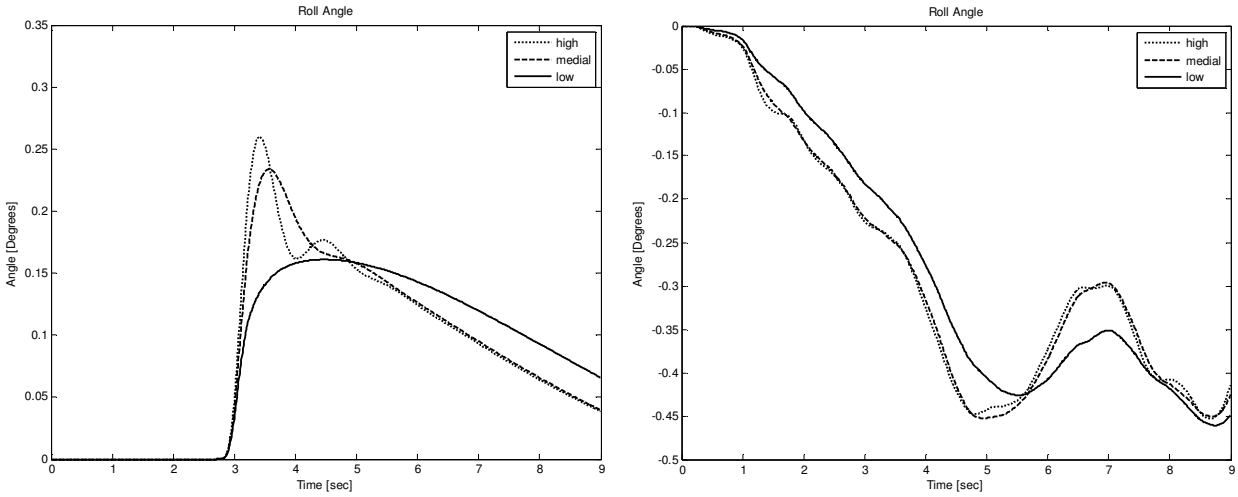

(a) (b)

Figure 3.7 GA Case 1: Front suspension stiffness (a) obstacle excitation, (b) road excitation

It is obvious that for the obstacle (Figure 3.7a), the lower stiffness produces a clearly better response, and that is the reason why the algorithm easily located that solution as the optimum. For the road input the answer is not that straightforward. The system and the excitation produce a topology of the solution such, that the two valleys that appear at the same approximate depth in the response of Figure 3.7b are each slightly attenuated or amplified by the stiffness in a way that final result is inversed. Even so, the first valley is significantly attenuated by the low stiffness value while the second valley is only slightly amplified as a result. The maximum roll angles in both cases are quite similar and this explains why the algorithm was unable to distinguish the optimum area between the two and got trapped in two different places of the design space. Another interesting observation is that the difference in the response by changing the stiffness from medial (25) to high (50) is very small. This creates sort of a plateau for a large range of values in that dimension of the solution space where the algorithm is very difficult to improve. This explains why the 10 best solutions contain 2 solutions with a low stiffness value and 8 dispersed in that high range, all with the same approximate objective function value. The graph shows that higher stiffness values within that range produces a slightly better final result.

The supports' damping parameters have not been mentioned so far because there seems to be no visible pattern and no individually optimal solution for each variable. Plotting these values in the same graph (Figure 3.8) proves this exact point.

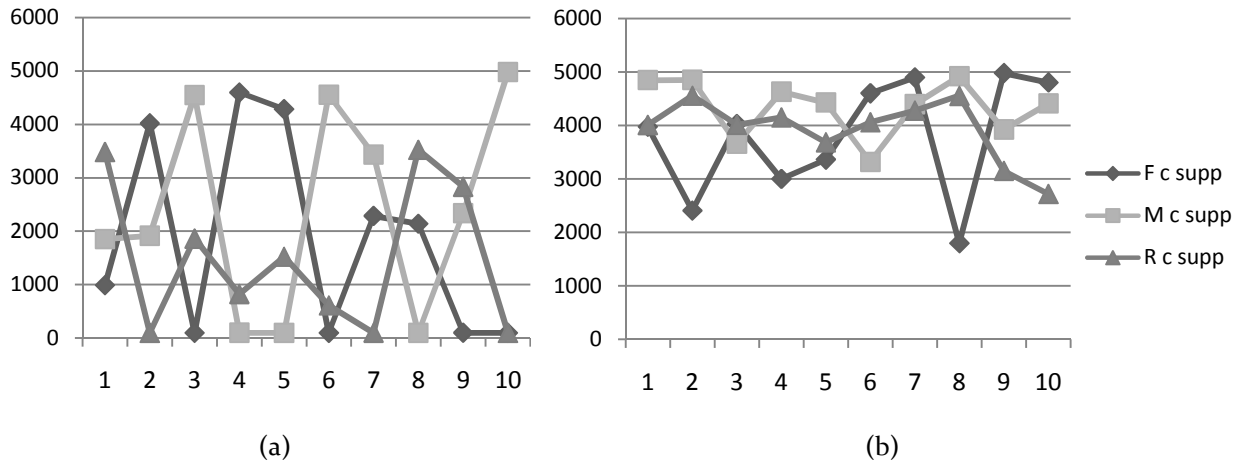

Figure 3.8 GA Case 1: Supports' damping (a) obstacle excitation, (b) road excitation

By a first look, these graphs may seem rather random and uncorrelated. On a closer examination though, one can discern that this is not actually the case. The individual variable values may fluctuate significantly, but on the contrary the sum of the three values on every run remains within a relatively tight range (Figure 3.9). It appears that this sum can be distributed among the three variables in numerous equivalent ways and produce the exact same final result.

This can be explained by the modeling of the tank and the sub-frame which supports it as rigid bodies, and the objective function selected since the roll of the tank affects all three supports in the same way. The supports act in parallel for containing the rolling of the tank's body and the respective individual damping values are added to provide the equivalent damping for each side of the tank. Therefore, there is no significant point in listing the values for the individual variables, but rather their sum is mentioned as the defining factor in the optimization.

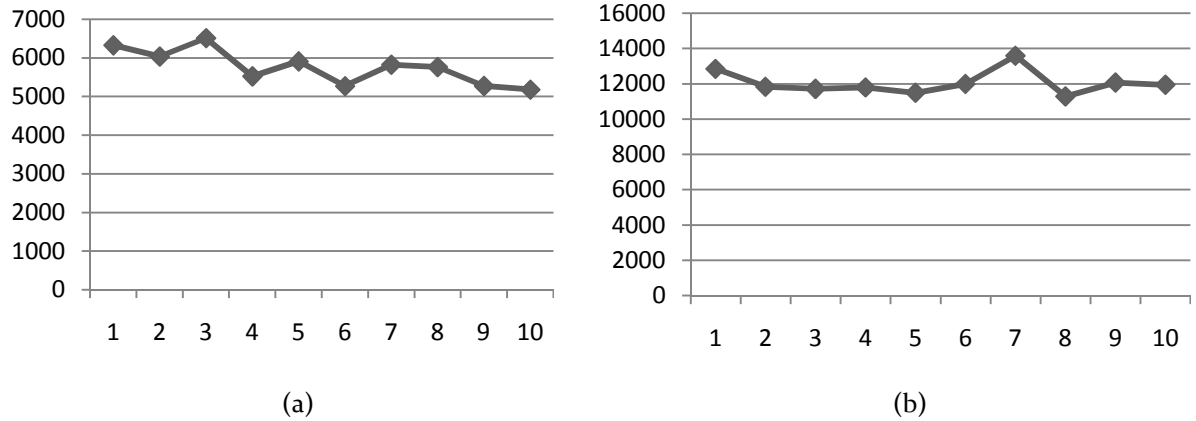

Figure 3.9 GA Case 1: Supports' damping sum (a) obstacle excitation, (b) road excitation

To sum this section, Table 3.6 shows the optimum design vectors found for each excitation input.

Table 3.6 GA Case 1: Optimum design vectors

GA	Obstacle excitation input	Road excitation input
F K susp	10001	21493
M K susp	10000	10000
R K susp	10000	10000
F c susp	49742	39024
M c susp	1003	1193
R c susp	1002	1000
F K supp	1000	1000
M K supp	1000	1000
R K supp	1001	1000
Σc supp	6329	12838
roll	0.1429	0.4498

In order to be able to make a more educated decision in the end, both optimum vectors are applied to the system for both excitations. The responses obtained are depicted in Figure 3.10. The continuous line represents the vector optimized for the obstacle and the dotted line represents the vector optimized for the road.

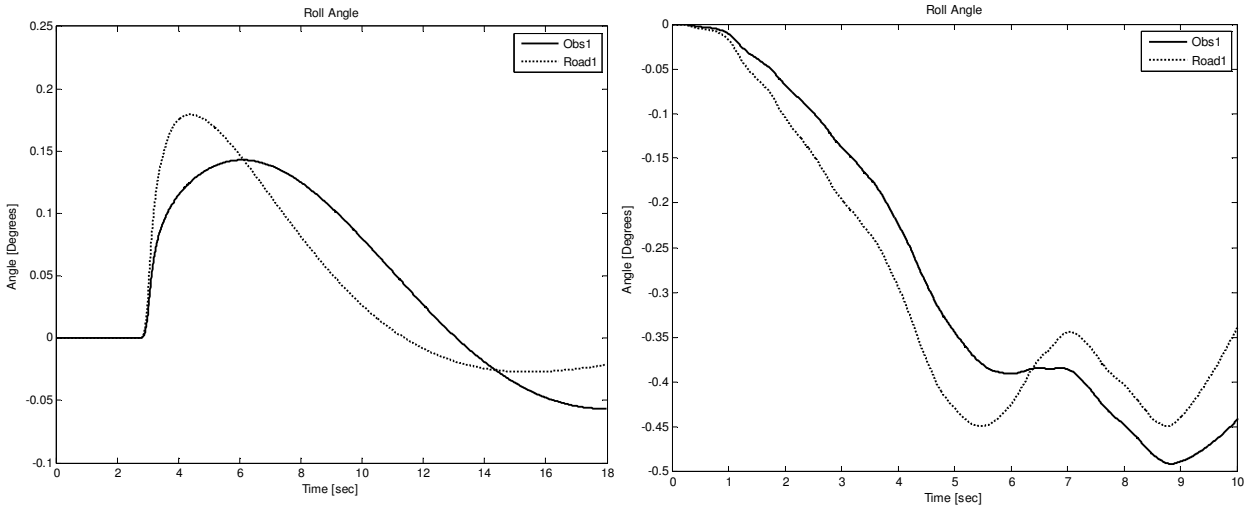

(a) (b)

Figure 3.10 GA Case 1: Optimized responses (a) obstacle excitation, (b) road excitation

3.2.2 Load Case 2: All compartments filled at 80%

The 6 compartments of the tank of the vehicle are partially filled, at 80% of their maximum capacity. Therefore the weight of the liquid inside the tank is 14500*0.8 = 11.600 kg and since the loading is symmetric, the center of gravity is still in the middle of the tank lengthwise. It should be mentioned again here, that in all the cases of partially filled compartments, the movement of the liquid inside the compartment is not modeled or taken into consideration and the tank with the liquid inside is modeled as a rigid body.

The ten out of 20 best design vectors found by the GA for the second loading case are presented in Table 3.7 and Table 3.8 for the obstacle and the road excitation input respectively.

Table 3.7 GA Case 2: Obstacle excitation

GA	1	2	3	4	5	6	7	8	9	10
F K susp	10000	10000	10000	10000	10000	10000	322574	10000	462750	298130
M K susp	10000	10000	10000	10000	10000	10000	10001	10000	10002	10001
R K susp	10000	10000	10000	10000	10000	10000	10001	10000	10000	10001
F c susp	49804	49248	47625	47264	45476	41727	46685	39585	36584	35604
M c susp	1000	1001	1000	1000	1000	5317	1000	3266	1000	1001
R c susp	1000	1001	1000	1000	1000	1000	1001	1001	14091	1000
F K supp	1000	1000	1000	1000	1000	1000	1000	1000	1000	1000
M K supp	1000	1000	1000	1000	1000	1000	1000	1000	1000	1000
R K supp	1000	1000	1000	1000	1000	1000	1000	1000	1000	1000
Σc supp	5755	5790	5433	5609	4911	5734	4763	5520	4865	4415
roll	0.1562	0.1563	0.1567	0.1568	0.1576	0.1586	0.1586	0.1591	0.1591	0.1592

Table 3.8 GA Case 2: Road excitation

GA	1	2	3	4	5	6	7	8	9	10
F K susp	10003	10001	380852	407952	386401	287384	395194	483525	366090	241131
M K susp	10000	10000	10000	10002	10000	10000	10000	10000	10000	10003
R K susp	10001	10001	10000	10000	20360	10001	10000	10000	69116	10002
F c susp	49734	43032	44088	49672	43419	39421	48817	44608	25050	28576
M c susp	1000	1000	1001	1000	1000	1000	1000	21682	6090	1003
R c susp	1001	1001	1000	9918	3899	1000	4938	1000	1000	1474
F K supp	1000	1000	1000	1001	1001	1000	1000	1000	1000	1000
M K supp	1000	1000	1000	1000	1000	1000	1001	1000	1000	1000
R K supp	1000	1000	1001	1001	1000	1002	1000	1000	1000	1000
Σc supp	11682	11533	9059	8865	9135	8787	8765	8800	9368	8383
roll	0.4590	0.4595	0.4607	0.4611	0.4613	0.4618	0.4620	0.4629	0.4633	0.4638

Figure 3.11 shows the graph of the maximum occurring roll angle for the ten best runs of every input. For the obstacle, the solutions lie within 2% and for the road within 1%.

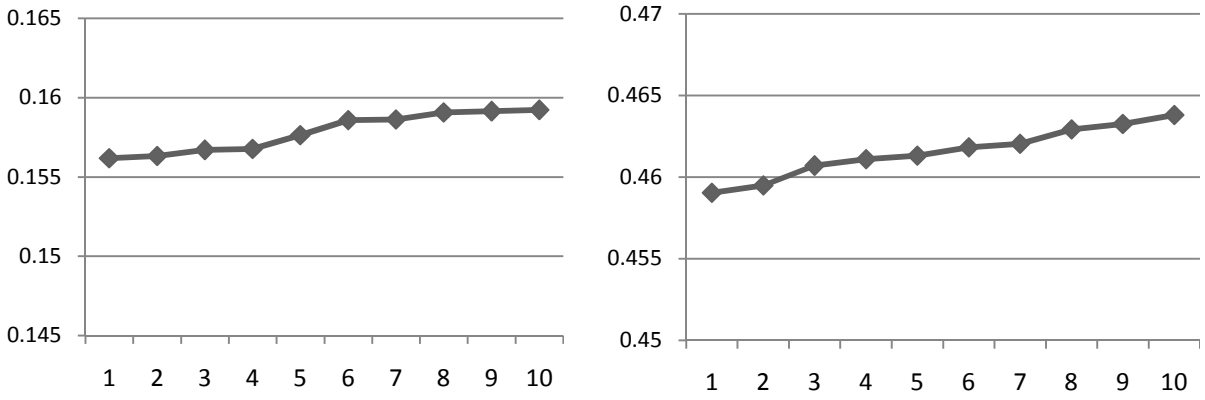

(a) (b)

Figure 3.11 GA Case 2: Roll angle (a) obstacle excitation, (b) road excitation

The results shown in Table 3.7 and Table 3.8 appear a little clearer than the previous load case. For both excitation inputs there seems to be a general agreement on the first 9 optimum parameters. The neighborhood of the global optimum seems to be similar and is located by the algorithm for both excitation inputs. Furthermore, the respective roll angles have increased compared to the previous load case once the tank has become emptier and therefore lighter. The reduced inertia of a smaller tank mass makes the system more sensitive to the same excitations.

As far as the supports' damping is concerned, a graph of the respective sums is presented in Figure 3.12 for reasons explained in section 3.2.1.

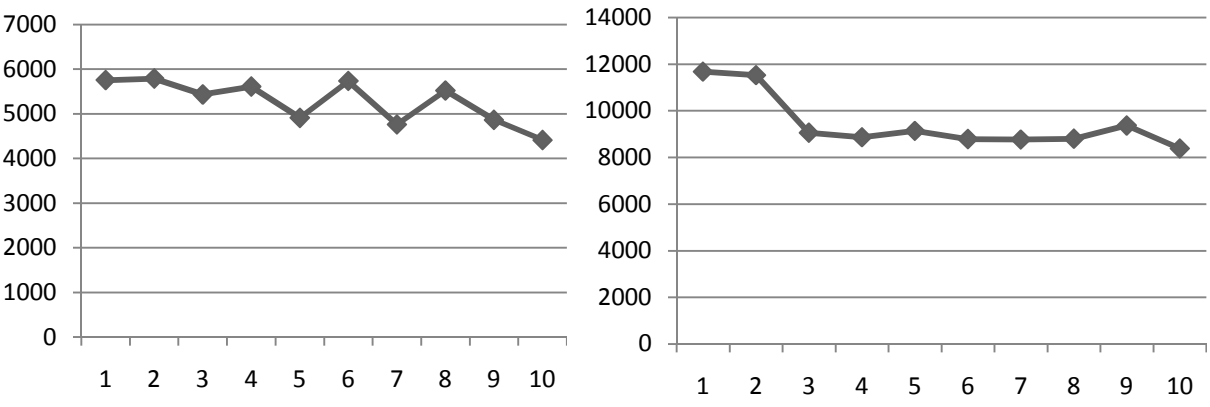

(a) (b)

Figure 3.12 GA Case 2: Supports' damping sum (a) obstacle excitation, (b) road excitation

There appears to be better homogeneity between the first four values of Figure 3.12a compared to the rest. Something interesting can thus be noticed by looking at the design vectors of Table 3.7 in correlation with the obtained roll angles as shown in Figure 3.11. First of all, these values are taken with more confidence since they are separated from the rest in their graph, in the same way that the best respective roll angles are separated from the rest in their graph. Moreover, as these values are kept relatively constant, there appears to be a direct relation between the front suspension damping and the roll angle, as expected by the linear modeling of the dampers. A higher suspension damping produces a lower roll angle as shown in Figure 3.13 for the obstacle excitation input. Of course the relation ceases to be this straightforward when more parameters come in play and their values are differentiated. What else is evident from Figure 3.13 is that the roll angle could in fact become lower and drop as low as 0.1561 just by setting the damping to 50000 which is the highest allowable limit.

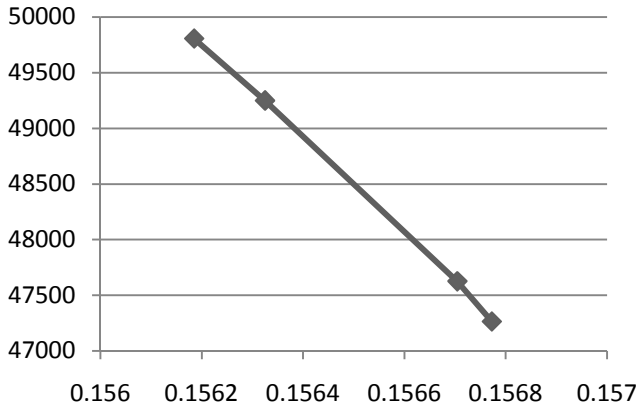

Figure 3.13 Relation between roll angle and front suspension damping

The large difference between the first two values and the rest in Figure 3.12b is explained by the respective values for the front suspension stiffness in the design vectors, as seen in Table 3.8, and the fact that, as mentioned in section 3.2.1, the system has a different balance point. Again for these two design vectors, as the supports' damping is kept constant, the relation between the front suspension damping and the roll angle is proportionate.

Table 3.9 shows the optimum design vectors found for each excitation input. The two vectors are practically identical with the exception of the supports' damping sum which is found to be twice as large for the road excitation.

Table 3.9 GA Case 3: Optimum design vectors

GA	Obstacle excitation input	Road excitation input
F K susp	10000	10003
M K susp	10000	10000
R K susp	10000	10001
F c susp	49804	49734
M c susp	1000	1000
R c susp	1000	1001
F K supp	1000	1000
M K supp	1000	1000
R K supp	1000	1000
Σc supp	5755	11681
roll	0.1562	0.4590

The responses obtained by these two vectors with each different input are depicted in Figure 3.14. The continuous line represents the vector optimized for the obstacle and the dotted line represents the vector optimized for the road.

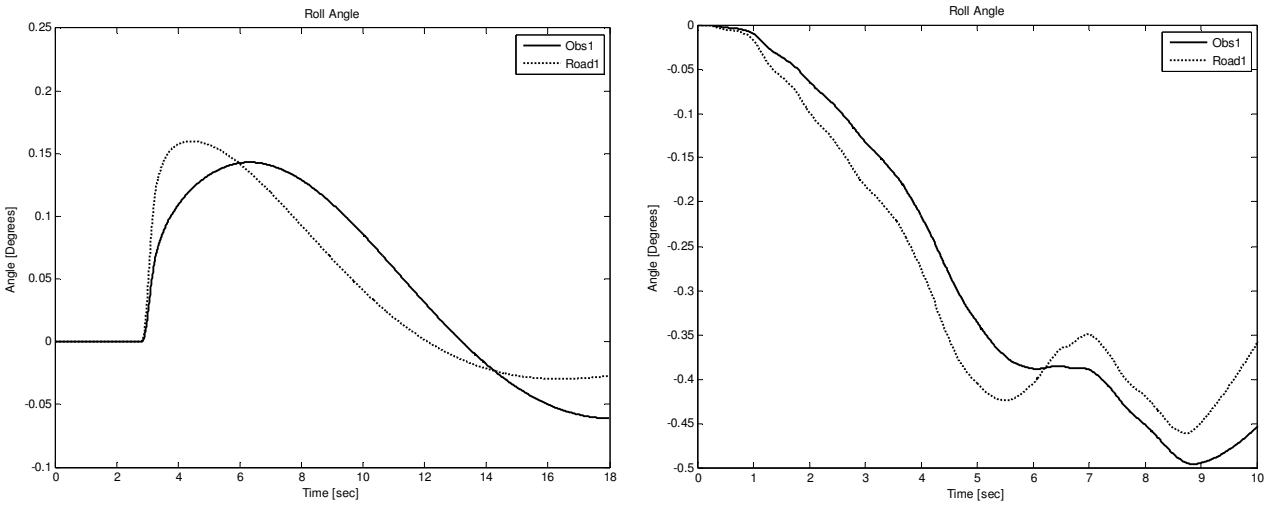

(a) (b)

Figure 3.14 GA Case 2: Optimized responses (a) obstacle excitation, (b) road excitation

3.2.3 Load Case 3: All compartments filled at 50%

In this case, the 6 compartments of the tank of the vehicle are filled in half. The weight of the liquid inside the tank is 14500*0.5=7250 kg.

Table 3.10 and Table 3.11 show the optimum design vectors found by the GA for the obstacle and road excitation input, respectively, for this particular load case.

Table 3.10 GA Case 3: Obstacle excitation

GA	1	2	3	4	5	6	7	8	9	10
F K susp	10000	10000	10000	10000	10000	10000	10000	10001	10000	10000
M K susp	10000	10000	10000	10001	10000	10000	10000	10000	10001	10000
R K susp	10000	10000	10000	10000	10000	10000	10000	10000	10001	10001
F c susp	49299	48349	48286	48593	47567	46479	45302	45039	42844	43185
M c susp	1000	1000	1000	1001	1000	1000	1000	1000	1001	1000
R c susp	1000	1000	1000	1000	1000	1000	1000	1000	1000	1000
F K supp	1000	1000	1000	1000	1000	1000	1000	1000	1000	1000
M K supp	1000	1000	1000	1000	1000	1000	1000	1000	1000	1000
R K supp	1000	1000	1000	1000	1000	1000	1000	1000	1000	1000
Σc supp	4707	4678	4695	4426	4767	4892	4752	4735	4629	4334
roll	0.1863	0.1866	0.1866	0.1866	0.1868	0.1872	0.1876	0.1877	0.1885	0.1885

Table 3.11 GA Case 3: Road excitation

GA	1	2	3	4	5	6	7	8	9	10
F K susp	10000	10000	10000	10001	10000	414640	398918	383816	484877	10000
M K susp	10000	10000	10000	10000	10000	10001	10000	10001	10000	10000
R K susp	10000	10000	10000	10000	10000	10001	10000	10000	10001	10000
F c susp	47508	48622	47962	41527	46529	1000	1001	1000	29918	35295
M c susp	1000	1000	1000	1000	12174	1000	1000	1000	3296	1000
R c susp	1000	1000	1001	1000	1000	1001	1001	1000	1000	1000
F K supp	1000	1000	1000	1000	1000	1000	1000	1000	1000	1000
M K supp	1000	1000	1000	1000	1000	1000	1000	1000	1000	1000
R K supp	1000	1000	1050	1000	1000	1000	1000	1000	1000	1000
Σc supp	5412	5779	5094	5136	5058	5688	5662	5857	5628	5280
roll	0.4952	0.4952	0.4974	0.4985	0.5006	0.5022	0.5025	0.5033	0.5034	0.5039

In Figure 3.15 the roll angle throughout the runs is depicted, as it appears in the above tables. The solutions lie within 1% for the obstacle excitation and within 2% for the road excitation.

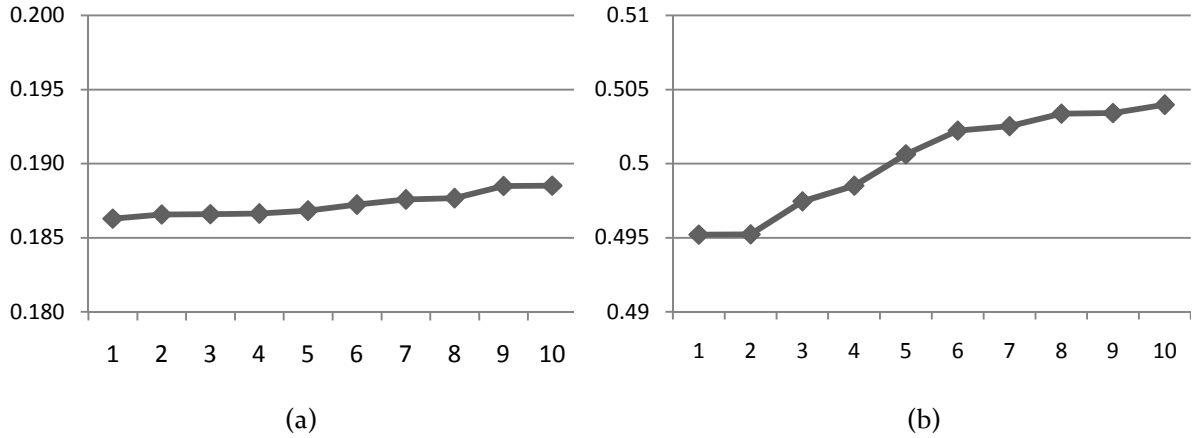

(a) (b)

Figure 3.15 GA Case 3: Roll angle (a) obstacle excitation, (b) road excitation

Again, in this load case, the results of the two optimization processes tend to agree to a large degree. The 9 first variables of the first few optimum vectors are practically the same, with all the values being set to the lowest allowable limit except for the front suspension damping which is very high. The supports' damping sum is shown in Figure 3.16.

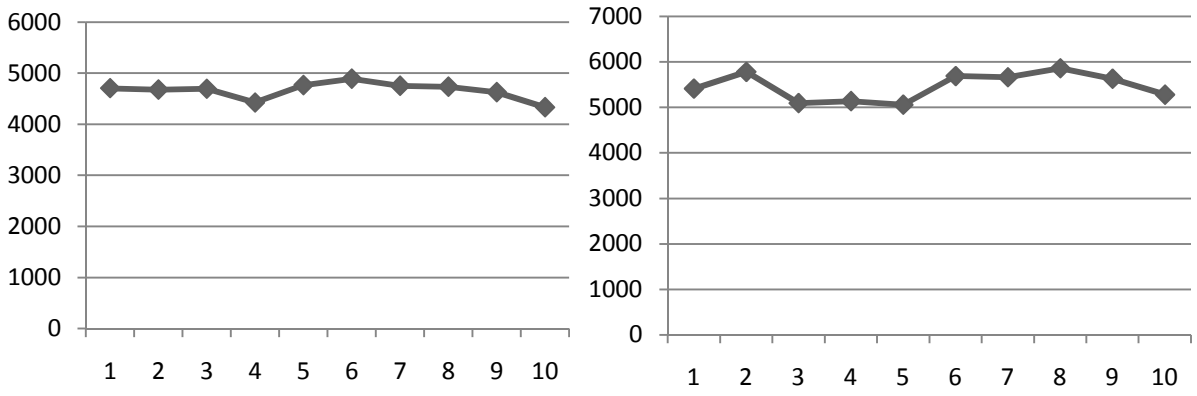

(a) (b)

Figure 3.16 GA Case 3: Supports' damping sum (a) obstacle excitation, (b) road excitation

For this particular load case, the supports' damping values are relatively close for the two inputs, compared to what has been the case so far.

As a result of all the above, Table 3.12 summarizes the optimum design vectors for each excitation input and Figure 3.17 depicts the responses obtained by these two vectors. The continuous line represents the vector optimized for the obstacle and the dotted line represents the vector optimized for the road. Since the design vectors are very similar, the responses obtained are also very similar.

Table 3.12 GA Case 3: Optimum design vectors

GA	Obstacle excitation input	Road excitation input
F K susp	10000	10000
M K susp	10000	10000
R K susp	10000	10000
F c susp	49299	47508
M c susp	1000	1000
R c susp	1000	1000
F K supp	1000	1000
M K supp	1000	1000
R K supp	1000	1000
Σc supp	4707	5412
roll	0.1863	0.4952

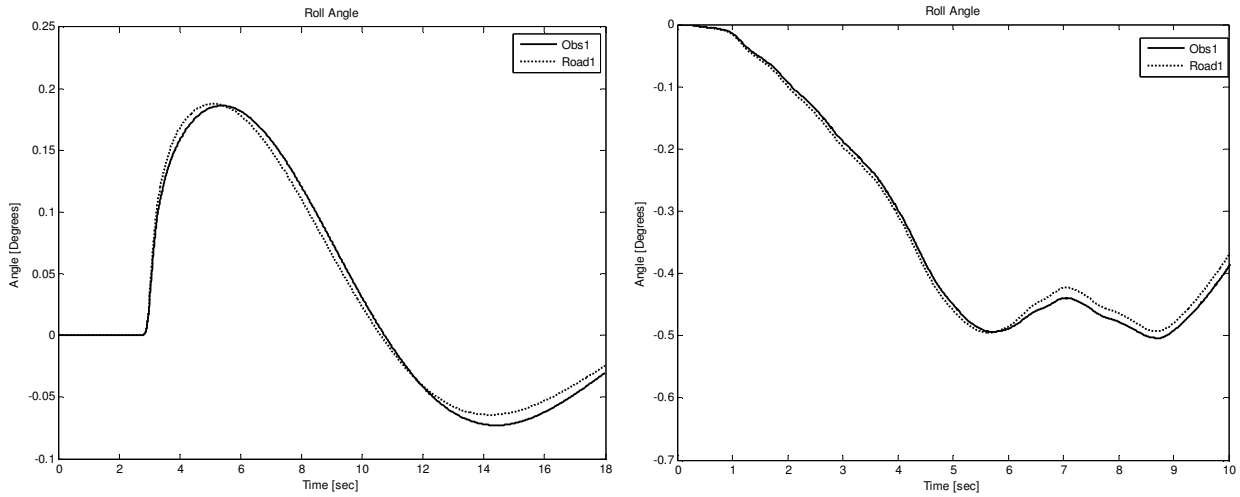

(a) (b)

Figure 3.17 GA Case 3: Optimized responses (a) obstacle excitation, (b) road excitation

3.2.4 Load Case 4: All compartments filled at 20%

In the last case the tank is only full by 20% which makes the tank very light and thus more susceptible to movement. The liquid carried inside the tank weighs 14500*0.2=2900 kg compared to the 14.500 kg of the first load case (section 3.2.1)

Table 3.13 and Table 3.14 show the ten best runs out of 20 that were executed for each road profile input.

Table 3.13 GA Case 4: Obstacle excitation

GA	1	2	3	4	5	6	7	8	9	10
F K susp	10000	10000	10000	10000	10000	10000	10000	10000	10000	10000
M K susp	10000	10000	10000	10000	10000	10001	10000	10000	10000	10000
R K susp	10000	10001	10000	10000	10000	10001	10000	10000	10000	10000
F c susp	49468	49165	49001	48264	47437	48670	46713	46776	43249	40976
M c susp	1000	1000	1000	1001	1000	1000	1000	1000	1000	1001
R c susp	1000	1000	1000	1000	1000	1000	1000	1000	1000	1000
F K supp	1000	1000	1000	1000	1000	1000	1000	1000	1000	1000
M K supp	1000	1000	1000	1000	1000	1000	1000	1000	1000	1000
R K supp	1000	1000	1000	1000	1000	1000	1000	1000	1000	1000
Σc supp	3487	3704	3402	3848	3780	3117	3293	3068	3496	3709
roll	0.246	0.2469	0.2469	0.2475	0.2476	0.2476	0.2480	0.2486	0.2494	0.2508

Table 3.14 GA Case 4: Road excitation

GA	1	2	3	4	5	6	7	8	9	10
F K susp	10000	10000	10000	10000	10000	10001	10000	10000	10000	10000
M K susp	10000	10000	10000	10000	10001	10000	10000	10000	10000	10000
R K susp	10000	10000	10001	10001	10001	10000	10000	10001	10000	10000
F c susp	49405	49074	48747	47477	45677	45854	44375	48799	38624	40317
M c susp	1001	1000	1000	1000	1001	1001	1000	1001	1000	3326
R c susp	1002	1000	1000	1000	1000	1000	1000	1000	1000	3009
F K supp	1000	1000	1000	1000	1000	1000	1000	1000	1000	1000
M K supp	1000	1000	1000	1000	1000	1000	1000	1000	1000	1000
R K supp	1000	1000	1000	1000	1000	1001	1000	1000	1000	1000
F c supp	7512	7562	7118	8312	7755	8056	7827	5999	8744	8547
roll	0.5707	0.5709	0.5716	0.5727	0.5727	0.5728	0.5735	0.5753	0.5776	0.5797

The general picture is maintained from the previous load cases and the optimization for both inputs tends to agree on the values of all variables, differing only on the supports' damping. An interesting observation that can be made is that, now that the tank is lighter and the response of the tank's roll angle to the excitation input is sharper, the local optimum (high front suspension stiffness) that appeared in the results of previous cases for the road excitation input has now completely disappeared. For the first load case, when the tank was the heaviest, the algorithm can barely keep from getting trapped in that local optimum, for the second case the algorithm was not trapped in local optima only 2 times and for the third case only 5 times.

The obtained values of the roll angle for the fourth load case are depicted in Figure 3.18 for the obstacle and for the road excitation input respectively. These values range within approximately 1.5% of the optimum found value for both cases.

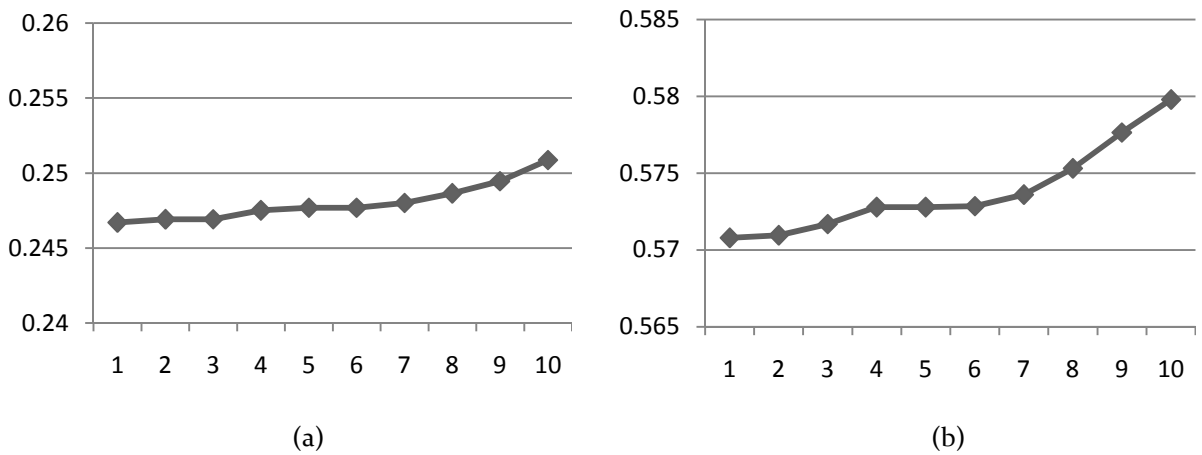

(a) (b)

Figure 3.18 GA Case 4: Roll angle (a) obstacle excitation, (b) road excitation

The optimum design vectors found for each input are presented in Table 3.15.

Table 3.15 GA Case 4: Optimum design vectors

GA	Obstacle excitation input	Road excitation input
F K susp	10000	10000
M K susp	10000	10000
R K susp	10000	10000
F c susp	49468	49405
M c susp	1000	1001
R c susp	1000	1002
F K supp	1000	1000
M K supp	1000	1000
R K supp	1000	1000
Σc supp	3488	7512
roll	0.2467	0.5707

Figure 3.19 shows the responses obtained by these two vectors with each different input. The continuous line represents the vector optimized for the obstacle and the dotted line represents the vector optimized for the road.

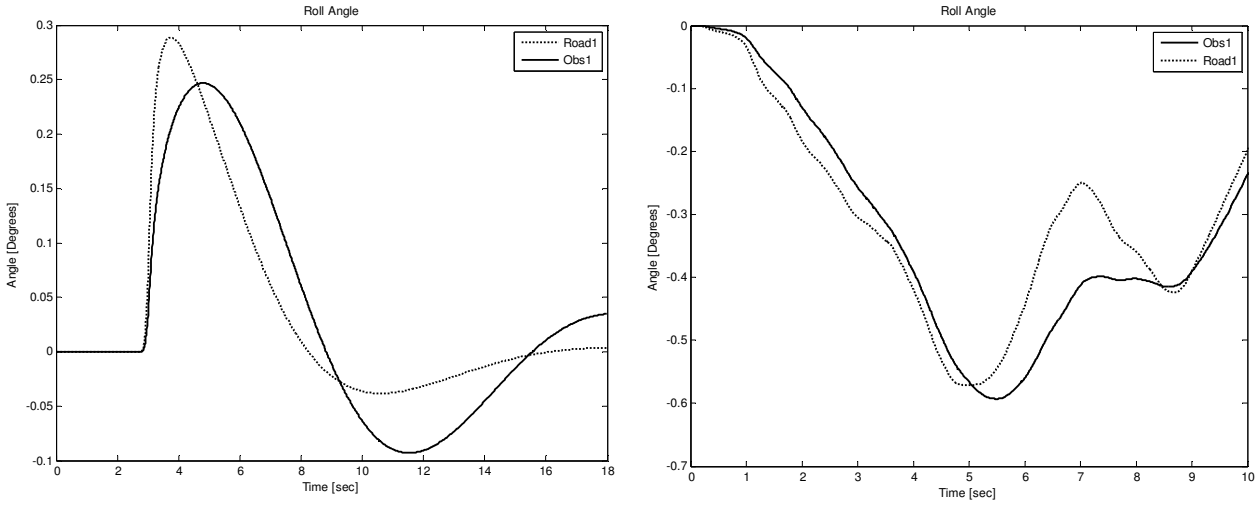

(a) (b)

Figure 3.19 GA Case 4: Optimized responses (a) obstacle excitation, (b) road excitation

3.3 Optimization with the BFGS method

The line-search optimizer used is part of the Vehicles Laboratory™ Toolbox Software Version 1.5.1 (MATLAB® R2008a). A number of 20 runs were executed per loading case per excitation input. The initial vectors were selected randomly from within the allowable range for every variable, following a uniform distribution. Out of the 20 runs, the 10 best were separated and presented here to be processed.

3.3.1 Load Case 1: All compartments filled at 100%

For the first load case, where the tank is 100% full, the 10 best design vectors obtained for the obstacle and the road excitation input are presented in Table 3.16 and Table 3.17 respectively.

Table 3.16 LS Case 1: Obstacle excitation

LS	1	2	3	4	5	6	7	8	9	10
F K susp	10000	482984	469040	445472	478561	498037	444463	470312	499553	453887
M K susp	10000	10000	10220	13143	12302	10703	25069	67237	77489	56276
R K susp	10000	10000	10463	21294	24811	42027	26877	10160	10262	31263
F c susp	50000	49222	49096	45030	45727	28821	40584	33716	28892	33484
M c susp	1003	5945	18064	22067	22790	17755	39951	46623	16476	16176
R c susp	1000	12063	15201	1127	24075	19451	16010	2273	3802	34310
F K supp	1000	1000	1000	1000	1000	1000	1000	1000	1000	1000
M K supp	1000	1000	1000	1000	1000	1000	1000	1000	1000	1000
R K supp	1000	1000	1000	1000	1000	1000	1000	1000	1000	1000
Σc supp	6122	5677	5536	5665	5497	5508	5449	5444	4961	5519
roll	0.1428	0.1448	0.1450	0.1453	0.1455	0.1459	0.1461	0.1465	0.1466	0.1469

Table 3.17 LS Case 1: Road excitation

LS	1	2	3	4	5	6	7	8	9	10
F K susp	347899	14029	435739	476596	473820	197983	281468	10000	10000	10001
M K susp	76551	13626	43918	24151	134096	23411	78360	10000	10000	10002
R K susp	254878	24946	231100	244451	111277	376656	224533	10000	10015	10004
F c susp	38554	45414	47207	21725	16605	38943	33183	50000	49792	49983
M c susp	10501	14847	37759	37529	29148	27716	40437	1000	9908	31159
R c susp	5691	24273	46970	38634	21167	7159	38022	17072	41659	25190
F K supp	1000	1000	1000	1000	1001	1000	1000	31702	12246	22330
M K supp	1000	1000	1000	1000	1001	1000	1000	31719	48918	39205
R K supp	1000	1000	1000	1000	1001	1000	1000	9917	4374	4313
Σc supp	11162	12960	11515	11742	11974	11109	11493	15000	8311	10216
roll	0.4572	0.4576	0.4590	0.4594	0.4597	0.4627	0.4638	0.6458	0.6480	0.6484

Figure 3.20 shows the graph of the roll angle during the ten best runs of every input as they appear in the above tables. Between best and the worst of these 10 angles there is a difference of 3% for the obstacle input and of a staggering 42% for the road excitation input.

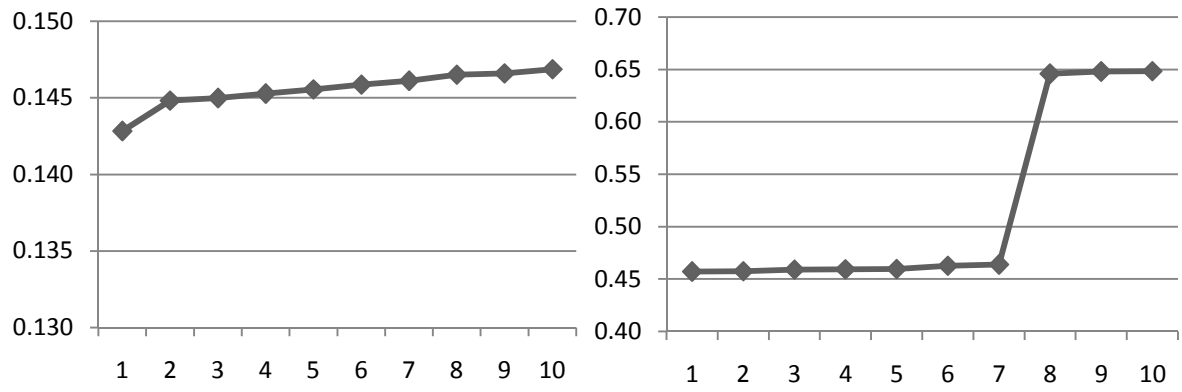

(a) (b)

Figure 3.20 LS Case 1: Roll angle (a) obstacle excitation, (b) road excitation

After the examination of the optimized design vectors in combination with Figure 3.20, various interesting observations can be made. For the obstacle excitation input, there appear to be at least two general directions of search in the solution space, differing mainly in the suspension stiffness value. The best solution obtained, which is significantly better than the rest, is found in the lower region of the suspension stiffness value range while all the other solutions are located in the higher region of the range. The fact that only one run out of 20 has located this optimum shows that for one, the algorithm can easily be trapped in local optima depending on the initial vector, but also that the topology of the solution space is such that the solution is not particularly easy to find.

A similar behavior, yet even more acute, can be noticed for the road excitation input. In this case, because of the nature of the excitation, the solution space is significantly more complex and highly non-convex. As a result, the algorithm is unable to produce a coherent set of optimized design vectors and appears to be very easily trapped in the numerous local optima that exist. The final result produced is practically inconclusive and unusable as to what the general location of the global optimum is. Moreover, there appears to be a relatively high homogeneity among the first 7 runs and the last three. Between the two groups, there is a very large difference in fitness values. This proves that the algorithm again got trapped near a local optimum which is significantly inferior in fitness, showing it is unable to perform a global search. The position of this local optimum inside the solution space seems to be related mainly

to the values of the supports' stiffness and the algorithm's inability to direct these parameters to the lower limit of their range.

Figure 3.21 shows the roll angle response of the system to both excitation inputs when the supports' stiffness of the system is modified. The continuous line in the plot represents the response for the 8th design vector of Table 3.17 and the dotted line shows the same system after the supports' stiffness has been set to the minimum allowable values, as it was found by the other optimized vectors. It is fairly obvious that the response is much better in the second case. As expected, when the stiffness is reduced, the oscillations of the system are attenuated in magnitude and the response becomes slower. However, the algorithm was unable to locate this clearly better solution due to the fact that it was trapped in a local optimum.

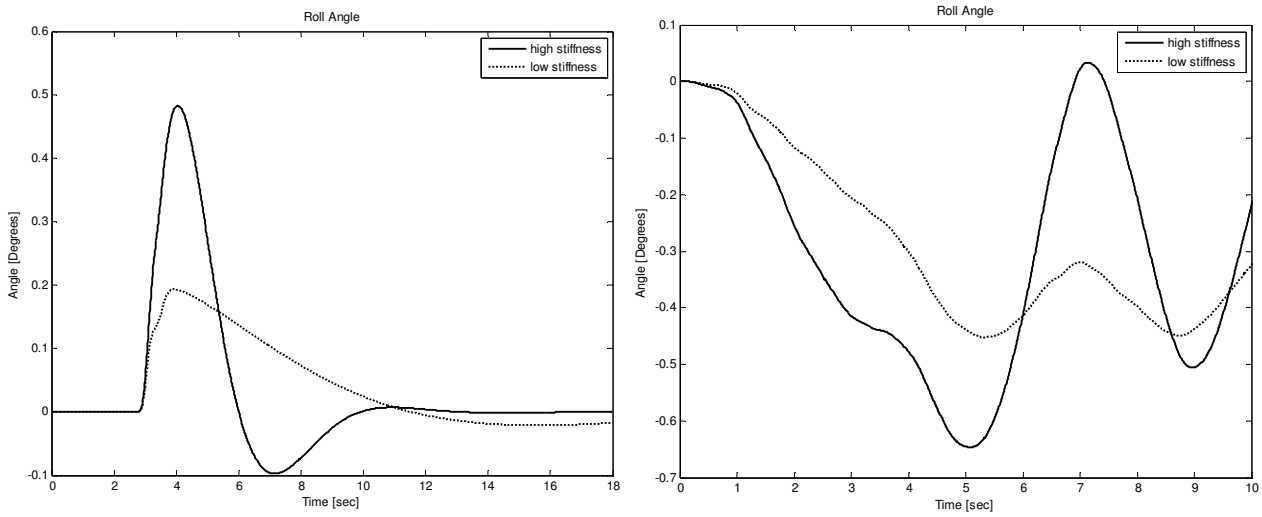

(a) (b)

Figure 3.21 LS Case 1: Support stiffness parameters (a) obstacle excitation, (b) road excitation

The optimum design vectors, as they were obtained so far for both excitation inputs in this load case, are repeated in Table 3.18 and the responses of both those systems are plotted in Figure 3.22. The continuous line represents the vector optimized for the obstacle and the dotted line represents the vector optimized for the road.

Table 3.18 LS Case 1: Optimum design vectors

LS	Obstacle excitation input	Road excitation input
F K susp	10000	347899
M K susp	10000	76551
R K susp	10000	254878
F c susp	50000	38554
M c susp	1003	10501
R c susp	1000	5691
F K supp	1000	1000
M K supp	1000	1000
R K supp	1000	1000
Σc supp	6122	11162
roll	0.1428	0.4572

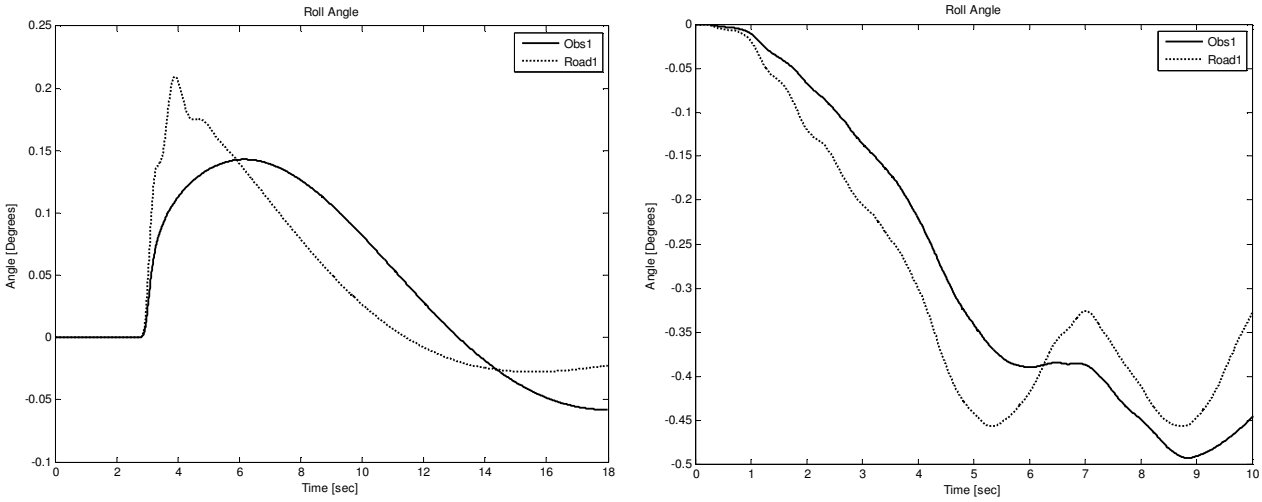

(a) (b)

Figure 3.22 LS Case 1: Optimized responses (a) obstacle excitation, (b) road excitation

3.3.2 Load Case 2: All compartments filled at 80%

For the second load case studied, the tank is by 20% lighter compared to the previous case and the results of the optimization are shown in Table 3.19 for the obstacle excitation input and in Table 3.20 for the road excitation input.

Table 3.19 LS Case 2: Obstacle excitation

LS	1	2	3	4	5	6	7	8	9	10
F K susp	10000	10000	10003	10000	405007	327787	415730	317149	475753	467097
M K susp	10003	10000	10000	10008	85232	71679	226919	97027	32558	157896
R K susp	10000	10003	10119	10082	10984	282117	188197	240768	489662	373701
F c susp	49258	49168	48410	47844	44298	47873	4703	33868	30995	11741
M c susp	3167	3561	16766	3445	25613	20502	38579	39487	35747	26272
R c susp	1222	1278	1104	18436	39494	13181	14298	17540	49969	29901
F K supp	1000	1000	1000	1000	1000	1000	1000	1000	1000	1000
M K supp	1000	1000	1000	1000	1000	1000	1000	1000	1000	1000
R K supp	1000	1000	1000	1000	1000	1000	1000	1000	1000	1000
Σc supp	5617	5583	5408	5292	4977	5029	4803	4967	4995	4986
roll	0.1565	0.1566	0.1581	0.1594	0.1621	0.1662	0.1662	0.1664	0.1664	0.1666

Table 3.20 LS Case 2: Road excitation

LS	1	2	3	4	5	6	7	8	9	10
F K susp	410832	364858	390585	379098	451975	383424	215613	305609	11127	394411
M K susp	172734	32618	87989	261112	306160	130976	270901	303731	10035	17337
R K susp	198848	252052	457116	70692	113192	283267	126027	208626	46262	457512
F c susp	42999	16779	47415	25051	22764	8096	38674	42398	20902	40058
M c susp	4580	19070	4270	5470	22147	45142	35664	36125	43903	24102
R c susp	6438	25760	36224	24198	48866	43379	3890	48309	41556	27205
F K supp	1000	1000	1000	1000	1000	1002	1004	1001	1000	1000
M K supp	1000	1000	1000	1000	1001	1003	1000	1000	1000	1001
R K supp	1000	1000	1000	1000	1000	1001	1006	1000	1000	33144
Σc supp	8290	8681	8371	8645	8742	8876	8558	8669	9121	9876
roll	0.4708	0.4723	0.4739	0.4743	0.4766	0.4779	0.4791	0.4794	0.4869	0.6574

Between the roll angle values of Table 3.19 there is a 6.4% deviation, while for the values of Table 3.20 there is a deviation of 3.4% excluding the last run, or approximately 40% if the last run is included. The roll angles of Table 3.19 are presented in Figure 3.23a and the first 9 values of Table 3.20 are shown in Figure 3.23b.

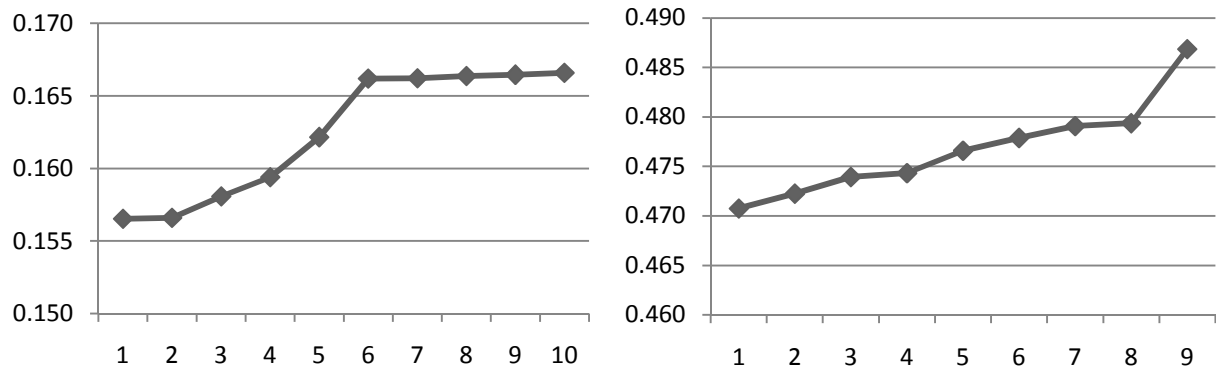

(a) (b)

Figure 3.23 LS Case 2: Roll angle (a) obstacle excitation, (b) road excitation

Clearly, for the case of the obstacle excitation input (Figure 3.23a), there is a significant difference between the group of the first few best solutions and the group of the 5 worst. As far as the nature of the solution space is concerned, by looking at the respective design vectors, it is evident that the first few vectors lie in the same approximate neighborhood of the design space. Yet the final results they produce, even though they are similar they are not especially close. This is a sign of non-convexity of the solution space and inability of the algorithm to overcome a local optimum so as to direct the search towards the better solution. On the other hand, the close proximity of the last five solutions fitness-wise, is a phenomenon not attributed to the location and approximation of the exact same local optimum in the solution space, but rather the existence of numerous local optima with the same objective function value dispersed in the entire search space. In other words, there appear to be numerous local optima of the same or extremely proximate objective function value scattered throughout the solution space and at the same time various local optima of better fitness value in the neighborhood of the global optimum, where the algorithm can also get trapped.

The same phenomenon yet even more amplified is observed for the road excitation input. As anticipated, the increased complexity of this excitation signal produces a more complex response and as a result the solution space is more diverse and with increased non-convexity. The local optima are more frequent which is indicated by the fact that none of the solutions found was approaching the global optimum. Instead the design vectors are scattered throughout the solution space. There only appears to be a general agreement on the supports' stiffness and damping sum values by the majority of the runs, which stresses the increased importance of these parameters compared to the rest, in the response of the system and consequently the whole optimization process.

The optimum solutions found for this particular load case are shown in Table 3.21 and the respective responses are plotted in Figure 3.24. The continuous line represents the vector optimized for the obstacle and the dotted line represents the vector optimized for the road.

Table 3.21 LS Case 2: Optimum design vectors

LS	Obstacle excitation input	Road excitation input
F K susp	10000	410832
M K susp	10003	172734
R K susp	10000	198848
F c susp	49258	42999
M c susp	3167	4580
R c susp	1222	6438
F K supp	1000	1000
M K supp	1000	1000
R K supp	1000	1000
Σc supp	5617	8290
roll	0.1565	0.4708

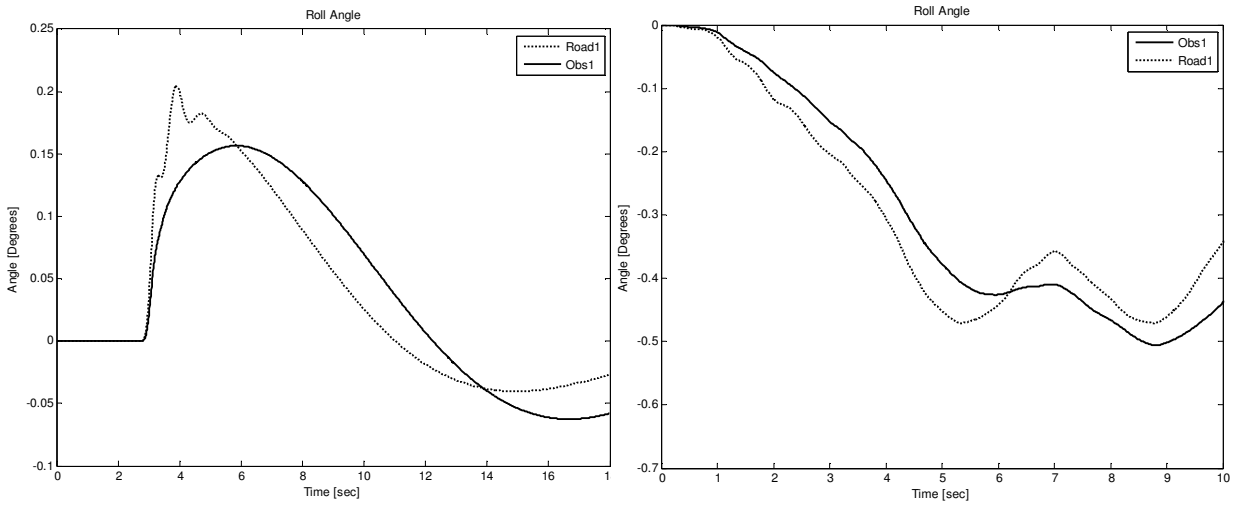

(a) (b)

Figure 3.24 LS Case 2: Optimized responses (a) obstacle excitation, (b) road excitation

3.3.3 Load Case 3: All compartments filled at 50%

In this load case the tank is half filled and therefore has half the weight compared to the first case. This should make the system more sensitive to the excitation and increase the magnitude of the response. Out of the 20 runs executed for the different inputs, the ten best are shown in Table 3.22 and Table 3.23.

Table 3.22 LS Case 3: Obstacle excitation

LS	1	2	3	4	5	6	7	8	9	10
F K susp	10000	10000	499992	498188	499362	496804	469906	496261	499096	488251
M K susp	10000	10000	10051	11131	10789	13121	21487	33129	10000	12980
R K susp	10000	10000	10001	21247	11022	21511	48872	26949	49758	78730
F c susp	50000	49999	49779	45626	48918	45444	26429	46202	38961	26915
M c susp	1000	1000	16921	14576	9646	2126	16426	43529	35662	24761
R c susp	1000	1000	2208	6519	22010	37342	19939	11787	21256	32731
F K supp	1000	1000	1000	1000	1000	1000	1000	1000	1000	1000
M K supp	1000	1000	1000	1000	1000	1000	1000	1000	1000	1000
R K supp	1000	1000	1000	1000	1000	1000	1000	1000	1000	1000
Σc supp	4711	4710	3806	3822	3806	3857	3730	3998	3955	3923
roll	0.1861	0.1861	0.1913	0.1916	0.1925	0.1932	0.1933	0.1937	0.1937	0.1944

Table 3.23 LS Case 3: Road excitation

LS	1	2	3	4	5	6	7	8	9	10
F K susp	495242	472386	470437	494633	499221	455687	499694	499996	488794	481187
M K susp	10832	10000	10042	10006	10000	12241	10586	10340	487382	312401
R K susp	10191	10001	11147	10002	10055	25435	28927	39770	163347	199922
F c susp	36911	40053	44367	31684	45290	9712	16704	46816	46065	15998
M c susp	5614	3075	1019	1412	3646	22939	40586	17298	29218	38018
R c susp	1275	1411	1012	6578	1275	9647	8175	33816	6279	46162
F K supp	1000	1000	1000	1000	1000	1000	1000	1000	1000	1000
M K supp	1000	1000	1000	1000	1000	1000	1000	1000	1000	1000
R K supp	1000	1000	1000	1000	1000	1000	1000	1000	1000	1000
Σc supp	5987	6024	6149	5908	6134	5207	5119	4700	5640	5851
roll	0.5036	0.5037	0.5038	0.5038	0.5040	0.5071	0.5092	0.5121	0.5257	0.5264

In order to visualize the quality of each solution, the roll angles obtained are shown in the graphs of Figure 3.25. For both excitation inputs the 10th best value lies within approximately 4.5% of the optimum one found.

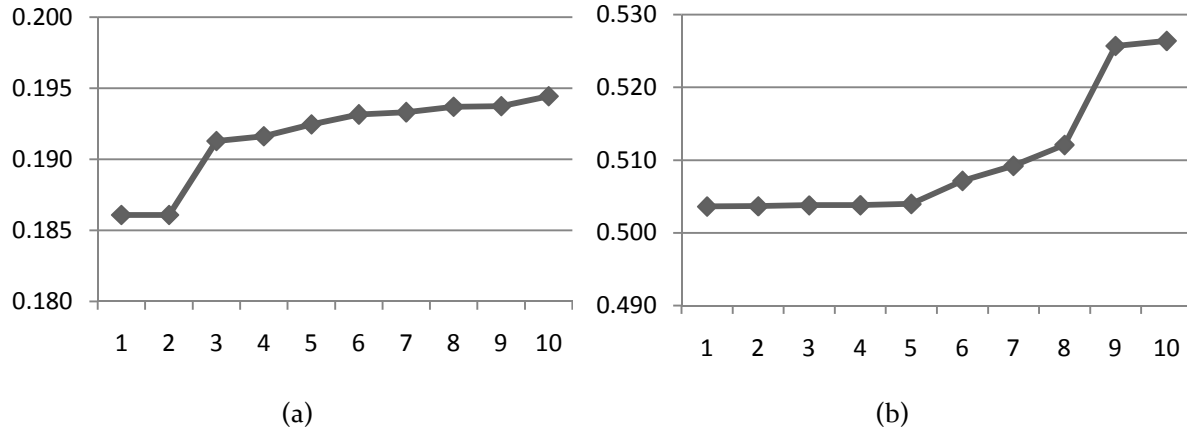

(a) (b)

Figure 3.25 LS Case 3: Roll angle (a) obstacle excitation, (b) road excitation

For the first excitation, it is apparent that the first two solutions produce a far superior result compared to the rest. In fact, by looking at the respective design vectors, these two solutions are practically identical, clear indication that this exact point in the solution space is a strong local optimum (or compared to what has been found so far the global optimum.) The other solutions appear to have been trapped while searching for a different strong local optimum, better approached by the 3rd solution as it seems.

For the second excitation, the five best solutions seem to be moving around the same general neighborhood and searching for the same strong local. The fitness values obtained are extremely close, perhaps even closer than would be normally expected by examining the respective design vectors. This could indicate that again, the design space has sort of a small plateau along some its dimensions, which inhibits the algorithm's effort to direct the search towards the local optimum solution.

Table 3.24 shows the optimum design vectors that were presented in the above tables for this particular load case and Figure 3.26 shows the response of the system for each of these vectors.

Table 3.24 LS Case 3: Optimum design vectors

LS	Obstacle excitation input	Road excitation input
F K susp	10000	495242
M K susp	10000	10832
R K susp	10000	10191
F c susp	50000	36911
M c susp	1000	5614
R c susp	1000	1275
F K supp	1000	1000
M K supp	1000	1000
R K supp	1000	1000
Σc supp	4711	5987
roll	0.1861	0.5036

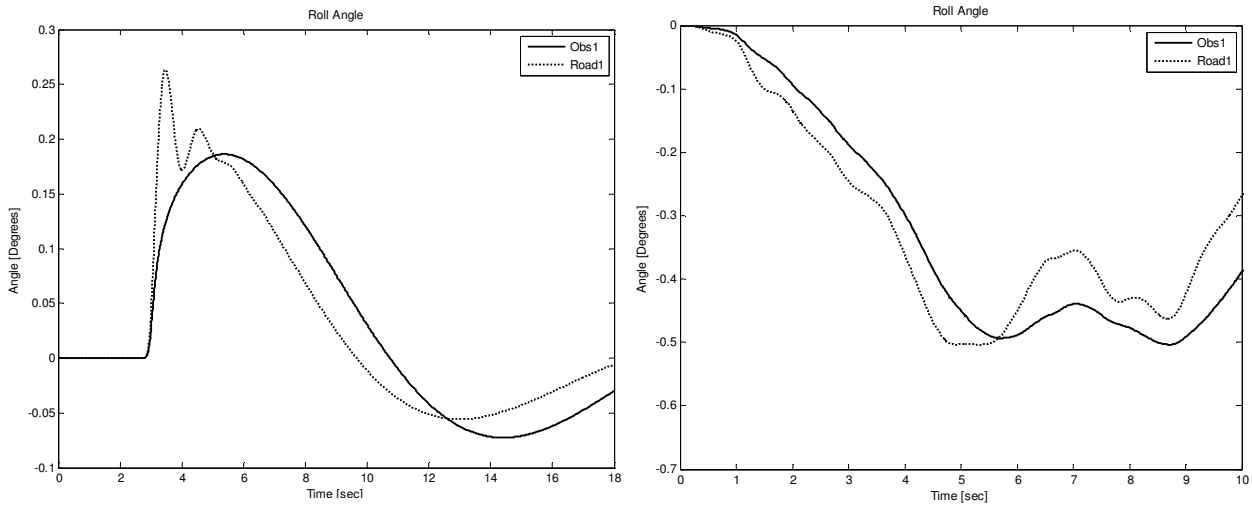

(a) (b)

Figure 3.26 LS Case 3: Optimized responses (a) obstacle excitation, (b) road excitation

It is very interesting to notice how Figure 3.26b shows two almost equally good responses of the system as far as the objective function is concerned, yet the two design vectors are optimized for completely different excitation inputs and are significantly different. This can be attributed to the fact that the optimized vector for the road excitation is not in fact the problem's global optimum solution. The algorithm was trapped in a completely different local optimum. However, comparing it to the optimum solution found by the GA for the same problem (section 3.2.3), although the distance between them in the solution space is significant, the two just happen to produce a very similar final result.

3.3.4 Load Case 4: All compartments filled at 20%

For the final loading case the tank is filled by only 20% and is extremely light making the system even more responsive to the excitations of the road. The optimization was executed 20 times for each excitation input with random initial vectors and the ten best results obtained are presented in Table 3.25 and Table 3.26.

Table 3.25 LS Case 4: Obstacle excitation

LS	1	2	3	4	5	6	7	8	9	10
F K susp	10000	10000	10001	499699	448650	499399	346233	494705	378698	482535
M K susp	10000	10000	10000	10013	69819	10135	10227	10068	11852	18992
R K susp	10046	10332	10991	167813	117294	104491	109484	145242	153775	232713
F c susp	49999	50000	49733	48350	49971	49120	48999	48755	45135	45277
M c susp	1000	1000	1303	10776	6834	36562	41712	42277	32739	24548
R c susp	1000	1000	1024	2762	1294	10812	5235	11805	1016	14438
F K supp	1000	1000	1000	1000	1000	1000	1000	1000	1000	1000
M K supp	1000	1000	1000	1000	1000	1000	1000	1000	1000	1000
R K supp	1000	1000	1000	1000	1000	1000	1000	1000	1000	1000
Σc supp	3535	3544	3522	3109	3150	3194	3279	3144	3163	3129
roll	0.2465	0.2465	0.2468	0.2602	0.2609	0.2621	0.2626	0.2630	0.2636	0.2644

Table 3.26 LS Case 4: Road excitation

LS	1	2	3	4	5	6	7	8	9	10
F K susp	10000	499944	499172	407341	467187	10150	241430	323180	277537	342204
M K susp	10008	10004	11314	120572	459244	12928	33111	129910	106910	148031
R K susp	74762	490596	307581	403087	333456	96858	499989	499982	490545	499918
F c susp	49967	41091	25096	49578	45874	49989	49966	49985	49556	49963
M c susp	1393	2987	2760	28904	46173	14427	1007	1012	4048	1029
R c susp	3027	1012	13156	18549	47412	5437	1003	1000	1943	2123
F K supp	1000	1000	1000	7810	3445	49927	49968	46743	48596	48199
M K supp	1000	1000	1000	5321	1357	49942	49996	47311	49947	49932
R K supp	1000	1000	1000	2688	11535	46593	49992	46364	45399	41530
Σc supp	11180	9591	5965	10246	11628	14248	301	349	318	315
roll	0.5720	0.5932	0.5951	0.6583	0.6848	0.7172	0.7647	0.7710	0.7729	0.7735

The roll angles for the ten best runs of every excitation are plotted in Figure 3.27.

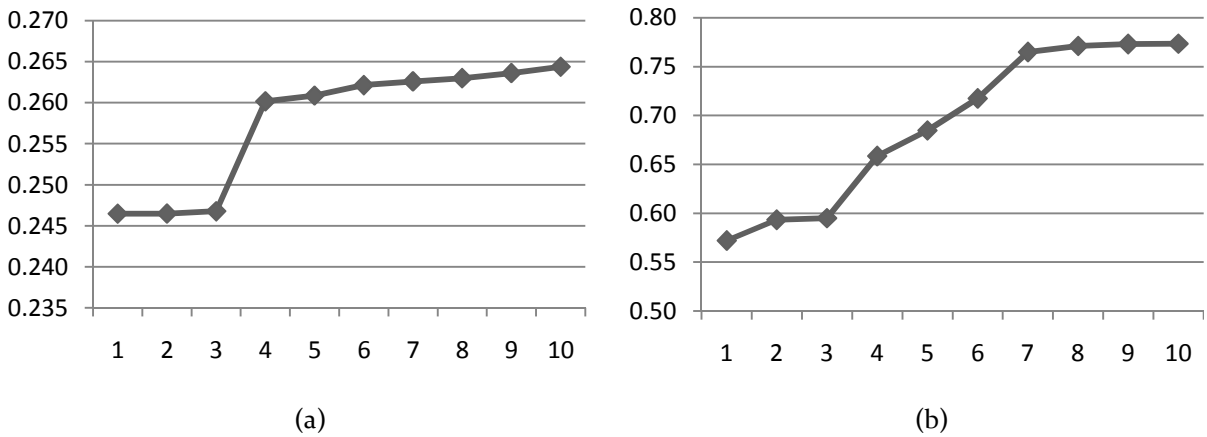

Figure 3.27 LS Case 4: Roll angle (a) obstacle excitation, (b) road excitation

Figure 3.27a clearly shows that the results obtained in the first three runs are significantly better than the rest. By examining the respective design vectors it is clear that these vectors have almost identical parameter values, meaning they have approached the same local optimum. The main difference with the other solutions is the extremely elevated front suspension stiffness value, which indicates the existence of another strong local optimum in that region, as has been noted previously. However, in this load case, because of the topology of the solution space due to the excitation, the two local optima have a large difference in their fitness value. The algorithm, unable to search globally, gets trapped in it anyway.

The general picture that can be extracted from Table 3.26 and Figure 3.27b seems somewhat expected. Due to the complexity of the solution space and the numerous local optima, only one solution out of 20 was able to separate itself from the rest and end up in the approximate area where the global optimum is located. However, again the algorithm could not avoid getting trapped in local optima during the process and the global optimum could not be located very closely. The best solution obtained is still quite poor. As far as the rest of the solutions are concerned, they were trapped very fast in local optima with much inferior fitness values, as the algorithm is unable to perform a global search. As long as the parameters of the support stiffness are located on the lower limit of the allowable range, the solutions produced are improved significantly, as it seems by the group of the first three design vectors.

In summation, the optimum design vectors found in this section are presented in Table 3.27 and the respective responses of the systems are plotted in Figure 3.28.

Table 3.27 LS Case 4: Optimum design vectors

LS	Obstacle excitation input	Road excitation input
F K susp	10000	10000
M K susp	10000	10008
R K susp	10046	74762
F c susp	49999	49967
M c susp	1000	1393
R c susp	1000	3027
F K supp	1000	1000
M K supp	1000	1000
R K supp	1000	1000
Σc supp	3535	11180
roll	0.2465	0.5720

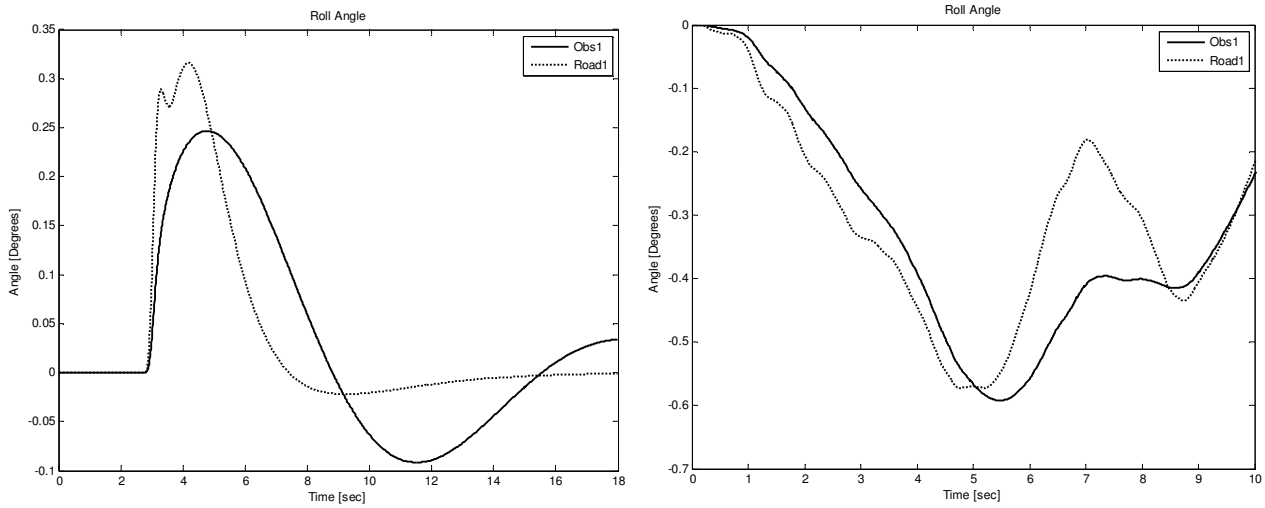

(a) (b)

Figure 3.28 LS Case 4: Optimized responses (a) obstacle excitation, (b) road excitation

In Figure 3.28a, the double peak that can be noticed in the response, is due to the deviation of the second design vector from the lower limit for the rear suspension stiffness.

Chapter 4

4 Conclusions

In the final chapter of the current work, all the conclusions that were drawn while conducting this study are analyzed. These include a comparison between the capabilities and general behavior of the algorithms used, a description of how the system's response is modified when the excitation input or the loading cases change, how the dynamic system behaves in general and why, and lastly the study's proposition for the values of the parameters in question. In the final section possible ways to expand the current work are described, as they arose through the close involvement and friction with the subject during the preparation of this study.

4.1 Optimization algorithms

During the course of the optimization, both algorithms were not always successful in locating the globally optimum solution. Each to a different extent, they either became trapped in local optima, close or far away from the general position of the global optimum in the design space or simply reached a point where they were for various reasons unable to further improve their position and fitness. Apart from the final values for the roll angle obtained by each method's optimum design vector, the frequency and location of the trapped solutions compared to the rest, and also the homogeneity in the parameter values of the solutions, help determine the general efficiency of the algorithms as well as their strengths, weaknesses and search capabilities. The following figures establish a comparison between the two methods' general efficiency and robustness. They show the ten best objective function values obtained out of a total of 20 for each load case (rows) and each excitation input (columns). The first column of the figures depicts the results for the obstacle excitation input and the second column those of the road profile. The dark-colored line represents the results of the genetic algorithm while the light-colored line the results of the BFGS method.

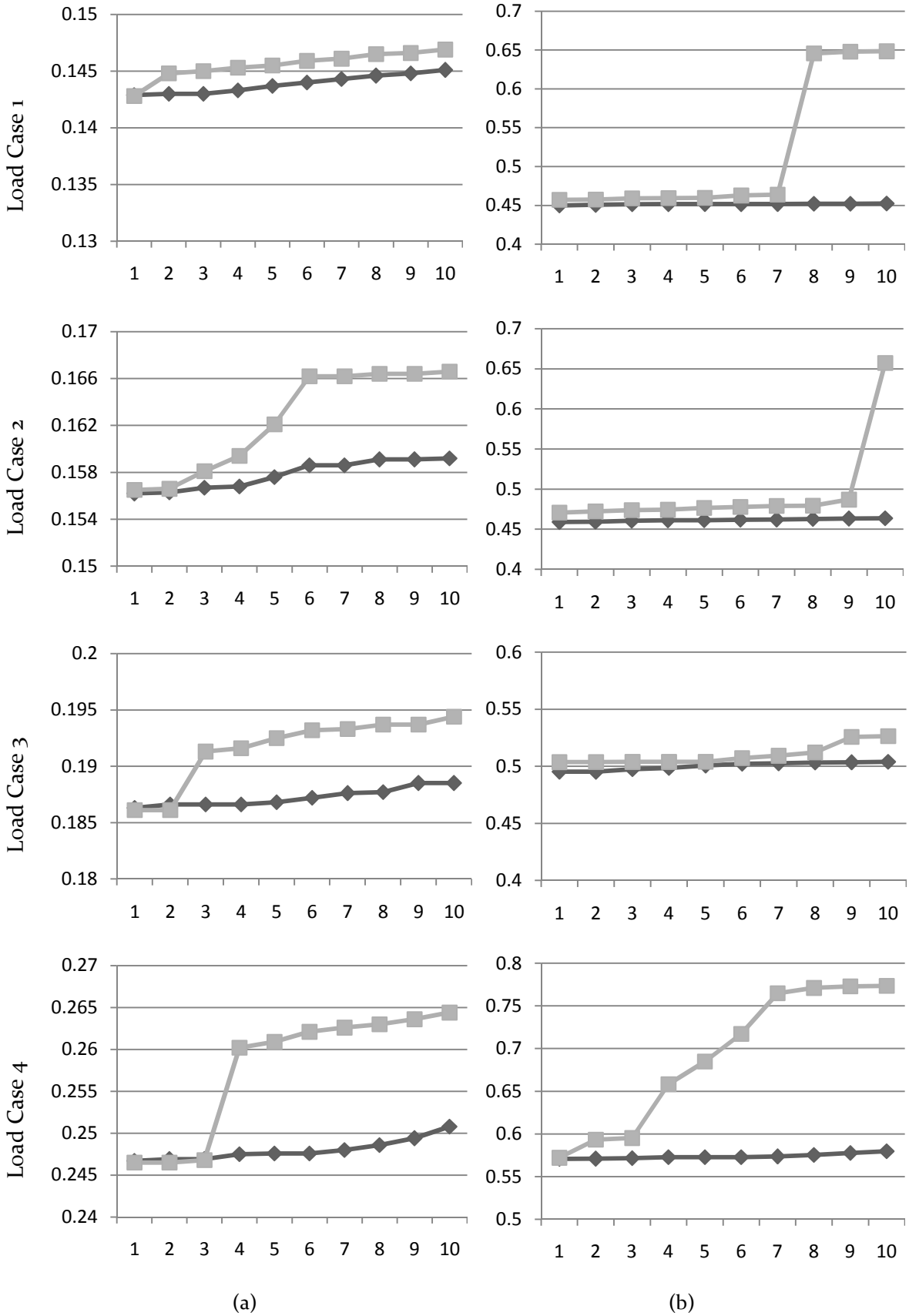

Figure 4.1 Roll angles per load case (a) obstacle excitation, (b) road excitation
GA: dark-colored line, BFGS: light-colored line

It is obvious that in general, the genetic algorithm produces superior results compared to the BFGS method for solving this problem. As the results of section 3.2 can also confirm, the GA shows good global search capabilities by scanning the entire search space efficiently and by avoiding being frequently trapped in local optima away from the global one. Even when the solution space of the problem was highly non-convex with multiple strong local optima, the GA was able to locate the optimum solution or at least arrive close to it. The results obtained had good repeatability, sign of a robust and reliable method. However, the algorithm showed weakness in locating the exact position of the global optimum and lacked strong local search capabilities. Once the population had converged in the neighborhood of the global optimum, it was difficult for the algorithm to locate its exact position or further improve the attained fitness. Instead, the final optimum solution obtained, lied very close to the global optimum in the design space and was not even necessarily a local optimum. This behavior was intensified when the optimum solution for an individual parameter was located on the boundaries of the design space and had to be approached from within the feasible region.

On the other hand the BFGS method produced much more diverse results within the group of the 20 runs of every test case. The tables of section 3.3 which contain the design vectors for the values presented in Figure 4.1, show that the solutions obtained have reduced homogeneity and do not lie very close to each other within the solution space. Since this method performs a single-point search of the solution space and moves from the initial point towards the strongest local optimum in the vicinity, it completely lacks global search and hill climbing capabilities. In complex problems, such as the one in hand, this means that it can be very easily trapped in local optima. However, this method has strong local search capabilities and the exact location of each optimum can be determined precisely. Depending on the position of the initial vector and/or the topology and convexity of the solution space the results obtained ranged from slightly better than the GA, when the local optimum found happened to be the global one, to significantly worse when the local optimum was random. In general the method is considered far less reliable than the GA for the particular type of problem.

4.2 Excitation input

The differences in the response of the system by changing the excitation input from the obstacle course to the road course are very noticeable in all the loading cases presented and to a large degree expected. For one, the roll angle time-response for the obstacle course is much simpler since the excitation itself is simpler. There is an initial peak at the point the pothole is

encountered on the road, then the system oscillates slightly and the excitation is damped according to the parameters selected. The relation between the parameters and the response is straightforward and fairly easy to determine due to the relatively simple nature of the system and the excitation. On the other hand, the road profile is significantly more complex and rich, with numerous peaks and valleys on both tracks which excite the system on many frequencies. These different peaks and valleys of the excitation signals of the two tracks are combined and attenuated or amplified according to the individual vehicle parameters, to produce the respective responses presented in the previous sections. The form of the response is very much attributed to the form of both track signals as well as the parameters selected.

With the road profile excitation, the solution space becomes more complex and highly non-convex. Therefore, the algorithms, and especially the BFGS method, are more susceptible to being trapped in local optima. This led the BFGS method to being terminated prematurely and faster than usual on numerous occasions –depending on the randomly selected initial vector- while it was trapped in a position far away from the global optimum.

As far as the individual parameters of the optimum design vectors are concerned, it is clear that between the two inputs, the main difference is expressed in the value of the supports' damping sum. For the same load case, the road profile generally demands a greater value for this parameter.

4.3 Load cases

By examining the responses produced for the different load cases it is clear that as the tank gets emptier and lighter, the reduced inertia of the tank mass makes the system more sensitive to the same excitations thus the response of the system is amplified. Figure 4.2 shows the optimized roll angle time-responses for every load case of the obstacle excitation input and Figure 4.3 is the respective graph for the road excitation input. The load cases are expressed by the percentage of the tank being filled in each.

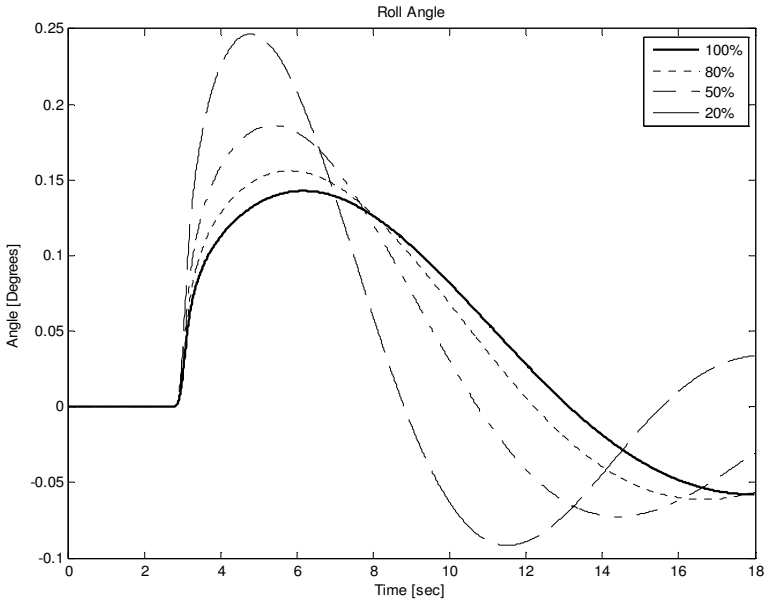

Figure 4.2: Optimized responses for the obstacle excitation

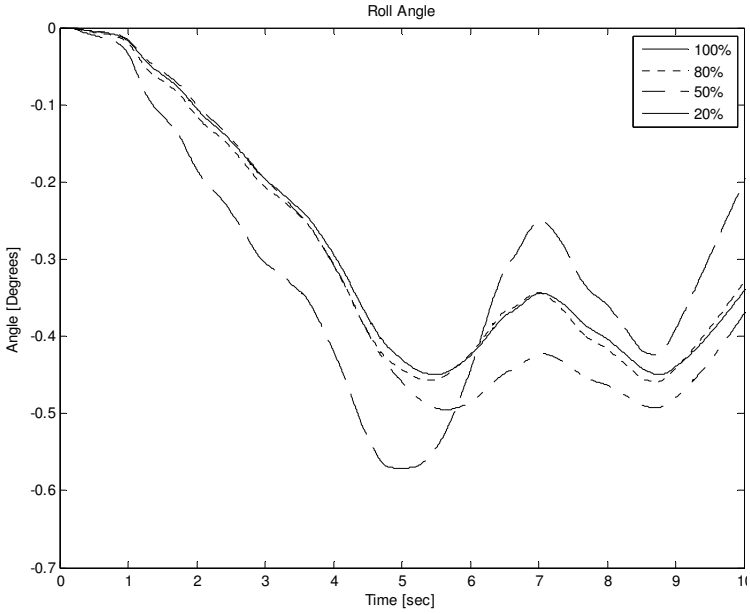

Figure 4.3: Optimized responses for the road excitation

From Figure 4.2 it is evident that the optimum response becomes sharper as the tank becomes lighter. The tank reacts faster to the initial disturbance and the maximum occurring roll angle increases in magnitude. The system oscillates more and it takes more time to return to the equilibrium state. Figure 4.3 shows that the optimum solutions are obtained when the two valleys which appear in the graph of the roll angle are of equal magnitude. For the fourth load case this does not seem to happen with the current settings, as it will be more clearly explained later on. The tank has become so light, even lighter than the weight of the chassis, and thus its movement is affected more intensely by the movement of the chassis. As a result, the initial

disturbances and the magnitude of the first valley cannot be attenuated enough, in the first place, in order for the two to become equal. (see also Figure 4.5) .

Table 4.1 shows the optimum design vectors as they were determined for the obstacle excitation input and Table 4.2 contains the respective vectors for the road profile input. The solutions presented for cases 1, 3 and 4 of Table 4.1 were located using the BFGS method and the rest by the GA.

Table 4.1 Optimum design vectors for the obstacle excitation

Obstacle excitation input	Case 1	Case 2	Case 3	Case 4
F K susp	10000	10000	10000	10000
M K susp	10000	10000	10000	10000
R K susp	10000	10000	10000	10046
F c susp	50000	49804	50000	49999
M c susp	1003	1000	1000	1000
R c susp	1000	1000	1000	1000
F K supp	1000	1000	1000	1000
M K supp	1000	1000	1000	1000
R K supp	1000	1000	1000	1000
Σc supp	6122	5755	4711	3535
roll	0.1428	0.1562	0.1861	0.2465

Table 4.2 Optimum design vectors for the road excitation

Road excitation input	Case 1	Case 2	Case 3	Case 4
F K susp	21493	10003	10000	10000
M K susp	10000	10000	10000	10000
R K susp	10000	10001	10000	10000
F c susp	39024	49734	47508	49405
M c susp	1193	1000	1000	1001
R c susp	1000	1001	1000	1002
F K supp	1000	1000	1000	1000
M K supp	1000	1000	1000	1000
R K supp	1000	1000	1000	1000
Σc supp	12838	11681	5412	7512
roll	0.4498	0.4590	0.4952	0.5707

It appears that, for the cases of the obstacle excitation input (Table 4.1), the only parameter of the optimum design vectors that practically changes from one load case to the next, is the value of the supports' damping sum. The other parameters remain almost unchanged, except for some minor deviations which do not generally affect the final result to a significant extent

and can be attributed to the innate inabilities and weaknesses of the algorithms' explained in section 4.1. For the road excitation input, shown in Table 4.2, the general picture is similar. The main difference between the design vectors lies again on the supports' damping sum value. For the first load case, the optimum design vector is also differentiated for the front suspension stiffness and damping values by a small margin. As has been explained earlier, when the tank is heavy, the inertia of the tank is increased and the system becomes less responsive. Slightly increasing the stiffness of the front suspension and lowering the damping seems to improve the final outcome by making the tank react faster on the initial disturbance.

The relation between the supports' damping and the filling percentage of the tank is shown in Figure 4.4

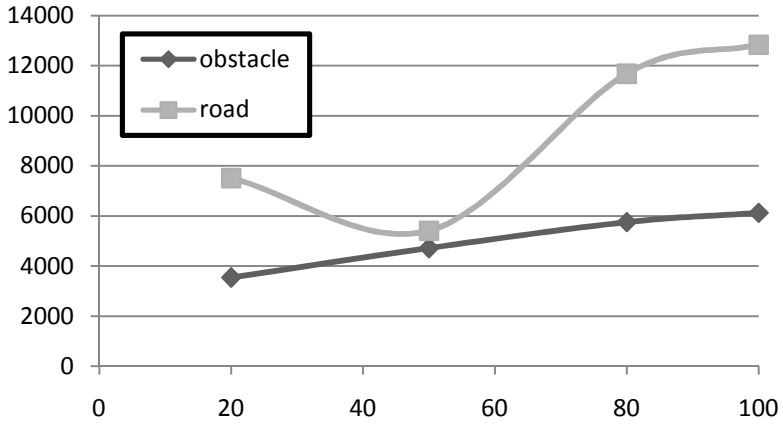

Figure 4.4 Supports' damping sum vs tank fill percent (a) obstacle excitation, (b) road excitation

It is interesting to notice how for the road profile input, the relation for the damping is not monotonous with the tank mass. For the third load case, when the tank is filled by 50%, the damping value found is significantly lower than expected. Various extra intermittent optimization test cases that were executed for the tank filled between 20 and 80% showed that the results do in fact follow this curve. Figure 4.5 shows the response to the same design vector as only the tank's mass increases. The dotted line represents the full tank, the continuous line is for a half-full tank and the dashed line represents a tank filled at 20%.

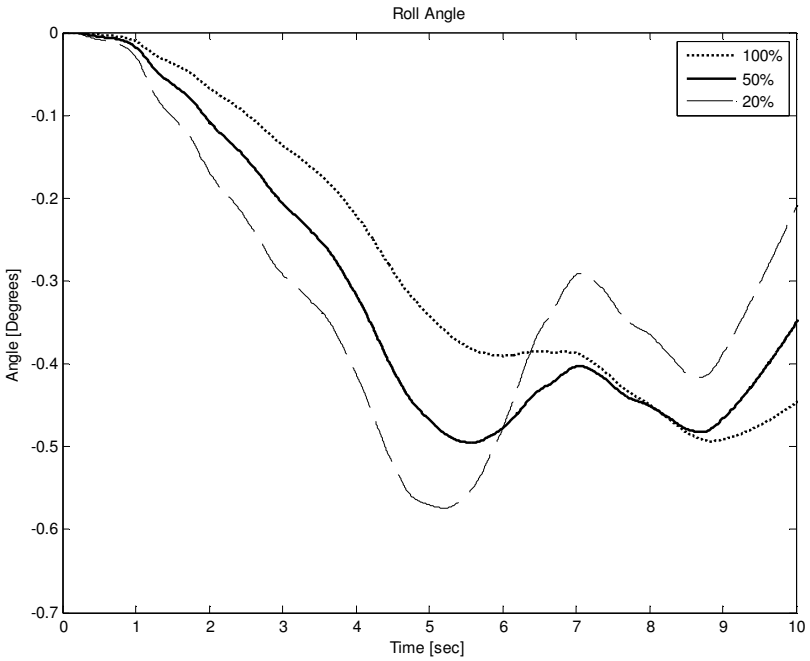

Figure 4.5 Roll angle vs tank fill percent for the road excitation

As it seems, as the tank's mass changes, the point of occurrence of the maximum roll angle in the response of the tank is shifted between the first and the second valley. It has already been mentioned, that the optimum solution is achieved when the two are of equal magnitude. When the tank is full and its inertia is high, the response is slower at first and the maximum angle appears at the second valley. Damping has to be increased in order to make the initial response faster and more intense so that the first valley is amplified and the second is attenuated. On the other hand, due to the low inertia, the response of the light tank is very fast at the beginning but the magnitude is also very high. Increasing the damping might indeed accelerate the initial response further but it will also dampen the magnitude of the disturbance which is more desirable in this case. Even so, because of the small inertia of the tank in this case, the two valleys for the light tank can never become equal so reducing the magnitude of the first of the two is the best that can be achieved.

4.4 Topology of the solution space

So far, it has been shown that the optimum solutions are found near the boundaries of the design space. With the exception of the supports' damping which varies with the load case, all the other variables are consistently driven towards the lowest limit, or in the case of the front suspension stiffness the upper limit of the respective allowable range.

As far as the suspensions are concerned, the sprung-to-unsprung mass ratio is extremely high due to the nature and loading of the vehicle. The inertia of the tank/chassis system is larger compared to the inertia of the wheels. When the suspension is softer, the unsprung mass (wheel system) is able to move more freely and absorb the vibrations from the road, so that they are not transferred to the vehicle. Since the roll angle of the tank is examined, reducing the amount of disturbances that pass from the wheels to the vehicle is the primary concern and therefore softer springs perform better. The same principle applies for the springs of the supports of the tank. However, in this case, since the chassis is much heavier than the wheels, the sprung-to-unsprung mass ratio is significantly lower than before and the movement of the unsprung mass is more difficult to be filtered. When the tank is approximately half filled, that ratio is close to 1. When the tank is heavier and the ratio increases and the response is better.

The different sprung-to-unsprung mass ratio that the two suspensions see, also explains why the contribution of the supports' parameters to the roll angle response is more important than that of the suspensions'. This has been made especially evident from the fact that the BFGS method, which does not possess good global search capabilities, is able to locate the optimum values for the supports' stiffness more consistently than any other parameter and more easily so as the tank gets lighter. When the tank is very light though (section 3.3.4), other factors also come in play. The tank is more influenced from all parameters and the solutions space becomes highly non-convex, which hinders the search for the algorithm and this picture is distorted. But, still, the increased importance of these parameters is also evident from the fact that their slight deviations away from the lowest value appear to be more harmful to the roll angle than the deviations of any other parameter (see Figure 3.20b, Figure 3.23b, Figure 3.27b and Table 3.17, Table 3.20, Table 3.26 respectively).

Damping on a dynamic system determines the rate at which the magnitude of the oscillation is reduced. When damping is low, the system oscillates until it gradually returns to the initial equilibrium state. As damping increases, it reaches a critical point where the response is such that the system returns to equilibrium as quickly as possible without oscillating. From that point on, as damping increases further, the system returns to equilibrium without oscillating but slower. Since the force produced by the damper is proportionate to the travel speed of the suspension, fast vertical movement of the wheel produces larger damping forces which resist movement. As the wheel meets an obstacle, it is inclined to move up or down at a speed determined by the vehicle's speed and the profile of the obstacle. In that case, a high damping

value restricts the suspension's travel speed and the suspension reacts initially as if it were stiffer.

The response of the roll angle is found to be optimal when the front suspension has a high damping value. The vehicle is lighter in the front, since the tank is in the back, and the sprung-to-unsprung mass ratio is lower for the front wheel. Increased damping makes the response, at the exact time the excitation is met by the wheel, faster and more intense but after that it reduces the overall magnitude more and makes the system return to stability faster. When damping is low, the initial response to the excitation is slower and milder but the overall magnitude is not damped as efficiently and the system needs more time to return to a state of equilibrium. Apparently the optimum spot between the two behaviors is found higher than the allowable range which drives this parameter to the highest allowable value. The middle and rear suspensions lie below the tank of the vehicle and therefore the sprung-to-unsprung mass ratio seen by them is significantly increased. It was found that high damping values for them do not really improve damping capabilities, but merely make the abnormalities of the road slightly more noticeable to the tank, as they make the suspensions appear artificially stiffer at the exact time the excitation is met by the wheel. As a result the optimal values for them are very low for this particular objective and therefore the respective parameters are driven to the lowest allowable limit.

As far as the damping of the tank's supports is concerned, it was found to be the only parameter that changed according to the loading. It has already been explained in section 3.2.1 how the modeling of the vehicle and tank as rigid bodies makes the use of individual damping values for the three supports redundant. The selection of the appropriate value for this parameter has to do with the mass of the tank and the profile of the excitation. Previously in this section it was discussed how damping affects the response at the time the excitation is met and how later on. This phenomenon is much clearer for this particular parameter because the optimum solution happens to be within the allowable range. Figure 4.6a shows the roll angle response to an obstacle with the use of the optimum damping value (continuous line), a lower value (dotted line) and a higher value (dashed line).

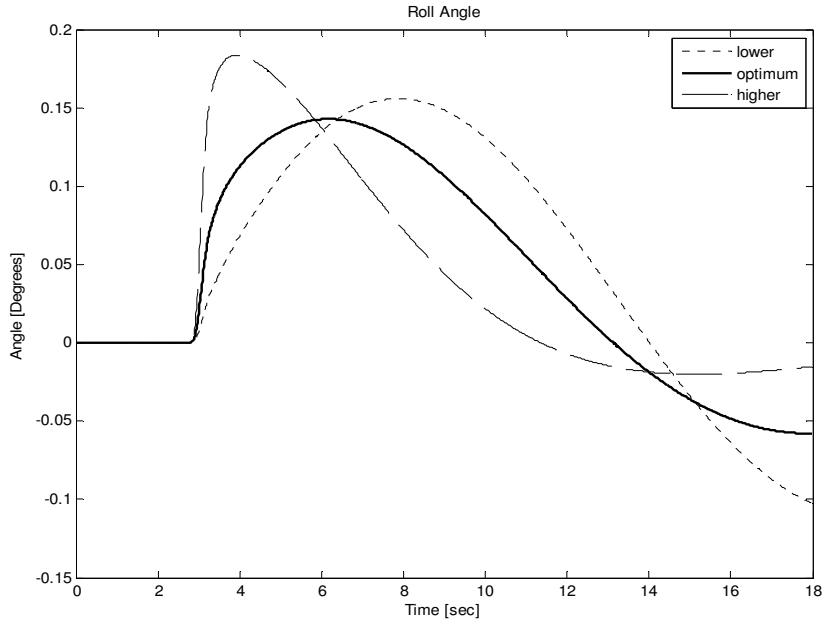

Figure 4.6 Roll angle response vs supports' damping

When damping is high, the sprung mass is moved more violently at the time of the excitation is encountered but this movement is damped faster later on. Lower than optimum damping produces a movement which is smoother and slower in the beginning but the resulting magnitude is higher and equilibrium is reached slower. For the obstacle excitation, it was found that, as the mass of the tank and its inertia increases, the optimum damping value also increases in order to compensate. For the case of the road excitation, it was found that the progression of the supports' damping parameter was not monotonous with the increase of the tank's mass (Figure 4.4). The dynamic behavior of the system proves far more complex due to the nature of the excitation and the optimum values obtained for that case represent the balance points between conflicting targets and behaviors of the system affecting the objective of the optimization (see also section 4.3).

4.5 Optimum solution

So far, through the preceding analysis, it has been shown and explained that the optimum design vectors for all the examined load cases and excitation inputs are quite similar and are neighboring in the design space. The front suspension damping is found to be very high in general, optimally placed near the upper limit of the allowable range, while the values of the suspension and support stiffnesses as well as the middle and rear suspension damping are optimally located at the lower limit of their respective allowable range (Table 4.1 and Table 4.2). The defining factor which differentiates the individual cases in the optimization is the supports' damping. The optimum value for each respective load case can be determined according to Figure 4.4. However, since the truck can only have one set of such components installed at any given time while the loading cases constantly change, there should be a value selected which can perform satisfactory for all cases.

In order to make an educated selection, the time-response of the roll angle for all the load cases is presented indicatively for the vectors with the highest (12838 N.s/m), median (6122 N.s/m) and the lowest (3535 N.s/m)damping value. These are the first vector of Table 4.2 for the road, and the first and last vectors of Table 4.1 for the obstacle, respectively. The results are shown in Figure 4.7. The high damping value is represented by the dotted line, the median value by the continuous line and the lowest value by the dashed line.

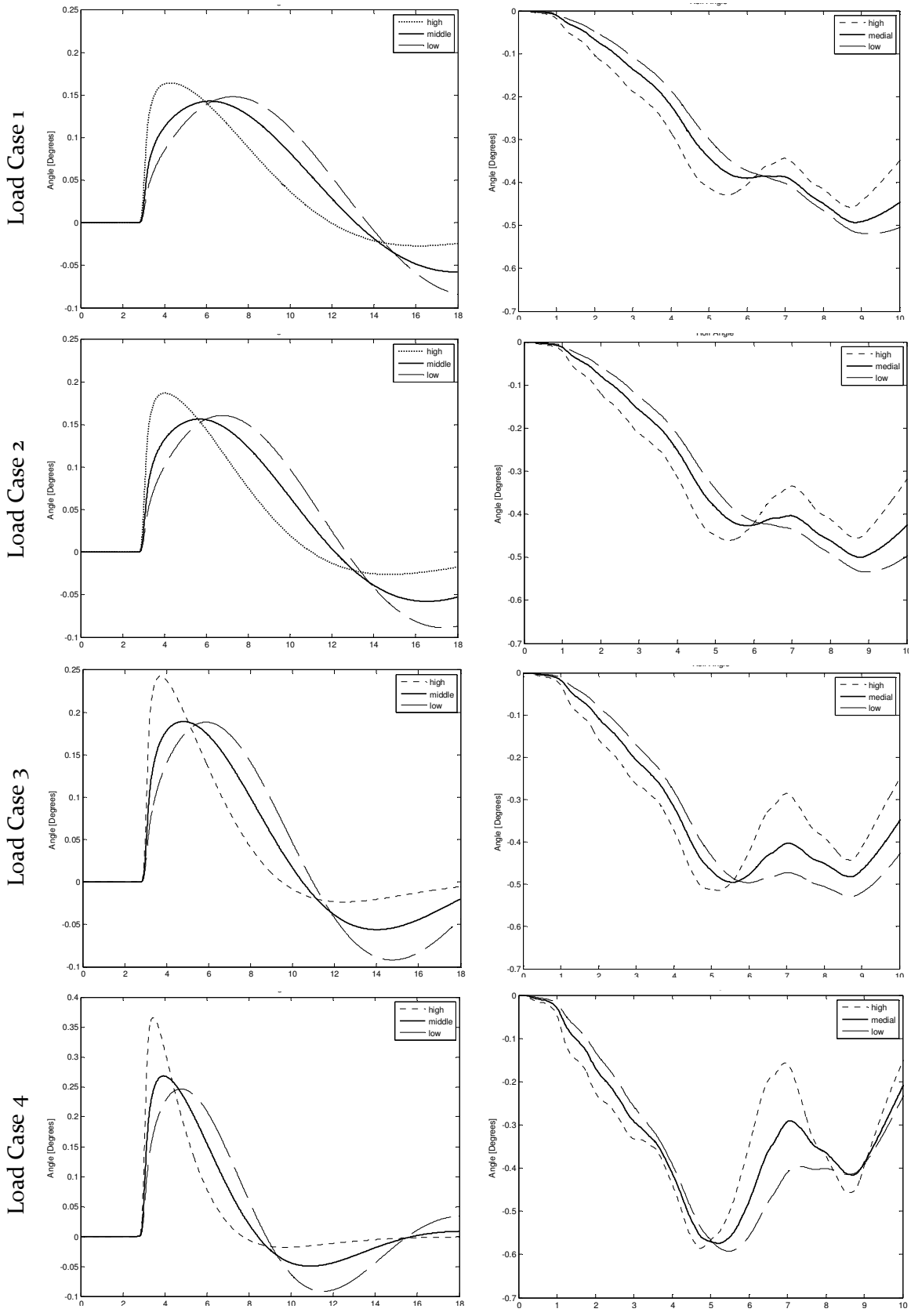

Figure 4.7 Roll angle response vs support damping (a) obstacle excitation, (b) road excitation high value: dotted line, medial: continuous line, low: dashed line

It appears that the high damping value is very ineffective for all the load cases of the obstacle course. Even though the excitation is damped faster, the respective peak is significantly higher and since the objective is the minimization of the roll angle, this solution seems too aggressive. From the above graphs, a high damping value is found to be optimal only when the tank is heavy and on a road course. When the lowest damping value is selected, the best performance is obtained when the tank is light on an obstacle course. For a light tank on the road course the response does appear somewhat smoother than the median value but the maximum occurring angle is higher. The median value performs best when the tank is not very light on an obstacle course or is light on the road. When the tank is heavy and on a road course, the response of the median value is smoother than that of the heavy damping but the peak is found to be higher.

An additional factor that should be taken into consideration is that the roll angles are increased as the tank gets lighter. This means that the gravity of the selection should be adjusted accordingly. When emphasis is given in minimizing the response of the light tank, the response of the heavy tank may be somewhat increased. However this way, the overall behavior remains more uniform and the supremum of the roll angles is kept lower.

As an all-around selection, a medial value seems like a safer and more sensible choice. The maximum roll angle remains at the same approximate level for all the load cases on the road course which is the primary terrain for the truck to move in, while the vehicle's behavior in case of the occasional obstacle still remains at a very good level. Among the values of the optimum vectors that were found in the optimal medial area of the range, the final selection was made between the values of the first vector of Table 4.1 for the obstacle (damping 6122 N.s/m)and the last vector of Table 4.2 for the road (damping 7512 N.s/m).

The respective graphs of the response are presented in Figure 4.8. The former vector is depicted with the continuous line while the latter with dotted line.

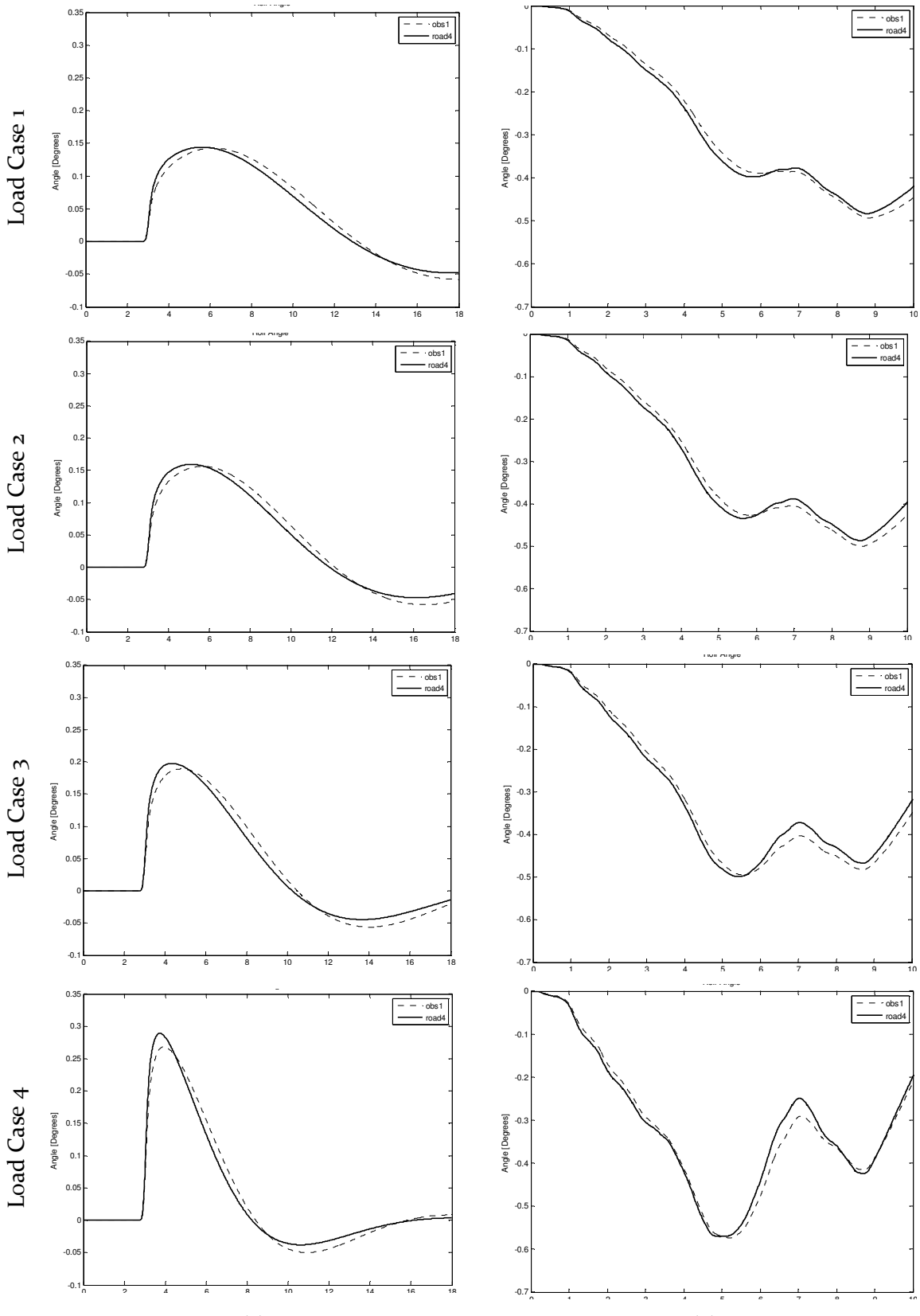

Figure 4.8 Roll angle response vs support damping (a) obstacle excitation, (b) road excitation high value: dotted line, medial: continuous line, low: dashed line

Between these two vectors, the differences in the response are rather minimal. As expected the one with the highest damping value performs slightly better on the road when the tank is heavy and the lower setting performs slightly better in all other cases. Between the two vectors, the one with the lower setting is selected to have an overall best performance. Since slight differences from this parameter are minimal as well as subjective on the load case, there is no need for such accuracy in the values of the damping sum. Instead, an optimal range or approximate setting should be defined. In that sense the optimum settings selected for the suspensions and supports of the truck are shown in

Vehicle Parameter	Optimum Design Vector
front suspension stiffness	10000
middle suspension stiffness	10000
rear suspension stiffness	10000
front suspension damping	50000
middle suspension damping	1000
rear suspension damping	1000
front support stiffness	1000
middle support stiffness	1000
rear support stiffness	1000
Sum of front, middle and rear support damping	~6000

4.6 Future Work

Throughout the whole optimization process for the purpose of this work, the genetic algorithm proved to be highly reliable and robust in all the cases examined. It exhibited good global search capabilities with high repeatability for the results obtained. Moreover, the initial scanning of the entire solution space and the location of the general neighborhood of the global optimum was relatively fast and efficient. However, the algorithm lacked strong local search capabilities towards the end of the search and near the boundaries of the design space and thus the exact position of the global optimum was rarely located precisely. On the other hand, the BFGS method was not able to locate the global optimum as successfully on most occasions and the algorithm was very easily trapped in local optima with much inferior objective function values. However, the local search capabilities of the algorithm were very strong. The characteristics of these two algorithms seem complementary and a combination of the two might prove more efficient than each separate algorithm. A hybrid optimization algorithm which combines the global search capabilities of the genetic algorithm during the initial stages of the search and the local search capabilities of the BFGS method after the neighborhood of the global optimum has been located, could produce superior results for the given problem.

In the current work the optimization was focused on a single objective; the minimization of the angular displacement (roll angle) of the vehicle's tank, as the general stability of the truck on the road is highly dependent on it. Perhaps it would be useful as well as interesting to widen the optimization by targeting multiple objectives at the same time and examining how the parameters and the results of the optimization are differentiated on such occasions. Other potential objectives could include the minimization of the tank's bounce or pitch movements or the minimization of the respective accelerations on the tank and the vibrations of the system.

Bibliography

A parenthetical author–date referencing system has been used throughout the study. Below is a list of the works cited, in alphabetical order.

1. Adeli, H. and Kumar, S. (1995), "Concurrent structural optimization on massively parallel supercomputer", *Journal of Structural Engineering*, 121(11), 1588-1597.
2. Anderson E. J., and Ferris M. C., (1994) "Genetic algorithms for combinatorial optimization: the assembly line balancing problem", *ORSA Journal on Computing,* 6, 161-173
3. Anon, *'Proposals for generalised road inputs to vehicles.'* ISO/TC 108/WGp draft No.3e, 1972
4. Barricelli, N.A. (1962), "Numerical testing of evolution theories", *ACT A Biotheoretica*, Vol. 16, 69-126.
5. Bean J. C., and Hadj-Alouane A. B., (1992), "A dual genetic algorithm for bounded integer programs", *University of Michigan Technical Report 92-53 to appear in RAIRO - RO*
6. Carroll, D.L. (1996), "Chemical Laser Modeling with Genetic Algorithms", *AIAA Journal*, 34(2), 338-346.
7. Chen, T.Y., and Chen, C.J. (1997), "Improvements of simple genetic algorithm in structural design", *Int. Journal Num. Meth. Eng*., Vol. 40, 1323-1334.
8. Coit D. W., Smith A. E., and Tate D. M., (1995) "Adaptive penalty methods for genetic optimization of constrained combinatorial problems", *ORSA Journal on Computing* in print
9. Fraser, A.S., "Symulation of genetic systems" (1962), *J. Theoret. Biol.*, 2, 329-346.
10. Galante, M. (1996), "Genetic Algorithms as an approach to optimize real-world trusses", *Int.Journal Num. Meth. Eng*.,39, 361-382.
11. Ghasemi, M.R., and Hinton, E. (1996), "Truss optimization using genetic algorithms", *in Topping B.H.V., (ed.) Advances in Computational Structures Technology, CIVIL-COMP Press*, Edinburgh, pp. 59-75.

12. Gillespie, T.D., "Fundamentals of Vehicle Dynamics", Society of Automotive Engineers, Inc, 400 Commonwealth Drive, Warrendale, PA

13. Goldberg, D.E. (1989), "Genetic algorithms in search, Optimization and Machine learning",Assidon-Weley, Reading, MA.

14. Grefenstette, J.J. (1990), A user's guide to GENESIS, Version 5.0, Computer Science Department, Vanderbilt University, Nashville, Tennessee, USA.

15. Groves, L., Michalewicz, Z., Elia, P., Janikow, C., "Genetic Algorithms for Drawing Directed Graphs", *Proceedings of the Fifth International Symposium on Methodologies of Intelligent Systems, North-Holland, Amsterdam*, pp. 268-276, 1990.

16. Holland J.H. (1975), "Adaptation in natural and artificial systems", University of Michigan Press, Ann Arbor.

17. Joines J. A., and Houck C. R., (1994), On the use of non-stationary penalty functions to solve nonlinear constrained optimization problems with GA's, *Proceedings of the First IEEE Conference on Evolutionary Computation,* 579-584

18. Juliff K., (1993) "A multi-chromosome genetic algorithm for pallet loading", *Proceedings of the Fifth International Conference on Genetic Algorithms* 467-473

19. Lagaros, N.D., (2000), "Βελτιστοποίηση κατασκευών με χρήση Εξελικτικών αλγορίθμων και Νευρωνικών Δικτύων", *PhD Dissertation*, National Technical University of Athens (NTUA).

20. Le Riche R. G., Knopf-Lenoir C., and Haftka R. T., (1995), "A segregated genetic algorithm for constrained structural optimization", *Proceedings of the Sixth International Conference on Genetic Algorithms,* 558-565

21. Lin, C.Y., and Hajela, P. (1992); "Genetic algorithms in optimization problems with discrete and integer design variables", *Eng. Opt*., vol. 19, pp. 309-327.

22. Martin, F.G., and Cockerham, C.C. (1960), "High speed selection study", in O. Kempthorne (ed.), *Biometrical Genetics, Pergamon Press*, pp. 35-45, London.

23. Michalewicz, Z., Vignaux, G.A., Hobbs, M. (1991), "A Non-standard Genetic Algorithm for Nonlinear Transportation Problem", *ORSA Journal on Computing*, 3(4), 307-316.

24. Michalewicz, Z., (1995) "Genetic algorithms numerical optimization and constraints", *Proceedings of the Sixth International Conference on Genetic Algorithms,* 151-158

25. Nagendra, S., Jestin, D., Gurdal, Z., Haftka, R.T. and Watson, L.T. (1996), "Improved genetic algorithm for the design of stiffened composite panels", *Computers & Structures*, 58(3), 543-555.

26. Ohsaki, M. (1995), "Genetic Algorithm for topology optimization of trusses", *Computers & Structures*, 57(2), 219-225.

27. Patton A. L., Punch III W. F., and Goodman E. D., (1995), "A standard GA approach to native protein conformation prediction", *Proceedings of the Sixth International Conference on Genetic Algorithms* 574-581

28. Richardson J.T., Palmer M.R., Liepins G., and Hilliard M. (1989) "Some guidelines for genetic algorithms with penalty functions", *Proceedings of the Third International Conference on Genetic Algorithms*, 191-197

29. Schwefel, H-P., (1995), "Evolution and Optimum Seeking", *John Wiley & Sons, Chichester,* UK.

30. Shyue-Jian Wu and Pei-Tse Chow (1995), "Integrated discrete and configuration optimization of trusses using genetic algorithms", *Computers & Structures*, 55(4), 695-702.

31. Siedlecki W., and Sklansky J., (1989), "Constrained genetic optimization via dynamic reward-penalty balancing and its use in pattern recognition", *Proceedings of the Third International Conference on Genetic Algorithms,* 141-150

32. Smith, A.E. and Tate,D.M., (1993) "Genetic optimization using a penalty function*" Proceedings of the Fifth International Conference on Genetic Algorithms* 499-505

33. Smith, S.F. (1980), "A Learning System Based on Genetic Algorithms", *PhD Dissertation*, University of Pittsburg.

34. Tate, D.M., and Smith,A.E, (1995), Unequal area facility layout using genetic search, *IIE Transactions,* 27, 465-472